

**CHARACTERIZATION OF AEROSOLS
IN CALIFORNIA
(ACHEX)**

FINAL REPORT

VOLUME IV

ANALYSIS AND INTERPRETATION OF DATA

**AIR RESOURCES BOARD
STATE OF CALIFORNIA**

TD
834.5
H5
v.4



Science Center
Rockwell International

SC524.25FR

CHARACTERIZATION OF AEROSOLS IN CALIFORNIA
(ACHEX)

FINAL REPORT

VOLUME IV

ANALYSIS AND INTERPRETATION OF DATA

Submitted to the
AIR RESOURCES BOARD
STATE OF CALIFORNIA

in
completion of
research under

ARB CONTRACT NO. 358

Prepared by

G. M. Hidy

with

LIBRARY
AIR RESOURCES BOARD
P. O. BOX 2815
SACRAMENTO, CA 95812

B. Appel
R. J. Charlson
W. E. Clark
D. Covert
S. K. Friedlander
R. Giauque
S. Heisler
W. W. Ho
J. J. Huntzicker
T. Novakov

L. W. Richards
R. Ragaini
T. B. Smith
G. Sverdrup
S. Twiss
A. Waggoner
H. H. Wang
J. J. Wesolowski
K. T. Whitby
W. White

September 30, 1974

Not for public release without approval of the Air Resources Board

SC524.25FR

TABLE OF CONTENTS

<u>Section</u>	<u>Title</u>	<u>Page No.</u>
I.	INTRODUCTION	1-1
	A. Objectives	1-1
	B. History and Completion of Program	1-2
	C. Contents of Final Report	1-3
II.	HISTORICAL PERSPECTIVE	2-1
III.	GENERAL CHARACTERIZATION OF AEROSOLS	3-1
	A. Physical Properties	3-1
	1. Mass Concentration	3-1
	2. Particle Size Distributions	3-4
	3. Particle Aging	3-19
	4. Particle Density	3-21
	5. Light Scattering and Smog	3-22
	B. Chemical Properties	3-41
	1. Chemical Composition	3-41
	2. Size Distribution	3-49
	3. Liquid Water Content	3-54
	4. Role of Ammonia	3-54
	5. Source Dominated and Receptor Chemistry	3-55
	C. Aerosol Background	3-60
IV.	PATTERNS OF DAILY CHANGE IN AEROMETRIC PARAMETERS	4-1
	A. Selected Episodes From the 1972 Program	4-1
	1. Pomona - October 24 and 25, 1972	4-1
	2. South Coast Basin - September 20 and 21, 1972	4-8
	3. South Coast Basin - October 5 and 6, 1972	4-26
	4. Background Measurements	4-36
	5. Fresno - August 31 and September 1, 1972	4-44
	B. Selected Episodes From the 1973 Program	4-48
	1. West Covina - July 23-26, 1973	4-48

SC524.25FR

TABLE OF CONTENTS

<u>Section</u>	<u>Title</u>	<u>Page No.</u>
	2. Pomona - August 16-17, 1973	4-55
	3. Rubidoux Episodes	4-57
	a. Case I - September 5-6, 1973	4-57
	b. Case II - September 19-20, 1973	4-61
	4. Dominguez Hills	4-64
	C. Concluding Remarks	4-69
V.	SULFUR AND NITROGEN AEROSOL CHEMISTRY	5-1
	A. Oxidized and Reduced Sulfur Species	5-1
	1. Sulfur and Motor Vehicle Emissions	5-8
	2. Evidence of Sulfate Photochemistry	5-12
	3. Estimated Rates of Conversion	5-18
	B. Nitrate Aerosols	5-20
	C. Mechanisms of Aerosol Formation	5-23
	1. Physical Constraints	5-24
	2. Chemical Reactions for Precursors	5-26
	a. Sulfate Reactions	5-27
	b. Nitrate Forming Reactions	5-33
	D. Application of Mechanisms to the Atmosphere	5-37
	1. Sulfate Formation	5-37
	2. Nitrate Formation	5-40
VI.	CARBON AEROSOL CHEMISTRY	6-1
	A. Characterization of Organic Fraction	6-1
	1. Total Carbon Analysis	6-1
	2. Solvent Extraction	6-2
	3. Physical Methods	6-10
	B. Mechanism of Organic Particle Formation	6-13
	C. Application to the Atmosphere	6-21

SC524.25FR

TABLE OF CONTENTS

<u>Section</u>	<u>Title</u>	<u>Page No.</u>
VII.	THE ROLE OF LIQUID WATER IN AEROSOL CHEMISTRY AND ATMOSPHERIC VISIBILITY	7-1
	A. Introduction	7-1
	B. Review of Theory Governing Liquid Water Content of Aerosol Particles	7-3
	C. Discussion of Experimental Results	7-7
	1. Laboratory Results From the Humidograph	7-7
	2. Humidograph Field Results	7-14
	a. Description of Sites	7-14
	b. Data Collection	7-17
	c. Computer Processing and Visual Display for Analysis	7-17
	3. Discussion of Humidograph Data	7-18
	4. Specific Discussion and Comparison with Chemical and Meteorological Data	7-19
	5. Waterometer Results	7-41
	a. Field Observations	7-41
	b. Results and Discussion	7-42
	6. A Comparison of Humidograph Results With Those of Other Techniques	7-55
	a. Comparison With Microbalance Weighing Results..	7-55
	b. Comparison With Calculations by Hanel.....	7-57
	D. Summary of Atmospheric Observations.....	7-57
VIII.	AEROSOLS AND SOURCES	8-1
	A. Size Distribution of Major Sources	8-1
	1. Characterization of the Freeway Aerosol Size Distribution	8-1
	B. Chemical Tracer Method	8-10
	1. Chemical Element Balance	8-12
	a. Chemical Composition of the Freeway Aerosol ...	8-13

SC524.25FR

TABLE OF CONTENTS

<u>Section</u>	<u>Title</u>	<u>Page No.</u>
	2. Secondary Constituents	8-18
	3. Emission Inventory Scale-up	8-18
	4. Results of Source Breakdown Calculations	8-20
	5. Carbon Balance	8-32
C.	Size Distributions of Primary Sources	8-36
	1. Coagulation of the Primary Distribution	8-44
	2. Growth Calculations	8-48
	3. Results of the Coagulation and Growth Calculations .	8-50
	4. Size Distribution of Chemical Elements	8-53
D.	Statistical Interpretation	8-62
	1. Introduction	8-62
	2. Statistical Methods	8-62
	a. Mass Concentrations of Nitrates, Sulfates, and Organics	8-66
	3. Light Scattering by Aerosols of Sulfate, Nitrate and Organic Mixtures	8-69
	a. Role of Water Vapor	8-76
	4. Source Contributions to the Aerosol	8-78
	a. Sources of Aerosol Precursors	8-78
	b. Calculations of Source Contributions	8-83
	c. Geographical Variations in Aerosol Composition .	8-84
	5. Summary and Conclusions	8-89
IX.	RECOMMENDED CONTROL STRATEGY FOR AEROSOLS	9-1
A.	Approach to Achievement of Standards	9-2
B.	Total Mass Concentration	9-3
	1. Significance of Secondary Contributions	9-3
	2. Primary Emissions and Natural Background	9-10
C.	The Visibility Standard	9-11
D.	Estimation of Emission Reductions	9-12

SC524.25FR

TABLE OF CONTENTS

<u>Section</u>	<u>Title</u>	<u>Page No.</u>
X.	INSTRUMENTATION FOR AEROSOL MONITORING	10-1
	A. Recommended Improved Standards	10-3
	1. Submicron Fraction	10-3
	2. Other Standards	10-4
	B. Approach to Instrumentation	10-4
	1. Monitoring Program	10-4
	2. Surveillance Stations	10-6
	3. Aerosol Research Laboratory	10-7
	C. Summary	10-7
XI.	ACKNOWLEDGEMENTS	11-1
XII.	REFERENCES	12-1
APPENDIX A.	A PRELIMINARY REPORT ON THE MISMATCH OF THE AEROSOL SIZE DISTRIBUTIONS OBTAINED DURING THE ACHEX	A-1
APPENDIX B.	THE AEROSOL SIZE DISTRIBUTION IN THE MOJAVE DESERT	B-1
APPENDIX C.	CONDENSATION NUCLEI COUNT VS. V_3 -/b _{scat}	C-1

LIST OF TABLES

<u>Number</u>	<u>Title</u>	<u>Page No.</u>
3-1	Summary of Results for Aerosol Mass Concentration by Filter Collection in the South Coast Air Basin During the Period July - October 1972 and 1973	3-2
3-2	Summary of Results for Aerosol Mass Concentration by Filter Collection and Analysis at Several Sites During the Period July - November 1972	3-3
3-3	Summary of Aerosol Physical Properties Achex I	3-8
3-4	Processes Affecting Evolution of Aerosols in a Unit Volume of Lower Atmosphere	3-20
3-5	Correlation Coefficients for b_{sp} Versus V_3 or V_3^-	3-34
3-6	Categories of Ambient Air Environments and Numerical Values for Their Parametric Description	3-38
3-7	Chemical Composition of Filter Collected Aerosol Samples ...	3-44
3-8	Summation of Total Filter Constituents	3-46
3-9	NASN Network Data for Nitrate and Sulfate in the South Coast Basin for 1968 (Annual 24-hr Average Values)	3-48
3-10	Mass Median Particle Diameter South Coast Air Basin, 1973 ..	3-51
3-11	Comparison of Theoretical and Experimental Ammonium Values..	3-56
3-12	Ammonia Concentrations vs Observed NH_4^+ ($\mu\text{g}/\text{m}^3$)	3-57
3-13	After Filter Chemistry for Samples Obtained Near the Harbor Freeway September 20, 1972 ($\mu\text{g}/\text{m}^3$)	3-58
3-14	Overall Averaged Analysis for Chemical Constituents of San Nicolas Island Aerosol (Basis $30 \mu\text{g}/\text{m}^3$ of Particle Concentration)	3-59
3-15	Total Filter Chemical Analysis of Selected Cases At Dominguez Hills (in $\mu\text{g}/\text{m}^3$)	3-61
3-16	Suspended Particulate Measurements at Nonurban California Locations (From Trijonis, Reference 17)	3-67

SC524.25FR

LIST OF TABLES

<u>Number</u>	<u>Title</u>	<u>Page No.</u>
4-1	Some Average Values of the Conversion Ratio for Secondary Aerosol Constituents in the South Coast Air Basin	4-71
5-1	Estimated Rates of Theoretically Possible Homogeneous Removal Paths for SO ₂ in a Simulated Polluted Atmosphere (from Calvert (27))	5-28
5-2	Heterogeneous Reactions to Form Sulfate	5-29
5-3	Reactions Potentially Involved in Nitrate Formation	5-34
5-4	Aqueous Reactions of Nitrogen Oxides	5-36
6-1	Solvent Extraction of 24-hour Filters	6-3
6-2	Comparison of Extraction Efficiency of Cyclohexane, Benzene and Benzene + MeOH-HCCl ₃	6-6
6-3	Comparison of Solvent Extraction and Thermal Analysis for Characterizing Carbonaceous Fractions ¹⁾	6-8
6-4	Non-Volatile Carbon Formation in Solvent Extracts of Atmospheric Particulate Samples	6-9
6-5	HRMS Analysis of Aerosol Samples in Heavy Smog at West Covina, July 23-24, 1973	6-12
6-6	Some Characteristic Ratios for the Organic Component as Determined by HRMS, Based on Analysis of Samples Taken at West Covina, July 23-24, 1973	6-14
6-7	Some Hydrocarbon Vapors in Souther California	6-15
6-8	Some Boiling Points and Vapor Pressures of Oxygenated Organic Compounds	6-16
6-9	Summary of Estimation of Non-Methane Hydrocarbon Fraction With Carbon Number Larger Than Six (concentrations in ppm)	6-18



SC524.25FR

LIST OF TABLES

<u>Number</u>	<u>Title</u>	<u>Page No.</u>
7-1	Deliquescent Compounds	7-5
7-2	Field Site Locations and Descriptions	7-15
7-3	Optically and Chemically Determined Sea Salt Concentrations.	7-27
7-4	Results of Chemical Analyses, Pasadena, California, 20-23 September 1972	7-32
8-1	Characteristics of the Freeway Aerosol Size Distribution Computed From the Difference Between Runs 54 and 55	8-3
8-2	Percentage Difference of Selected Aerosol, Particle Chemistry, and Gas Chemistry With the Wind From the Freeway	8-5
8-3	Chemical Element Concentrations From Harbor Freeway 9/20/72.	8-15
8-4	Contributions of Non-Freeway Sources to Harbor Freeway Filter Samples 9/20/72	8-16
8-5	Elemental Concentrations in Primary Freeway Aerosol	8-17
8-6	Primary Particulate Inputs Relative to Automobile	8-19
8-7	24-Hour Source Breakdown Based on Chemical Element Balance .	8-21
8-8	2-Hour Source Breakdown Based on Chemical Element Balance...	8-22
8-9A	Measured and Calculated Element Concentration	8-24
8-9B	Measured and Calculated Element Concentration	8-25
8-10A	Estimated Source Contributions - 2 Hr Filters	8-26
8-10B	Estimated Source Contributions - 24 Hr Filters	8-27
8-11	Measured and Calculated Element Concentrations	8-28
8-12	Assignment of Non-Organic Secondary Species to Chemical Compounds and Associated Water	8-33
8-13	Carbon Balance Based on 1972 Data	8-37
8-14	Carbon Balance	8-38
8-15	Ratio of Number Concentration to Pb Concentration	8-45
8-16	Fraction of Chemical Species on Particles Smaller than 1.5 μm	8-56
8-17	"Two-Hour" Samples Used in Regression Analysis and Mobile Van Averages	8-63
8-18	Notation, Units, and Analytical Techniques	8-64

SC524.25FR

LIST OF TABLES

<u>Number</u>	<u>Title</u>	<u>Page No.</u>
8-19	Estimated Breakdown of Aerosol Mass Concentration for Two-Hour Aerosol Samples at Mobile Van	8-68
8-20	Ratio of Mass on After Filter (Particle Diameters Less Than 0.5 μ) to Mass on Total Filter (Particle Diameter Less Than 15 μ) for Individual Aerosol Components	8-70
8-21	Estimated Breakdown of Light Scattering Coefficient for Two-Hour Aerosol Samples at Mobile Van	8-74
8-22	Inventory of Estimated Reactive Gas Emissions in the Los Angeles Basin Compiled from Most Recent Inventories by Local Air Pollution Control Districts: Los Angeles (1973), Orange County (1972), San Bernardino (1972), and Riverside (1970)	8-79
9-1	Estimated Influence of Auto Exhaust Control on Ambient Sulfate Levels (All Values Given in $\mu\text{g}/\text{m}^3$ SO ₂ Equivalents)	9-9
10-1	Ambient Air Quality Standards for Particulates	10-1
10-2	Recommended Instrument Hierarchy for Measuring Atmospheric Aerosols	10-2
A-1	Royco 220 Temperatures	A-26
B-1	Particle Size Ranges and Time at Each Step for WAA	B-18
B-2	Mean and Relative Standard Deviation of Particle Voltage Pulses From the ARB Royco PC 220 (Serial No. 431) Optical Particle Counter With the Original and Sheath Air Sample Inlets	B-18
B-3	Particle Size Ranges for the Optical Single Particle Counters	B-19
B-4	Summary of Averaged Data for Goldstone	B-20
B-5	Aerosol and Meteorological Parameters for Associated Plots in Figures B-11 - B-14	B-21
B-6	Particle Density, Chemistry, and Gaseous Chemistry at Goldstone	B-22
C-1	Identifiable Categories of Urban and Non-Urban Concentrations of CNC and K = V3-/BS	C-5
C-2	The Range, Mean, and Percent Standard Deviation of BSCAT, V3-, and VT for Categories of Clean Continental and Urban Conditions	C-7



SC524.25FR

LIST OF FIGURES

<u>Number</u>	<u>Title</u>	<u>Page No.</u>
2-1	Hypothetical Presentation of Bimodal Mass Distribution Based on Work on Urban Aerosols Through 1971.....	2-4
3-1	Aerosol Mass Distributions vs. Particle Size	3-5
3-2	Total Filter and Afterfilter Mass vs. Hi-Vol Mass	3-6
3-3	Number Distribution of Particles	3-9
3-4	Surface and Volume Distributions Taken at Pomona on October 24, 1972	3-12
3-5	Comparison of Surface and Volume Distributions for Background and Motor Vehicle Source Enriched (Near Harbor Freeway) Sites	3-13
3-6	Evolution of the Volume Distribution of Smog Aerosol Taken at Pomona, CA. 8/17/73	3-15
3-7	Comparisons of the Volume Distributions of Atmospheric Aerosols Measured in Different Urban and Nonurban Locations	3-18
3-8	Variation in Apparent Particle Density With Relative Humidity	3-23
3-9	Ratio of Light Scattering Coefficient to Mass Concentration for Uniform Spherical Particles of Unit Density, Refractive Index 1.5, and Diameter D_p .	3-26
3-10	Correlation of Light Scattering Coefficient With Aerosol Mass Concentration in 60 Two-Hour Samples at Mobile Van Sites.....	3-27
3-11	Correlations Between b_{scat} and the Aerosol Volume in Different Size Ranges.....	3-29
3-12	Particle Size Distributions Before and After the Arrival of Smog.....	3-30
3-13	Extinction Due to the Aerosol as a Function of V_3 -.....	3-32

SC524.25FR

LIST OF FIGURES

<u>Number</u>	<u>Title</u>	<u>Page No.</u>
3-14	Correlation of b_{sp} vs. V_3 for ACHEX-1 Data	3-39
3-15	Parameter K as a Function of the Log-Normal Size Distribution Parameters for a White Aerosol	3-40
3-16	Variation in V_3/b_{sp} vs. DGV_3 for the Pomona Data in 1972 ...	3-42
3-17	Variation of V_3/b_{sp} vs. DGV_3 for the Harbor Freeway Data ...	3-43
3-18	Mass Distributions of $SO_4^{=}$ and NO_3^- With Particle Size	3-50
3-19	Mass Distributions of Ni and Pb With Particle Size	3-52
3-20	Mass Distributions of Na, Al, and Fe With Particle Size	3-53
3-21	Comparison Between Trace Material Concentration in the Los Angeles Atmosphere and the Offshore Background on San Nicolas Island. Data for Average Concentrations in Pasadena were Based on Results in 1969 Reported by Miller et al. (16), Except for $SO_4^{=}$ and NO_3^- Which are Average Values From the National Air Surveillance Network	3-63
3-22	Variation in the Cu/Na Ratio With Distance From the Ocean ..	3-65
3-23	Variation in the K/Na Ratio With Distance From the Ocean ...	3-66
4-1	Diurnal Patterns of Pollutant Gases Taken at Pomona on October 24-25, 1972	4-2
4-2	Diurnal Patterns of Aerosol Parameters Taken at Pomona on October 24-25, 1972.....	4-5
4-3	Diurnal Patterns of Chemical Species for Pomona - October 24-25, 1972	4-6
4-4	Diurnal Patterns for Riverside, Pasadena, and Harbor Freeway on September 20-21, 1972	4-9
4-5A	Diurnal Patterns of Chemical Species (Inorganic Fraction) on September 19-20, 1972	4-21
4-5B	Diurnal Patterns of Chemical Species (Carbon, and Oxidized and Reduced Sulfur and Nitrogen) for Harbor Freeway on September 19-20, 1972	4-22

SC524.25FR

LIST OF FIGURES

<u>Number</u>	<u>Title</u>	<u>Page No.</u>
4-6	Diurnal Patterns of Heavy Elements for Pasadena - September 20, 1972	4-23
4-7	Diurnal Patterns of Heavy Elements for Riverside - September 19-20, 1972	4-23
4-8	Diurnal Patterns for Riverside, Pasadena, and Pomona on October 5-6, 1972	4-27
4-9	Diurnal Patterns of Heavy Elements for Pomona on October 5-6, 1972	4-37
4-10	Diurnal Patterns for Hunter-Liggett on September 13-14, 1972.	4-39
4-11	Diurnal Patterns for Fresno on August 30-31, 1972	4-45
4-12	Diurnal Patterns of Heavy Elements for Fresno August 31 - September 1, 1972	4-47
4-13	Diurnal Changes at West Covina - July 24, 1973 First Day of Intense Pollution Episode	4-49
4-14	Diurnal Changes at West Covina - July 24-25, 1973 Second Day of Intense Pollution Episode	4-51
4-15	Diurnal Changes at West Covina - July 26, 1973 Third Day of Intense Pollution Episode	4-52
4-16	Diurnal Changes at West Covina - July 23-26, 1973	4-53
4-17	Diurnal Changes at Pomona August 16-17, 1973.....	4-56
4-18	Diurnal Patterns for Aerosol Constituents for Pomona August 17, 1973	4-58
4-19	Diurnal Changes at Rubidoux September 5-6, 1973	4-59
4-20	Diurnal Patterns for Aerosol Constituents for Rubidoux A(VH), B(VI), C(VJ) September 1973	4-60
4-21	Diurnal Change at Rubidoux September 19, 1973	4-62
4-22	Diurnal Changes at Dominguez Hills October 4-5, 1973	4-65
4-23	Diurnal Changes at Dominguez Hills October 10-11, 1973	4-66

SC524.25FR

LIST OF FIGURES

<u>Number</u>	<u>Title</u>	<u>Page No.</u>
4-24	Diurnal Patterns of Aerosol Constituents for Dominguez Hills A(WK), B(WL)	4-68
4-25	The Variation of Nitrate and Sulfate Levels in Time and Space.	4-70
4-26	24-Hour Average Size Distributions for Sulfate at Receptor Sites, 1973	4-73
4-27	24-Hour Average Size Distributions for Sulfate and Nitrate at Dominguez Hills, 1973	4-74
4-28	24-Hour Average Size Distributions for Nitrate at Receptor Sites, 1973	4-75
5-1	Sulfur 2p Photoelectron Spectra of Ambient Pollution-Aerosol Samples Collected in ACHEX and Analyzed by Craig <u>et al.</u> (22)	5-2
5-2	SO ₂ and Particulate S ⁺ and S ⁻ Collected Using Sticky (ST) and Nonsticky (NS) Substrates. The Wind Direction (WD) is Indicated	5-3
5-3	Correlation Between Sulfur and Lead - Harbor Freeway (Downwind Conditions)	5-9
5-4	Correlation Between Oxidized Sulfur (S ⁺) and Lead - Pasadena, Pomona, and Riverside	5-11
5-5	Correlation Between Reduced Sulfur (S ⁻) and Lead - Pasadena, Pomona, and Riverside	5-13
5-6	Correlation Between Sulfur and Lead - San Jose	5-14
5-7a	Scatter Diagram of the Ratio of Particulate Sulfate on Total Filter as Sulfur to Sulfur Dioxide Reduced to Sulfur vs. Relative Humidity	5-15
5-7b	Scatter Diagram of the Ratio of Particulate Sulfate on After Filter as Sulfur to Sulfur Dioxide Reduced to Sulfur vs. Relative Humidity	5-16
5-8	Scatter Diagram of the Conversion Ratio f _S Based on Particles Less Than 0.5 μm vs. 2 Hour Averaged Ozone Concentration ...	5-17

SC524.25FR

LIST OF FIGURES

<u>Number</u>	<u>Title</u>	<u>Page No.</u>
5-9	Scatter Diagram of the Conversion Ratio f_S Based on Particles Less Than $0.5 \mu\text{m}$ vs Total Carbon Less Than $0.5 \mu\text{m}$ Diameter..	5-19
5-10	Scatter Diagram of the Nitrogen Oxide Conversion Ratio f_N vs. Two Hour Averaged NO_2 Concentration	5-21
5-11	Scatter Diagram of the Particle to Gas Phase Nitrogen Ratio Against Ozone	5-22
5-12	The Dependence of the Sulfate Conversion Ratio on the Product of the Ozone and Non-Methane Hydrocarbon Concentrations	5-39
6-1	Benzene vs Cyclohexane Extractables	6-4
6-2	Story's Model of Organic Aerosol Formation	6-20
6-3	Mass Concentration of Aerosol Formation from Olefin-Ozone Reaction as a Function Olefin Concentration	6-22
7-1	Laboratory Measurements of Light Scattering Ratio, b_{sp}/b_{sp} (RH=20%), vs. Relative Humidity-Smoothed Curves	7-8
7-2	Humidogram of H_2SO_4 Aerosol and H_2SO_4 Aerosol Plus NH_3	7-9
7-3	Humidograms of Nitrate Aerosols	7-10
7-4	Humidograms of Aerosil R and Carbowax R	7-12
7-5	Humidograms of Internal and External Mixtures	7-13
7-6	Humidograms at Point Reyes Lighthouse, CA 1630 24 Aug. 72 to 0600 25 Aug. 72	7-20
7-7	Comparison of Humidograms at Richmond, CA; Pasadena, CA; Tyson, MO	7-21
7-8	Humidogram at Richmond, California	7-23
7-9	Averaged Humidograms at Pt. Reyes, California	7-24
7-10	Humidograms at Pt. Reyes, California Taken During Periods for Which Chemical Analyses Were Made	7-25

SC524.25FR

LIST OF FIGURES

<u>Number</u>	<u>Title</u>	<u>Page No.</u>
7-11	Averaged Humidogram, Pasadena, California 20 Sep. to 02 Oct. 72	7-29
7-12	Averaged Humidograms at Pasadena, California Corresponding to Chemical Analyses, See Table 7-4	7-30
7-13	Relative Concentrations (Fraction by Weight of Total) of Some Chemical Components of South Coastal Basin Aerosol. California Institute of Technology, Pasadena, California, 20-23 Sep. 1972	7-31
7-14	Averaged Humidogram, Fresno, California 29 Aug. 72 to 08 Sep. 72	7-34
7-15	Averaged Humidogram, Hunter Liggett Military Reservation 13 Sep. 72 to 15 Sep. 72	7-35
7-16	Averaged Humidograms at Montana de Oro State Beach, California and El Capitan State Beach, California	7-37
7-17	Humidograms for St. Louis Area, 21 to 28 Sep. 73	7-38
7-18	Humidogram of Hygroscopic Aerosol, Denver, Colorado 21 Nov. 73	7-40
7-19	Liquid Water Concentration in Atmospheric Aerosols at Pasadena, September 15, 1972	7-43
7-20	Liquid Water Concentration in Atmospheric Aerosols at Pasadena, September 20, 1972	7-44
7-21	Liquid Water Concentration in Atmospheric Aerosols at Pasadena, September 9, 1972	7-45
7-22	Liquid Water Concentration in Atmospheric Aerosols at Pomona, October 4-5, 1972	7-46
7-23	Liquid Water Concentration in Atmospheric Aerosols at Goldstone Tracking Station November 1972	7-48
7-24	Weight Fraction of Liquid Water as a Function of Relative Humidity for the Los Angeles Basin Area.....	7-49
7-25	Comparison of Light Scattering Coefficient With the Liquid Water Concentration in Atmospheric Aerosols	7-52



SC524.25FR

LIST OF FIGURES

<u>Number</u>	<u>Title</u>	<u>Page No.</u>
7-26	Correlation of b_{scat} vs. Liquid Water Content for 1972 and 1973	7-53
7-27	Comparison of Microbalance and Humidograph Results	7-56
7-28	Humidograms From Hanel's Calculated Values of Light Scattering Ratio as a Function of Relative Humidity (80) ...	7-58
8-1	Plot of the Surface Size Distributions, $\Delta S/\Delta \log D_p$ for Run 54 When the Wind was From the Freeway, Run 55 When the Wind was Toward the Freeway, and the Difference Distribution, Run 54 Minus Run 55 for D_p Less Than $.15 \mu m$.	8-3
8-2	Schematic of the Battelle-Columbus Auto Dilution Tunnel and Smog Chamber.....	8-6
8-3	Comparisons of the Surface Distributions for the Freeway Difference Size Distribution, Run 54 Minus Run 55, from the Harbor Freeway with Aerosol Size Distributions Measured in the Battelle Dilution Tunnel at Idle, 35 mph, and 50 mph.....	8-7
8-4	Size Distributions of Sea Salt, Soil Dust and Freeway Aerosols.....	8-41
8-5	Volume Distribution of Goldstone Aerosol, Primarily Soil Dust in Origin, Normalized to Total Volume	8-42
8-6	Freeway Aerosol Volume Distribution Normalized to Lead.....	8-43
8-7	Results of Coagulation Calculations. Measured Freeway Distribution is Shown	8-47
8-8	Primary Volume Distribution Based on Chemical Element Balance, and Final Volume Distribution After Secondary Conversion Calculations for Pomona	8-51
8-9	Primary Number Distribution Based on Chemical Element Balance, and Final Number Distribution After Secondary Conversion Calculations for Pomona.....	8-52

SC524.25FR

LIST OF FIGURES

<u>Number</u>	<u>Title</u>	<u>Page No.</u>
8-10	Primary Volume Distribution Based on Chemical Element Balance, and Final Volume Distribution After Secondary Conversion Calculations for Pasadena.....	8-54
8-11	Primary Number Distribution Based on Chemical Element Balance, and Final Number Distribution After Secondary Conversion Calculations for Pasadena	8-55
8-12	Calculated Values of b_s as a Function of Volume of Converted Material: Power Law Growth Equation with $\gamma=2.8$	8-59
8-13	Ratios $b_{scat}/mass$ from Two-Hour Samples at Mobile Van, Plotted as a Function of $SO_4/MASS$, $NO_3/MASS$, and Relative Humidity	8-72
8-14	Influence of Relative Humidity on $b_{scat}/mass$ Based on Statistical Analysis of Nitrate Behavior and Total Aerosol.	8-77
8-15	Patterns of Pollutant Transport in Afternoon	8-81
8-16	Geographical Distribution of Aerosol Mass Concentration Given as # ($\mu g/m^3$) and Estimated Breakdown by Component ...	8-85
8-17	Geographical Distribution of Aerosol Light Scattering Coefficient ($10^{-4}m^{-1}$) and Estimated Breakdown by Component.	8-86
8-18	Geographical Distribution of Aerosol Mass Concentration ($\mu g/m^3$) and Estimated Breakdown by Source Type	8-87
8-19	Geographical Distribution of Aerosol Light Scattering Concentration (m^{-1}) and Estimated Breakdown by Source Type.	8-88
9-1	Distribution by Source of Aerosol Mass Concentration for Filter Samples Collected Over Two Hour Periods, and Equilibrated to Air at Less Than 50% Relative Humidity.....	9-4
9-2	Comparison of the Distribution of Sources for Aerosol Mass Concentrations and Light Scattering in the South Coast Air Basin.....	9-6
A-1	Mismatch of Volume-Size Distributions at the Harbor Freeway..	A-12
A-2	Sketch of ARB Mobile Laboratory	A-13
A-3	Effect of Diluter on Volume-Size Distribution Measurement Point Arguello	A-14



SC524.25FR

LIST OF FIGURES

<u>Number</u>	<u>Title</u>	<u>Page No.</u>
A-4	Sheath Air Sample Inlet for the ARB and EPA Royco PC 220 Optical Particle Counters.....	A-15
A-5	Results of a Change in Refractive Index for Run 49 at the Harbor Freeway	A-16
A-6	Aerosol Inlet to Mobility Tube	A-17
A-7a	Aerosol Surface Distribution at Pt. Arguello	A-18
A-7b	Aerosol Volume Distribution at Pt. Arguello	A-19
A-8	Mismatch for Runs 40 Through 55	A-20
A-9	Mismatch for Runs 56 Through 61	A-21
A-10	The Method for Determining the Mismatch Parameter	A-22
A-11	Mismatch Parameter as a Function of Relative Humidity	A-23
A-12	Mismatch Parameter as a Function of Temperature	A-24
A-13	Mismatch Parameter as a Function of the Difference in the Inside and Outside Relative Humidities	A-25
B-1	Location of the Mobile Laboratory	B-23
B-2	Location of Instrumentation in the Mobile Laboratory	B-23
B-3	Sampling and Recording Times in the Ten-Minute Cycle	B-24
B-4	Variability in Electrometer Current, Particle Number, Surface Area, and Volume Due to Instrument Noise	B-24
B-5	Sheath Air Sample Inlet for the Royco PC220 Optical Particle Counter	B-25
B-6	Conical Sample Inlet for the Royco PC 245 Optical Particle Counter	B-25
B-7	Sampling Efficiency of the Conical Inlet vs. Particle Size ...	B-26
B-8	MCA Channel Number vs. Particle Diameter for the Royco PC 220 Optical Particle Using DOP Aerosols With a Refractive Index of 1.49	B-26

SC524.25FR

LIST OF FIGURES

<u>Number</u>	<u>Title</u>	<u>* Page No.</u>
B-9	MCA Channel Number vs. Particle Diameter for the Royco PC 245 Optical Particle Counter Using DOP Aerosols With a Refractive Index of 1.49.....	B-27
B-10	Plot of the Diurnal Variation of Selected Ten-Minute Averages Obtained at Goldstone.....	B-27
B-11	A Comparison of the Background Volume Distributions During a Very Clean Period and an Evening with Higher Total Volume	B-28
B-12	A Comparison of the Volume Distributions of Background Aerosols Sampled at Goldstone and Fort Collins, Colorado .	B-28
B-13	Incursion of Aged Aerosol From the South Coast Basin	B-29
B-14	A Comparison of the Aged Aerosol Sampled at Goldstone and Pomona	B-29
B-15	Total Mass of Aerosol at Goldstone Determined From the Total Filter	B-30
C-1	Condensation Nuclei Concentration vs. K with Superimposed Aerosol Classifications	C-2
C-2	Condensation Nuclei Concentration vs. K for ACHEX II Data ..	C-3
C-3	Condensation Nuclei Concentration vs. K for ACHEX I and II Data, Except Aged Polluted Urban Category With $K < 13$	C-4

SC524.25FR

I. INTRODUCTION

Some of the more pressing questions of air pollution requiring improved knowledge are those dealing with aerosols. Although airborne particles represent a small fraction of the trace constituent loading in air, they contribute significantly to environmental degradation as a potential hazard to health, a visibility reducer, and a possible agent of weather modification. Despite many years of investigation, the origins and evolution of atmospheric aerosols remain poorly understood quantitatively, compared with trace gases. Recognizing this, the California Air Resources Board (ARB) sponsored the California Aerosol Characterization Experiment (ACHEX), a major experiment in air chemistry devoted to a detailed study of aerosols in urban and remote sites of California.

The first phase of the study (ACHEX-1), was devoted to the development of observational systems for the program and to the acquisition of a wide variety of data characterizing atmospheric aerosols sampled primarily in late summer and fall of 1972. The second phase (ACHEX-11), was a continuation of observations and analysis, with primary emphasis on smog aerosols in the South Coast Air Basin.

A. OBJECTIVES

The objectives of ACHEX-1 were:

- 1) To characterize the aerosols in the South Coast, the San Francisco Bay area, and the San Joaquin Valley Basins in terms of their physical and chemical properties, interaction with atmospheric gases, and natural and anthropogenic origins.
- 2) To evaluate the amount of atmospheric aerosol in the cited three major air basins which can be related to: (a) primary emissions, such as, from auto exhausts or smokestacks; and (b) secondary production, due to physical and chemical processes taking place in the atmosphere.
- 3) To identify those major sources of particles and chemically reactive gases which can be related to aerosol pollution and visibility reduction.

SC524.25FR

- 4) To estimate, from aerosol source characterization in the three major regions, the extent to which the ambient air quality standards can be achieved by existing technology.
- 5) To evaluate the applicability of the aerosol analysis instrumentation employed in this study for use in other monitoring networks. Special emphasis was placed on an improved practical indicator (Index) for relating ambient aerosol properties to potential health hazards and to visibility reduction according to established California standards.

The objectives of the second increment of the program, ACHEX II, reflected the increased emphasis on photochemical processes and were recast in form:

- 1) To characterize aerosols in the South Coast Basin in terms of their physical and chemical properties and their interaction with atmospheric gases.
- 2) To improve knowledge of secondary aerosol formation processes by investigating the evolution of aerosols under conditions of photochemical smog formation.
- 3) To estimate the primary and secondary aerosol contributions to the total airborne particulate concentration in the South Coast Basin.
- 4) To evaluate the significance of anthropogenic sources and uncontrolables, including meteorological factors, natural sources, and water in the evolution of the respirable and visibility degrading aerosol.
- 5) To recommend from the characterization of aerosols and their sources, the key ingredients for a control strategy in the South Coast Basin.
- 6) To evaluate the applicability of instrumentation employed in this study for use in future monitoring programs.

B. HISTORY AND COMPLETION OF PROGRAM

The California Aerosol Characterization Experiment (ACHEX) was originally planned as a two-year program, with the observations scheduled to optimize acquisition of data during the latter half of 1972. As the objectives note, the project emphasized primary particle sources, secondary particle formation in the atmosphere, and their relation to changes in visibility. In California,

SC524.25FR

the "secondary" production of aerosols by chemical and physical processes in the atmosphere is believed to be especially important.

Because of unusual, unseasonably good weather in late 1972, few days were encountered in which adequate data could be obtained for characterizing the heavy hazes frequently observed in Southern California. Such weather conditions were so persistent that it was decided to terminate the 1972 program early and return to the field in 1973 to seek cases of more intense photochemical smog.

The ACHEX was redesigned in the spring of 1973 to apply a stronger focus on photochemical aerosol. In the late summer of 1973 a second observational program was implemented exclusively for the South Coast Basin. During this effort, weather and smog evolution was more consistent with conditions normally encountered and an important supplement to the 1972 data base was obtained.

After completion of the 1973 field study, considerable data analysis and sample analysis was undertaken to support the project objectives.

C. CONTENTS OF FINAL REPORT

This document is one of four volumes making up the final report describing the methods and results of the study. In this volume, the analysis and interpretation of the results is discussed in some detail. The other three volumes include: Volume (I) the summary of results and conclusions; (II) the experimental methods and analytical techniques, and (III) the data.

The following sections begin with a brief historical setting to place the results of ACHEX in perspective. This is followed by some general results characterizing the properties of atmospheric aerosols based on the ACHEX program. Then the details of diurnal changes in aerosols are summarized as they relate to diurnal patterns of variation in other aerometric parameters. This discussion leads into a detailed discussion of the behavior of the key chemical ingredients of the aerosol, the sulfur, nitrogen, carbon and water components. The relation between atmospheric aerosols and sources is then considered, with a discussion of possible control strategy for visibility improvement. The volume is completed with a chapter on the evaluation of aerosol instrumentation and its impact on upgraded monitoring or surveillance.

SC524.25FR

II. HISTORICAL PERSPECTIVE

Perhaps the first air pollutant to be commonly identified is atmospheric haze resulting from dispersion of smoke, fumes, or blowing dust. It has long been known that the suspended particles making up atmospheric aerosols are a hazard to human health. Furthermore, the light scattering by haze particles is the dominant factor in visibility degradation when the relative humidity is below 70%. These considerations have led the State of California to establish ambient air quality standards for airborne particles on the basis of total mass concentration of $75 \mu\text{g}/\text{m}^3$ annual average, and for visibility reduction in terms of visual range realized at relative humidity 70% or below.

As a result of many studies over the past several years, questions have been raised about the applicability of high volume filter sampling as a useful measure of pollution aerosol. For example, recent work has indicated that particles less than about $3 \mu\text{m}$ diameter are of principal interest for respiratory disease. Furthermore, there is evidence from several studies that man's contribution to the ambient aerosol burden is principally composed of particles smaller than $1 \mu\text{m}$ diameter. The high volume filter is believed to collect all particles below about $20 \mu\text{m}$ diameter, but gives (potentially) undue weighting to the supermicron particle fraction.

If chemical analysis is to be undertaken on monitored aerosol samples, other questions arise about the high volume filter procedure. For example, one must be concerned with the interaction of reactive gases with the filter substrate or with the collected material accumulated on the filter mat. Inaccuracies in measurement of sulfate on glass fiber media have been attributed to SO_2 absorption on the glass fiber filters. Nitrates and organic material also may be formed on the filter as reactive gases pass through it.

Despite the many questions about the sampling and the gravimetric analysis, the aerosol monitoring in the United States continues to rely on the high volume filter with glass fiber substrates.

While the monitoring of aerosols to meet the regulatory requirements for California is a legal requirement, the Air Resources Board has recognized that there is a close, but uncertain, relationship between intense hazes in

SC524.25FR

many air basins and chemical reactions in the ambient mixture of trace pollutants. Indeed, the smog chamber work in the early fifties of Haagen-Smit, Stephens, Hanst and others (see, for example, Leighton⁽¹⁾) provided strong evidence for aerosol formation as a part of photochemical smog.

It has long been recognized that the quantity of sulfate and nitrate in atmospheric aerosols cannot be accounted for by primary anthropogenic or natural emissions. These components are virtually universally present in large quantities in all tropospheric aerosol samples. Their concentrations are normally larger than those of the metals. However, only in the sixties have workers fully appreciated the significance of processes of "secondary" particle formation in contributing to the atmospheric burden of these constituents.

Sulfate and nitrate have been monitored for some time in selected cities, along with a solvent soluble fraction associated with organic material. Like sulfate and nitrate, it has not been possible to account fully for the amount of organics in aerosols without being concerned with chemical processes in the atmosphere. It has been recognized for some time that organics make up a substantial part of urban aerosols, but their sources remain unaccounted for in past work. In fact even today, few aerosol studies of any kind have attempted to construct a complete material balance in collected particles, either directly or by indirect calculation using suitable scaling factors.

About two years before the major increase in California's concern about atmospheric hazes in 1971, the development of new instrumentation and techniques for chemical analysis promoted interest in a series of new field experiments on aerosol behavior. The new developments permitted essentially continuous monitoring of certain physical properties of urban aerosols, particularly their size-number distribution and light scattering capacity. In addition, analytical methods became available with sufficient sensitivity to investigate changes in urban aerosol chemistry over periods of four hours or less. These innovations combined with improved continuous meteorological and pollutant gas analyzers led to a major experiment aimed at characterizing the daily evolution of smog aerosol over Los Angeles.⁽²⁾ This program was conducted at the Keck Laboratories of the California Institute of Technology in

SC524.25FR

August and early September 1969. The early results of this study were reported in Aerosols and Air Chemistry.⁽³⁾ The Pasadena Smog Experiment yielded a wide variety of new data characterizing the nature of changes in the physical and chemical properties of aerosols in smog over a few 24-hr periods. Although the observations were very detailed, the bulk of the analysis was done for a single 24-hr period.

The following measurements were made during the 1969 Pasadena aerosol study:

- 1) Continuous observations of size distribution of particles over the range 50Å to several microns using a variety of instruments.
- 2) Chemical nature of various size fractions of the aerosol collected in a cascade impactor over continuous time intervals as short as two hours.
- 3) Optical properties using a single wavelength and a multi-wavelength continuous recording integrating nephelometer.

At the same time that the aerosol and nuclei measurements were made, trace gas concentrations were monitored, including hydrocarbons, nitrogen oxides (NO_x), ozone and SO_2 . Meteorological variables such as wind speed and direction, temperature, humidity and flux of solar radiation also were recorded. The 1969 data indicated that:

- 1) Visibility is closely related to changes in humidity and in particle concentration over the 0.1 μm -1.0 μm diameter size range. The particle concentration showed a maximum at midday which corresponded with a maximum in ozone concentration.
- 2) The daytime interaction between aerosols and the photochemically reactive atmosphere was manifested mainly in the particle size range exceeding 0.1 μm diameter and less than a few microns in diameter.
- 3) There was a persistent bimodality in the mass distribution with respect to particle size. The pollution contribution was found in the small particles while the natural background was identified principally with the large particle fractions. The distribution of certain chemical constituents reflected the bimodal pattern. The results deduced from the study are shown schematically in Figure 2-1. This is a hypothesis about the distribution of



SC524.25FR

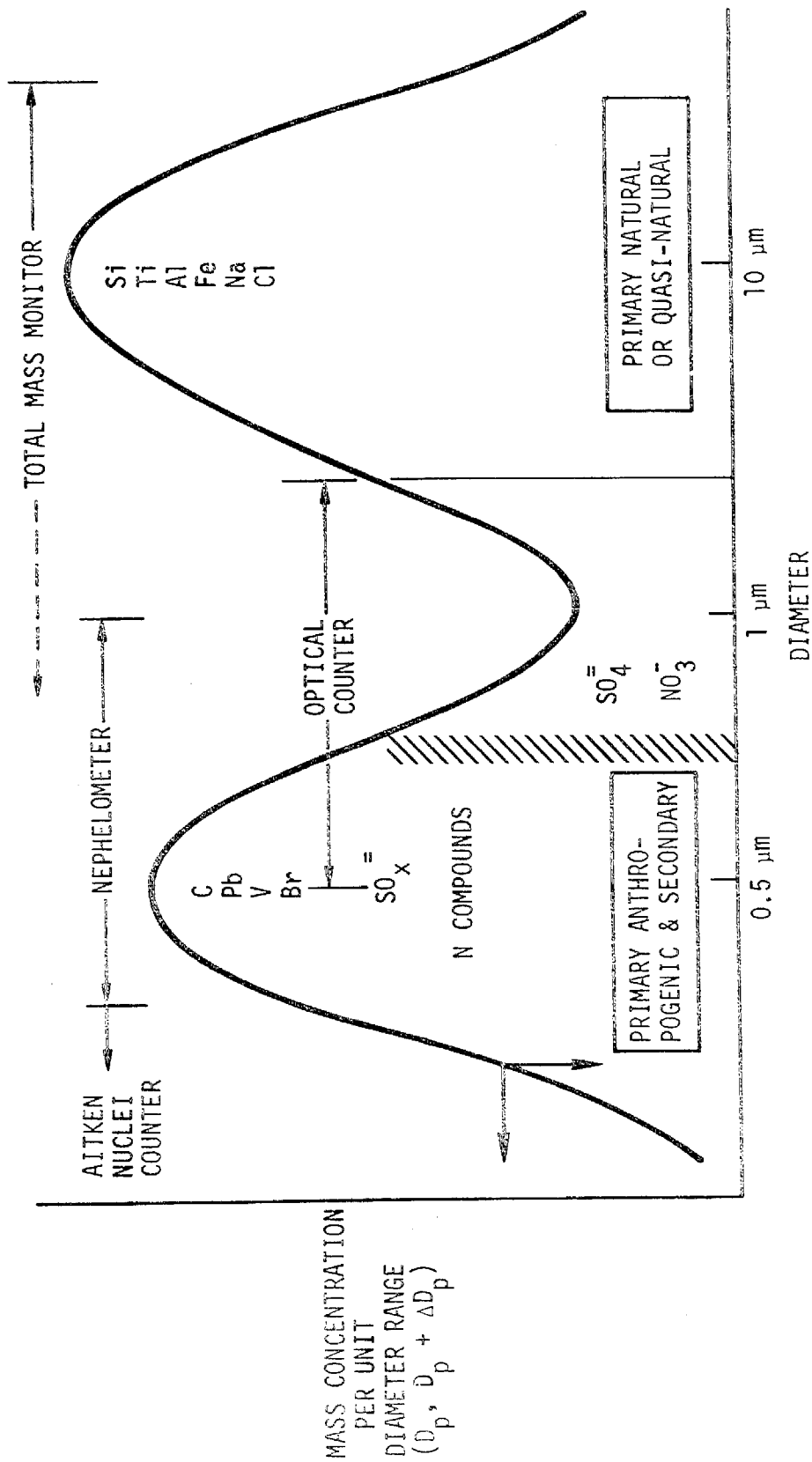


Figure 2-1. Hypothetical Presentation of Bimodal Mass Distribution
Based on Work on Urban Aerosols Through 1971

SC524.25FR

components and their origins.

4) There are significant diurnal changes in sulfur (sulfates, sulfites) and nitrogen-bearing compounds (nitrates, pyridinium and amino compounds) in the aerosol particles and the suspended material was unusually rich in non-carbonate carbon (\approx 30% by mass).

5) A method was tested for estimating the contributions of major primary sources to the Pasadena aerosol through its chemical composition. This procedure was found to be useful for characterizing the Los Angeles aerosol in relation to other cities.

These results demonstrated the feasibility of investigating the evolution of aerosols in sufficient detail to penetrate the complex physical and chemical interactions taking place in smoggy air.

They could be interpreted in the following way as related to control strategy:

- 1) Major increases in visibility will require substantial improvements in control of sub-micron particles in a range where removal efficiency of existing control equipment is relatively low.
- 2) Humidity is an uncontrollable factor in visibility degradation but must be accounted for in a uniformly applicable ambient air quality standard.
- 3) To achieve air quality goals, very stringent controls on gases such as NO_x , reactive hydrocarbons, and SO_2 are required because of the high photochemical reactivity to produce aerosols.
- 4) Measurement of total mass alone by filtration is an inadequate monitoring procedure, without further qualification.
- 5) Because of implications to health effects, monitoring of ambient aerosols should include routine checking for specific chemical elements or compounds such as lead or non-carbonate carbon.

The knowledge gained from the 1969 Pasadena study and a later 1971 investigation in Denver provided the technical basis for the experimental design of the ACHEX. Deliberations by the Air Resources Board in 1971 resulted in a request for proposals on the investigation of aerosols in California. The funding for the conduct of ACHEX was derived from the response to this request.

SC524.25FR

At the time the ACHEX was conceived, the state of development of computerized data acquisition, collection procedures for aerosol chemical analysis, and some analytical methods remained at the limits of technology, requiring considerable research in parallel with the operational aspects of ACHEX. Thus, the ACHEX program represented a pioneering effort in the application of new measurement and data acquisition systems to urban aerosol study, as well as in implementation of new, previously untested techniques for chemical analysis.

Several operational "firsts" attributed to the ACHEX should be kept in mind in the light of widespread progress in aerosol science during the past three years. These are:

- 1) A complete transportable aerometric laboratory was designed, built and operated which observed pollutant gases, aerosols, and meteorological variables.
- 2) A minicomputer system with on-line data surveillance capability was used to acquire and partially analyze data from both gas and aerosol analyzers.
- 3) Continuous observations were made over the particle diameter range between 50^oÅ and 30 μm.
- 4) Aerosol samples were collected on a two-hr basis for size fractionated, detailed chemical analysis to obtain results for aerosol changes compatible with the scale of changes in smog gas reactions.
- 5) Aerosol chemical analysis by combined wet chemical and physical methods, which included photoelectron spectroscopy, x-ray analysis, and high resolution mass spectroscopy.
- 6) The ACHEX was the first major field study devoted principally to aerosol chemistry.
- 7) The study involved the first attempt to measure aerosol mass concentration semicontinuously by β-ray attenuation.
- 8) The ACHEX used separate filter media for organic and inorganic aerosol chemical analysis.
- 9) ACHEX first used chromatographic instruments operationally for continuous measurement of hydrocarbon and sulfur containing gases.

SC524.25FR

- 10) The ACHEX provided detailed "snapshot" data of aerosol and trace gas behavior at several rural and urban locations in California.
- 11) Humidified nephelometry was tested extensively and used to investigate in the field the hygroscopicity of urban and non-urban aerosols.
- 12) The liquid water content of the aerosol was measured semicontinuously by a microwave method, and over extended periods by chromatographic filter analysis.
- 13) The field study was designed to explore extensively the influence of sources and meteorological transport on aerosol behavior.
- 14) The ACHEX used the chemical tracer approach combined with material balance to quantify the role of primary and secondary sources of particles.
- 15) The ACHEX confirmed the importance of $\text{SO}_4^{=}$, NO_3^- , condensed hydrocarbons, NH_4^+ and H_2O in dominating the aerosol mass and light scattering in Southern California.
- 16) The investigation confirmed the multimodal nature of the volume-size distribution and the chemical composition distribution for aerosols in California.
- 17) The study has shown clearly the importance of photochemical processes in aerosol formation in smog.
- 18) The study provided data to distinguish between the behavior of liquid water in particles as contrasted to relative humidity.

SC524.25FR

III. GENERAL CHARACTERIZATION OF AEROSOLS

This section deals with the general character of aerosols in California air as indicated by the ACHEX and related measurements. The discussion begins with a review of important physical properties of aerosols sampled in urban and nonurban sites. Then, several aspects of the chemical properties of airborne particles are summarized. Completing the section is a brief discussion of the aerosol background.

A. PHYSICAL PROPERTIES

From the standpoint of the present regulatory structure for air pollution, the physical properties of suspended particles of greatest interest include the total mass concentration, measured in $\mu\text{g}/\text{m}^3$ with a resolution of a 24-hour averaged value, and the visibility, which depends on the particle size concentration distribution as well as the index of refraction of the airborne material.

The monitoring and surveillance of aerosols in the past have relied on the high volume filter sampler and the use of a continuous device measuring qualitatively the coefficient of stain on a paper tape filter. Future activity undoubtedly will make use of filter-collected aerosols for continuity of the long-term data base as well as for chemical analysis of samples. However, it is expected that on-line, continuous measurement instruments also will be implemented that will replace the paper tape (COH) device presently used.

1. MASS CONCENTRATION

Extensive measurements of mass concentration by hi-vol samplers were made in the ACHEX simultaneously with two-hour filter measurements of total mass. The exposure to aerosols in different locations is illustrated in the data tabulated in Tables 3-1 and 3-2. These data indicate that the South Coast Basin was the area with heaviest particulate pollution, with a gradation of aerosol concentration increasing toward the east. Individuals will experience exposure as high as $200 \mu\text{g}/\text{m}^3$ on a 24-hour basis, with a range of much higher levels on two-hour intervals during the day.

SC524.25FR

TABLE 3-1

SUMMARY OF RESULTS FOR AEROSOL MASS CONCENTRATION BY FILTER COLLECTION IN THE SOUTH COAST AIR BASIN DURING THE PERIOD JULY - OCTOBER 1972 AND 1973. (DATA GIVEN FOR TOTAL FILTERS IN $\mu\text{g}/\text{m}^3$ AS AVERAGE OVER SAMPLES TAKEN; NUMBERS IN PARENTHESES REFER TO RANGE AT A GIVEN SITE.)

	No. of Samples For Total Mass 24 hr. 2 hr.	Total		Sulfate		Nitrate		Lead		Non-Carbonates	
		24 hr.	2 hr.	24 hr.	2 hr.	24 hr.	2 hr.	24 hr.	2 hr.	24 hr.	2 hr.
A. West/Coastal											
Dominguez Hills	2	18	113 (46.7-213)	3.64	19.66 (1.51-50.3)	4.11	9.43 (2.69-27.3)	2.42	2.81 (.897-12.5)	--	11.5 (3.6-34.4)
Harbor Freeway	2	23	94 (29.5-175)	5.8	-(*)	6.3	-(*)	6.3	-(*)	--	27.2 (16.4-39.2)
B. Central											
Pasadena	8	66	77.2 (54-117)	6.43 (2.9-11)	4.11 (0.46-9.42)	6.29 (3.5-7.2)	--	1.5 (0.8-2.0)	0.959 (.31-1.67)	--	26.3 (22.9-30.9)
West Covina	5	35	181 (123-241)	20.4 (6.48-32.1)	21.4 (3.38-69.5)	8.98 (6.8-12.0)	18.3 (6.0-50.2)	2.84 (1.72-3.75)	3.71 (1.7-7.63)	--	17.2 (5.87-38.6)
C. Eastern											
Pomona	7	76	137 (87-180)	10.3 (4.4-19)	52.5 (22.33-51.8)	15.1 (4.81-36.4)	21.6 (9.15-64.0)	2.1 (1.7-2.9)	2.54 (1.4-3.28)	--	31.1 (13.5-39.8)
Riverside/ Rubidoux	12	68	148 (55-284)	8.3 (1.96-21.2)	17.0 (0.99-48.2)	19.2 (6.9-42.4)	50.2 (8.29-247)	1.47 (.64-2.37)	1.64 (.37-3.32)	--	32.0 (18.8-58.4)

* 1972 Only

† Silver membrane filters used

SC524.25FR

TABLE 3-2

SUMMARY OF RESULTS FOR AEROSOL MASS CONCENTRATION BY FILTER COLLECTION AND ANALYSIS AT SEVERAL SITES DURING THE PERIOD JULY - NOVEMBER 1972. (DATA GIVEN IN $\mu\text{g}/\text{m}^3$ AS AVERAGE OVER SAMPLE PERIOD; NUMBERS IN PARENTHESES REFER TO RANGE AT A GIVEN SITE.)

Site	# of Samples Hi-Vol	Total		Sulfate		Nitrate		Lead	
		24 hr.	2 hr.	24 hr.	2 hr.	24 hr.	2 hr.	24 hr.	2 hr.
A. San Francisco Bay Area									
San Jose	10	95.8 (71.9-122)	72.4 (33.2-158)	4.3 (1.0-16.6)	1.4 (.3-4.2)	6.55 (1.58-12.3)	---	1.93 (.97-3.35)	2.22 (.38-7.35)
Richmond/ San Pablo	2	75.4	41.2 (8.83-134)	3.6	---	1.20	---	0.143	---
SFO Airport	1	61.6	---	2.2	---	5.63	---	1.53	---
B. Central Valley									
Fresno	2	153	130 (70.6-170)	3.6	3.8 (1.49-15.9)	7.67	N.D. (ESCA)	.876	1.01 (.46-2.66)
C. Non-Urban									
Pt. Arguello (marine)	1	185	148.2	6.5	---	0.985	---	.029	---
Goldstone (desert)	1	42.4	23.8 (6.9-42.3)	1.2	---	1.5	---	0.074	0.083 (0.018-0.156)
Hunter- Liggett	1	64.0	---	2.9	---	2.72	---	0.118	---

SC524.25FR

Generally a substantial portion of the aerosol sampled is in the sub-micron fraction. The distribution of mass is illustrated for several cases studied with the impactor data in Figure 3-1. In urban locations, approximately 30% by mass of the aerosol is concentrated below 0.5 μm diameter.

A comparison of 24-hour average high volume filter data with the sum of two-hour average total filter and after filter data are given in Figure 3-2. Here there is a systematic correlation between the three parameters. Empirically the hi-vol mass is related to the total filter and after mass by the following correlations:

$$\text{Total filter } (\mu\text{g}/\text{m}^3) = 0.87 \text{ Hi-vol mass conc. } (\mu\text{g}/\text{m}^3) \quad (3.1)$$

$$\text{After filter conc. } (D_p < 0.5 \mu\text{m}) (\mu\text{g}/\text{m}^3) = 0.28 \text{ Hi-vol mass conc. } (\mu\text{g}/\text{m}^3) \quad (3.2)$$

2. PARTICLE SIZE DISTRIBUTIONS

The data from the continuous-reading instrumentation represent the most comprehensive set of results obtained to date in any study of this kind. The initial analysis by the University of Minnesota staff has noted a wide range of aerosol behavior, depending on the location of sampling and the local sources or atmospheric chemistry. Examination of the aerosol data has been made in terms of the number-particle size distribution and its integral moments. In particular, the former is defined in terms of the distribution function

$$\frac{dN}{dD_p} = n(D_p),$$

which is the number of particles per unit volume in the size range D_p and $D_p + \Delta D_p$. The moments of the distribution function of interest are

$$\text{Total number concentration} \quad N = \int n(D_p) dD_p$$

$$\text{Surface concentration} \quad S = \pi \int D_p^2 n(D_p) dD_p$$

$$\text{Volume concentration} \quad V = \frac{\pi}{6} \int D_p^3 n(D_p) dD_p$$

SC524.25FR

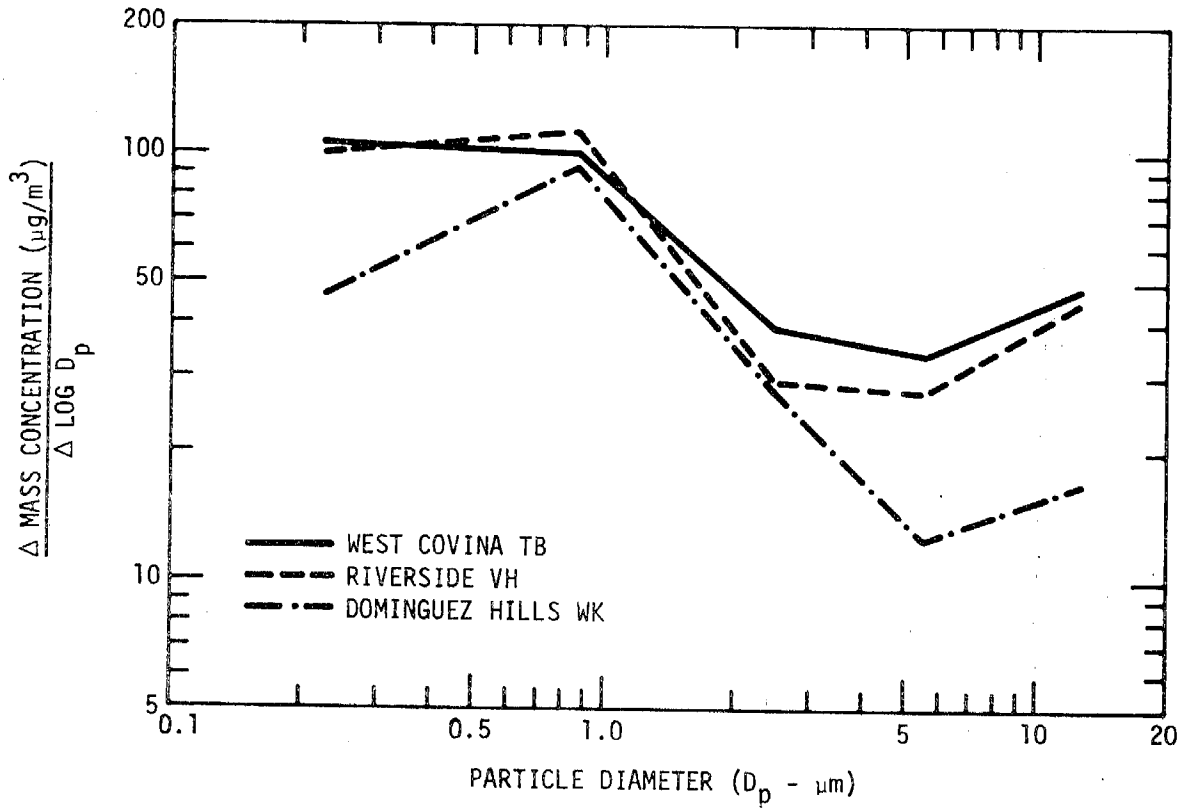


Figure 3-1. Aerosol Mass Distributions vs. Particle Size

SC524.25FR

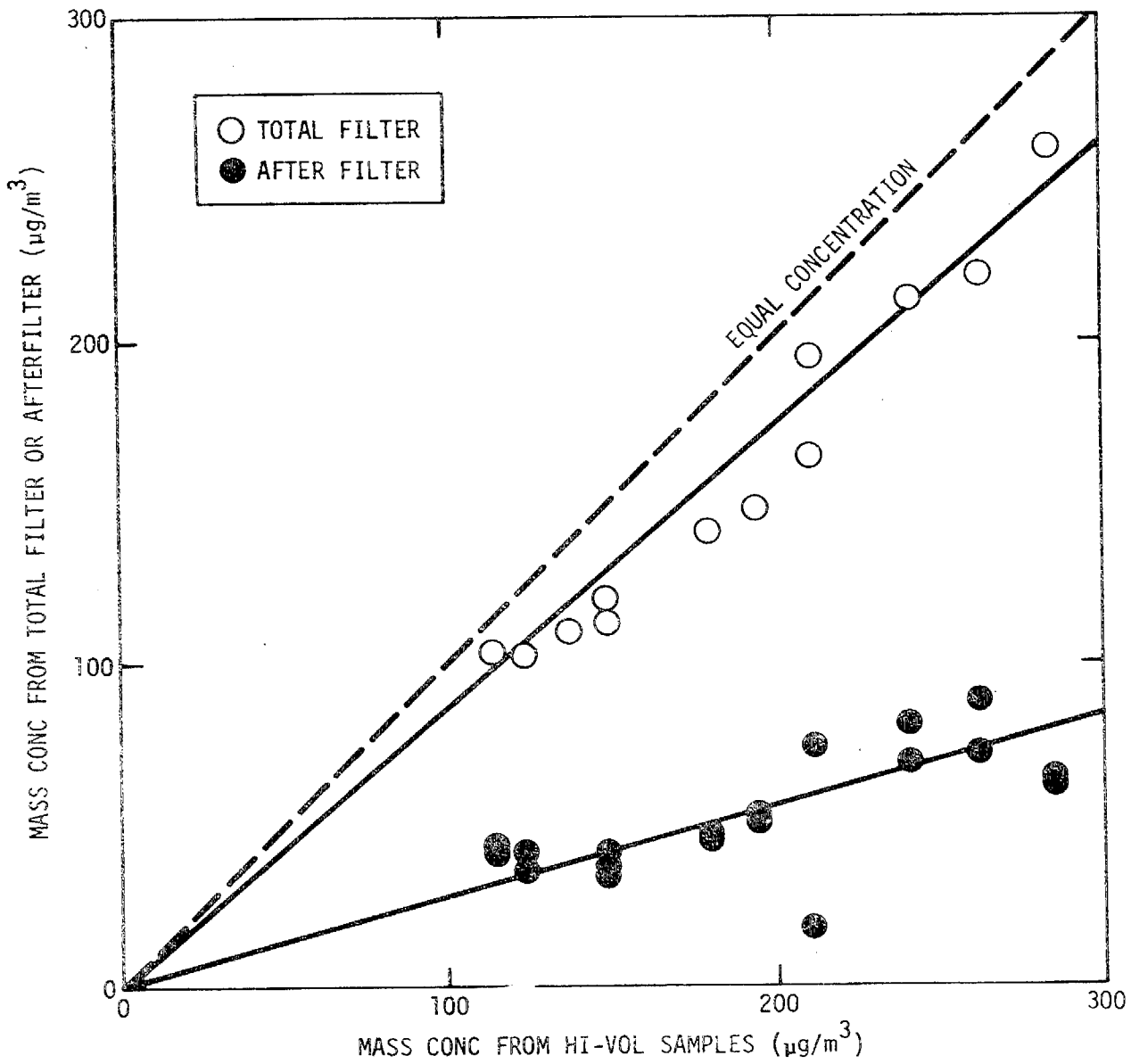


Figure 3-2. Total Filter and Afterfilter Mass vs. Hi-Vol Mass

SC524.25FR

The notation for the particle size ranges of interest is as follows:

- N Concentration (second letter or number denotes particle size range: T = total, 3- = < 1 μm , 2- = < 0.1 μm , 3 = 0.1 to 1 μm , 4 = 1 to 10 μm , 5 = 10 to 38 μm)
- S Surface (second letter or number denotes particle size range: T = total, 3- = < 1 μm , 2- = < 0.1 μm , 3 = 0.1 to 1 μm , 4 = 1 to 10 μm , 5 = 10 to 38 μm)
- V Volume (second letter or number denotes particle size range: T = total, 3- = < 1 μm , 2- = < 0.0 μm , 3 = 0.1 to 1 μm , 4 = 1 to 10 μm , 5 = 10 to 38 μm).

The aerosol physical properties that have been examined in any detail so far stem from the measurements primarily coming from the mobile laboratory. Typical data taken during the study are shown in Table 3-3. These results cover a selected list of test cases reflecting different conditions at the sites where the mobile laboratory was located during the 1972 program. Similar results were obtained in 1973. These observations range over a wide variety of meteorological and aerometric conditions. The b_{scat} range covered is from $0.35 \times 10^{-4} \text{ m}^{-1}$ to $15.9 \times 10^{-4} \text{ m}^{-1}$. The lowest b_{scat} was in Point Arguello, with the highest in Pomona. The Aitken nuclei concentration measured from very low values, ~ 50 particles/cm³ in Goldstone, to $> 2 \times 10^6$ particles/cm³ near the Harbor Freeway.

Various parameters expressing surface concentration and volume concentration (i.e., the second and third moments of the number size distribution function) also are tabulated.

The differences between size distributions from various conditions, such as receptor sites or source-dominated sites, can be illustrated well by considering various moments of the size distribution function. For example, the number distribution of particles is shown in Figure 3-3. Several distribution functions are shown in this figure. On the ordinate is plotted the parameter dN/dD_p . This corresponds to the number of particles per unit volume in a size range between D_p and $D_p + dD_p$. On the abscissa is the diameter D_p , given in μm . From the distribution functions plotted in this way, several characteristic distribution functions have been chosen. One was from Pomona, during the time when the b_{scat} value was maximum, on October 24, 1972. Another

SC524.25FR

distribution function was chosen for later in that day, when b_{scat} was considerably reduced.

Three background size distributions are shown: one from Goldstone, one from Point Arguello, and one from Hunter-Liggett. The Point Arguello sample is of particular interest, because this was taken under conditions of a strong contribution of sea spray aerosol to the large-particle fraction. Also shown is a size distribution from the Harbor Freeway indicating a motor vehicle source dominated aerosol, which shows a large number of particles in the range $< 0.1 \mu\text{m}$ in diameter.

Plotted as the number-size distribution in Figure 3-3, the number distributions are remarkably similar in their general features, except in the region below $\sim 0.5 \mu\text{m}$ in diameter. The upper size range, from $5 \mu\text{m}$ to $\sim 30 \mu\text{m}$ in diameter, indicates a strong overlap between all of the spectra shown for illustration. The lower extreme of the spectra, the highest particle concentrations achieved in the region $< 0.10 \mu\text{m}$ in diameter are associated with the fresh combustion aerosol coming from off the motor vehicles at the Harbor Freeway.

At Pomona, the concentration of sub-micron particles is somewhat lower than for fresh combustion aerosol concentrations in the two time periods considered. There is a rather interesting distinction in the range between 0.1 and $1.0 \mu\text{m}$ diameter. This undoubtedly is related to the very high b_{scat} observed at that time. The distribution functions from Goldstone, Point Arguello, and Hunter-Liggett show a marked reduction in small particles in the sub-micron range, compared with the urban aerosols. This is a characteristic of aerosol distributions measured from nonurban or remote sites, where the tiny particles have essentially been removed by collision processes or by growth processes, to accumulate in the larger particle range $> 0.5 \mu\text{m}$ diameter. The general shape of the averaged size distribution follows a power law, with a decrease of D_p^{-4} in the middle ranges of particle size; however, in the extreme ranges of large particles, the size distribution tends to drop off with a sharper slope, one that can be drawn through the data is a $-19/4$ slope above $5 \mu\text{m}$ diameter. In the extreme range of smaller sizes, the individual spectra show much greater scatter, associated with

SC524.25FR

either growth processes or combustion sources. However, illustrative cases of aged aerosol indicate a $D_p^{-5/2}$ below $\sim 0.1 \mu\text{m}$ diameter.

The moments of the size distribution, either the second moment (the surface distribution) or the third moment (the volume distribution), tend to display more detailed features of the size spectra than the number distribution in Figure 3-3. These moments are particularly useful for examining the midsize range, where the D_p^{-4} power law fit may be somewhat misleading. The second and third moments of the distribution functions in Figure 3-3 are shown in Figures 3-4 and 3-5. In Figure 3-4 are two sets of data, one representing observed conditions of heavy haze at Pomona on October 24, 1972. A second case, later in the same day, is shown for comparison. In this episode, heavy haze was observed in the morning, which was accompanied later in the day by a significant buildup in oxidant. By afternoon, the photochemical activity became lighter, and the aerosols were considerably lower in concentration. In both cases, it is readily seen that the sub-micron portion of the volume and surface spectra are strongly contributing to the physical properties of the haze; the principal maximum in the surface and volume distributions is in the optical scattering range between 0.1 and $1.0 \mu\text{m}$ diameter. There are very major differences in b_{scat} between morning and evening, accompanying the concentration changes. The influence of particle aging is suggested in that there is a dramatic decrease in particle volume in the $0.3 \mu\text{m}$ diameter region from morning to evening, but a "background" peak level remains in volume concentration at $\sim 6 \mu\text{m}$.

The contrast between airborne particles from anthropogenic sources like the automobile and the aerosol background is illustrated in Figure 3-5. Here, a surface and volume distribution for a case strongly influenced by motor vehicle exhaust at the Harbor Freeway is compared with background samples at Point Arguello, Goldstone, and Hunter-Liggett. The anthropogenic contribution from combustion processes involving motor vehicles strongly influences the sub-micron range of particles, particularly below $0.1 \mu\text{m}$ diameter, as expected from previous work. The distinction between the background samples and material samples near sources and at receptor sites like Pomona is very apparent in that the urban aerosol is principally different

SC524.25FR

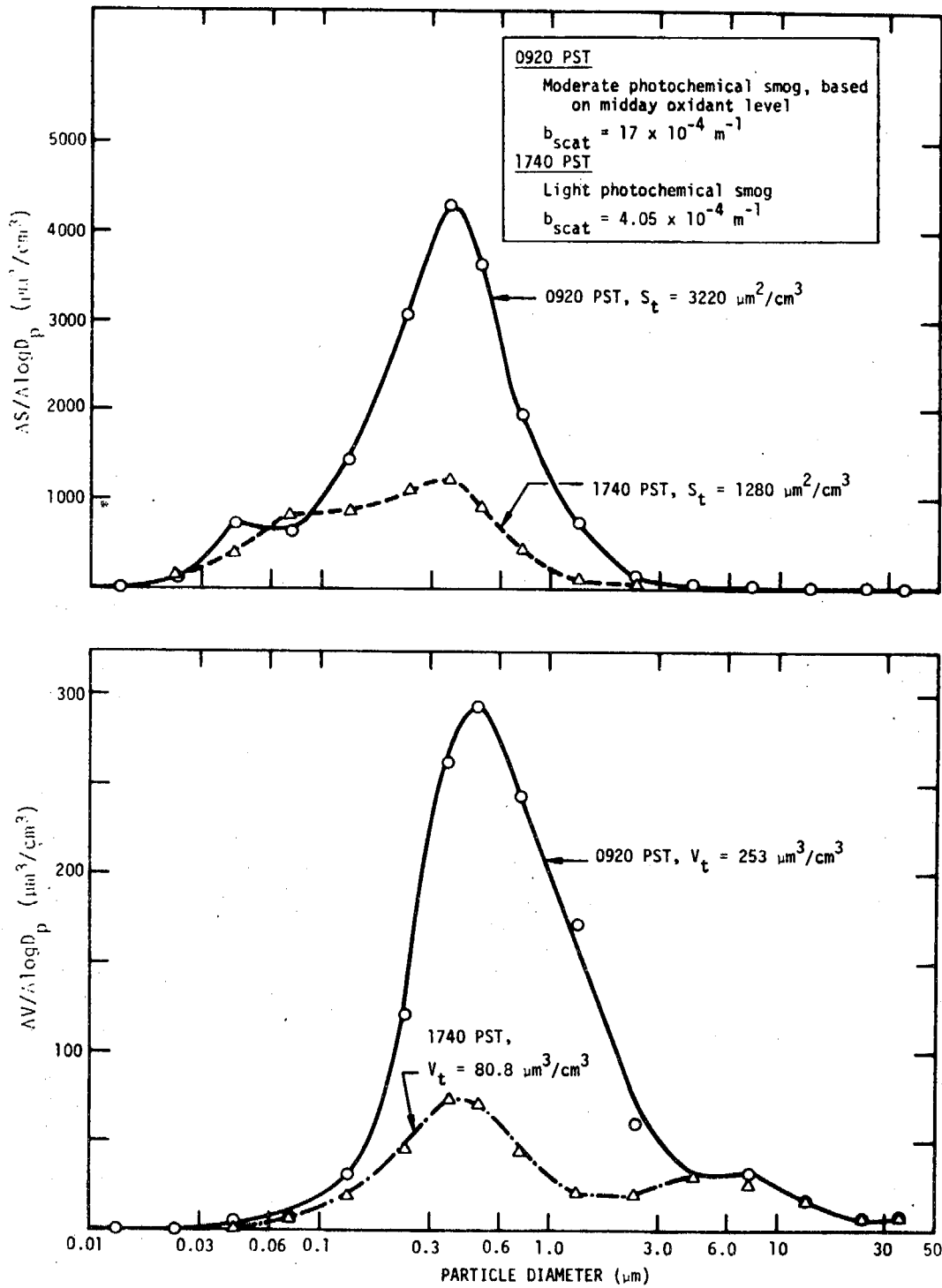


Figure 3-4. Surface and Volume Distributions Taken at Pomona on October 24, 1972

SC524.25FR

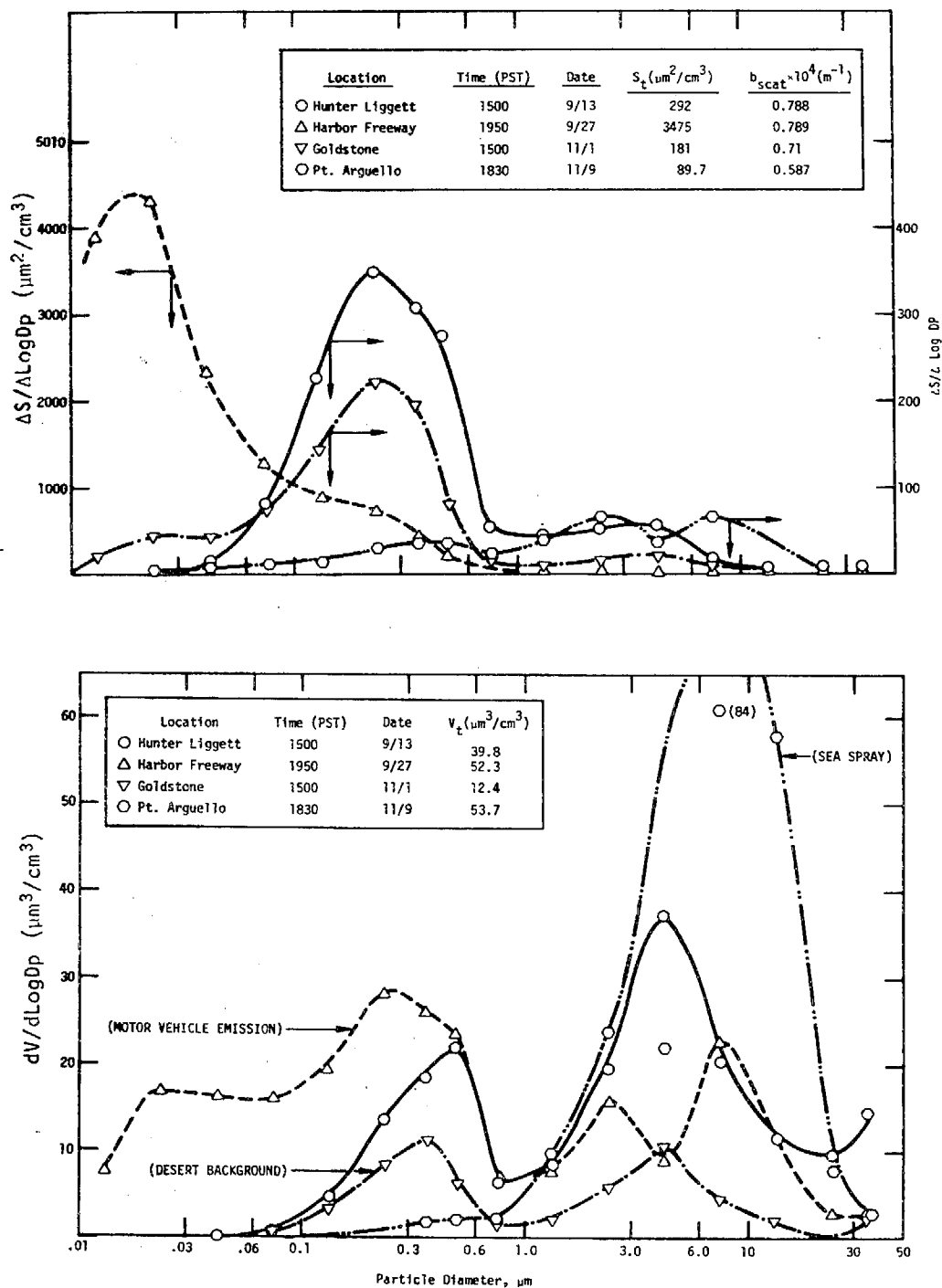


Figure 3-5. Comparison of Surface and Volume Distributions for Background and Motor Vehicle Source Enriched (Near Harbor Freeway) Sites

SC524.25FR

In the sub-micron range. The dramatic local influence of the sea on the large particle fraction under light to moderate winds also can be seen in the comparison between the marine sample at Point Arguello and the other two background locations. The minimum in volume distribution at $\sim 1.0 \mu\text{m}$ diameter again appears in these days, as in many previous observations elsewhere.

The significance of aerosol growth during the morning as the smog chemistry evolves is shown in Figure 3-6. Two volume-size spectra are shown for averaged data at Pomona in August, 1973. A comparison is made between the volume distribution in early morning and in mid-morning during a period of moderate smog. It is illustrated well in these data that the major change in evolution of smog aerosol takes place in the $0.1 \mu\text{m}$ to $1.0 \mu\text{m}$ diameter range. As will be shown below, this is precisely the particle size range that influences light scattering most strongly.

The typical background desert condition based on the Goldstone data was a total volume on the order of 8 to $13 \mu\text{m}^3/\text{cm}^3$ with the amount below $1 \mu\text{m}$ at 3 - $4 \mu\text{m}^3/\text{cm}^3$. The nuclei count was a few thousand. In contrast with other background data obtained at Fort Collins, Colorado, the volume of aerosol greater than $1 \mu\text{m}$ is much less, being only 60 to 70% of the total volume. The occurrence of rain just before the sampling period makes it impossible to claim that typical background conditions over a long period of time were measured. Although large amounts of windblown dust had been expected at Goldstone, no evidence of such dust was recorded. The maximum volume greater than $1 \mu\text{m}$ was about $12 \mu\text{m}^3/\text{cm}^3$.

When the wind was from the north at Goldstone, the lowest volumes ever recorded with the Minnesota Aerosol Analyzer System were obtained. The average total volume over a three-hour period was $1.85 \mu\text{m}^3/\text{cm}^3$. The low volume is probably due to the rain which fell at Goldstone prior to the sampling period. The rain does not explain the low nuclei counts (less than 100) which were found.

At the end of the sampling period an incursion of aged smog aerosol from the South Coast Basin of California was observed. This episode, when contrasted with the earlier, exceptionally clean conditions, has provided valuable

SC524.25FR

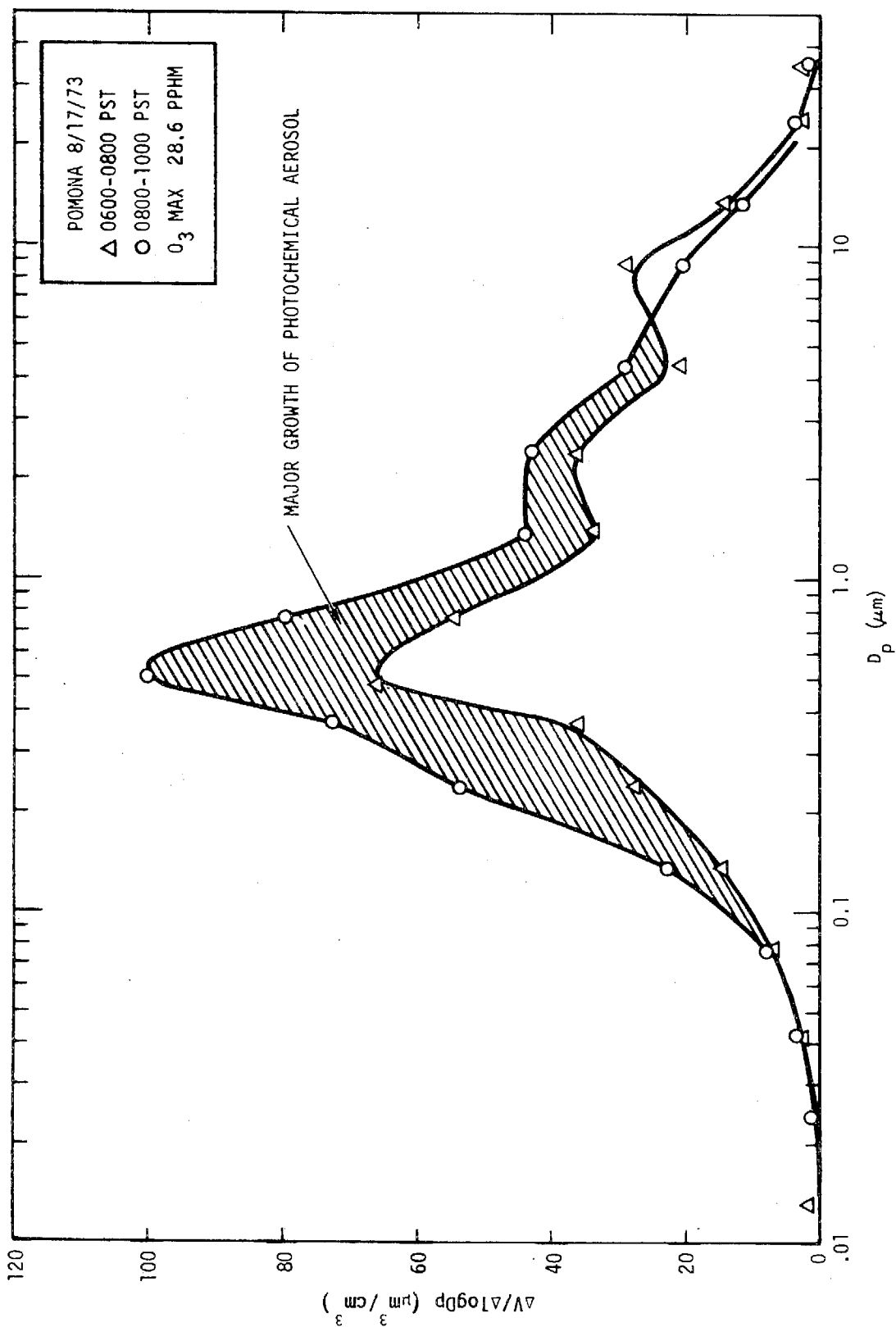


Figure 3-6. Evolution of the Volume Distribution of Smog Aerosol Taken at Pomona, Ca. 8/17/73

SC524.25FR

insights into the characteristics of aged air pollution aerosols. A total volume of $43.1 \mu\text{m}^3/\text{cm}^3$, with $31.5 \mu\text{m}^3/\text{cm}^3$ smaller than $1 \mu\text{m}$, represents aerosol concentrations of the same order of magnitude as those measured in the South Coast Basin on days of light smog.

Most of the data from Hunter-Liggett suggested that the results were affected most of the time by incursions of aged, diluted air pollution, either from sparse local sources or by pollution from the San Joaquin Valley. Aitken nuclei counts were on the order of 2,000 per cm^3 , and the volume size distribution was typically bimodal, with $10 \mu\text{m}^3/\text{cm}^3$ smaller than $1 \mu\text{m}$ and $15 \mu\text{m}^3/\text{cm}^3$ larger than $1 \mu\text{m}$. Surprisingly, the ozone concentration reached 0.1 ppm, indicating that there was some photochemical activity. The sodium-to-mass ratio was about the same as at San Pablo, being higher than the more inland sites but not as high as the seaside sites.

At Point Arguello clean maritime air was sampled. During one period of heavy surf, a high concentration of salt aerosol was sampled. The distribution was unimodal, with the volume distribution mode at $10 \mu\text{m}$. The total volume concentration was $332 \mu\text{m}^3/\text{cm}^3$ with only 3% of the volume smaller than $1 \mu\text{m}$. Under conditions of low surf, the total volume was $7 \mu\text{m}^3/\text{cm}^3$ with 10% smaller than $1 \mu\text{m}$. Aitken count for the maritime air was relatively constant at about $100/\text{cm}^3$.

Size distributions measured with a portable electrical aerosol analyzer and optical counter at King River, Big Sur, Morro Bay and Point Reyes typically gave sub-micron aerosol volumes of 1 to $10 \mu\text{m}^3/\text{cm}^3$ and total volumes of 10 to $20 \mu\text{m}^3/\text{cm}^3$.

Measurements made with the portable system at Santa Monica on September 21, 1972, gave sub-micron aerosol volumes that decreased from 69 early in the morning to $10.6 \mu\text{m}^3/\text{cm}^3$ in the evening, even though the wind was from the sea during this whole time. This indicates that rather high concentrations of sub-micron aerosol, presumably from air pollution episodes over the land can be blown out to sea and return.

From measurements of the size distribution, concentration, and chemistry of aerosols sampled during a 24-hour intensive period from 2100 on September 19 to 2100 on September 20, 1972, alongside the Harbor Freeway in Los Angeles, it

SC524.25FR

is possible to draw a number of conclusions regarding the nature of freeway aerosols⁽⁴⁾:

- 1) The fresh aerosol sampled at a distance of 70M from the freeway is mostly below $0.15 \mu\text{m}$ in diameter. The direct freeway contribution was $17.1 \mu\text{m}^3/\text{cm}^3$ during the morning rush hour. The nuclei count was between two and three million particles/ cm^3 and the surface area for the fresh aerosol was $2870 \mu\text{m}^2/\text{cm}^3$.
- 2) Calculation of particle density from the ratios of the filter-measured mass concentration to the volume concentration from the in situ instruments was a strong function of relative humidity. Indicated densities ranged from approximately 1 at 100% to 2.1 for the dry particles.
- 3) The direct freeway contribution accounts for 99.4% of the aerosol number concentration during the rush hour. Because of its high number concentration, the aerosol coagulates rapidly, by both monodisperse and heterodisperse coagulation.

In Figure 3-7 the volume distribution of fresh aerosol coming from the freeway during the morning rush hour is compared with a number of distributions from other places.

Fresh combustion aerosol from aircraft taking off from the San Francisco Airport was found to be similar to the freeway aerosol, except that the concentration was lower and the aerosol came in bursts.

The light to medium pollution aerosols sampled at Fresno and Pomona were found to be similar in chemistry and size distribution to those reported previously in the 1969 Pasadena study⁽⁵⁾.

The observed shape of the aerosol particle size distribution was affected by a mismatch between the two optical particle counters, one of which was outside the laboratory and the other inside. The mismatch was a function of the relative humidity and the temperature difference between the inside and outside, and is discussed further in Appendix A. The data presented in this report are as recorded, and do not include a correction for this effect.

SC524.25FR

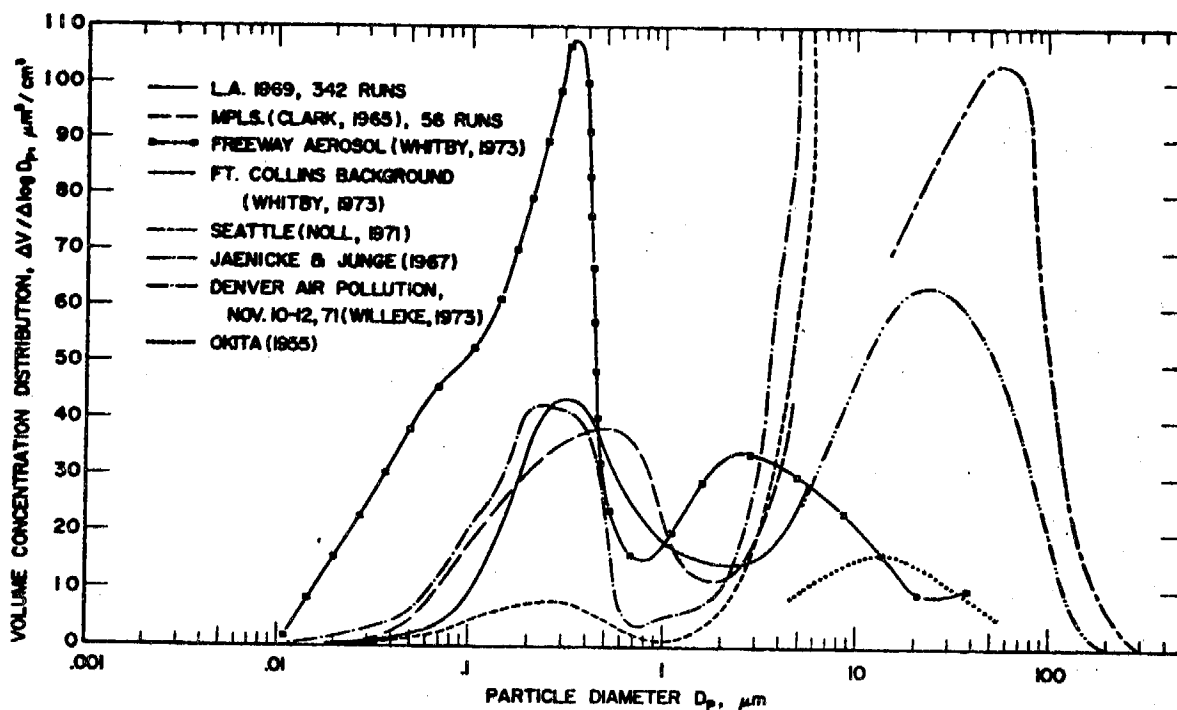


Figure 3-7. Comparisons of the Volume Distributions of Atmospheric Aerosols Measured in Different Urban and Nonurban Locations. Note the Variation in the Relative Proportions of Aerosol in the Sub-micron Mode. Note especially the Large Volume of Sub-micron Aerosol Alongside the Harbor Freeway

SC524.25FR

3. PARTICLE AGING

The aging processes of aerosols in the atmosphere are listed in Table 3-4. Here, the cases are classified in terms of processes that transfer particles from one size range to another in the spectrum, but do not remove mass from an elemental volume, and/or processes that physically transfer particles from parcels of air. In California during the summer and fall, rain cloud processes exert a limited influence on aerosol aging. Thus, apparent regularities in the size spectra should be controlled by "dry" mechanisms. Evaluation by Hidy⁽⁶⁾ suggests that, near the ground, atmospheric diffusion is important for the behavior of particles. Even in the absence of active particle growth processes near the ground, changes in the size spectrum will be influenced strongly by thermal coagulation in the range $D_p \leq 0.1 \mu\text{m}$, while collision processes are weaker in the range of larger particles. The extreme range of large particles must be strongly cut off by sedimentation.

The sample spectra illustrated in Figure 3-3 display a wide range of behavior, but they are very similar in the particle size range beyond $D_p \approx 0.5$ to $1 \mu\text{m}$. There is a precedent for such regularities, derived in theoretical models of Friedlander⁽⁷⁾ and later reviewed by Hidy⁽⁸⁾. A quasi-steady state, consisting of a balance between the sources feeding the lower end of the size spectrum with tiny particles and the sedimentation losses at the upper end of the spectrum, can truncate the size spectrum above $\sim 5 \mu\text{m}$ diameter. Friedlander has estimated that the sedimentation subrange should decrease in concentration as $D_p^{-\alpha}$, where $\alpha = 19/4$, for an aerosol in a quasi-steady state. Interestingly enough, this power law dependence appears to be consistent with the data in Figure 3-3, except possibly for the Point Arguello case, which was strongly influenced by fresh sea spray aerosol.

In another calculation, involving the constraints of the quasi-steady state and self preservation of size distributions, Hidy⁽⁶⁾ reviewed Schwarz's unpublished calculation and suggested that the sedimentation subrange should exist, and would follow a power law in the upper extreme of the size spectrum with $\alpha \geq 4$, depending on the distribution of volume concentration with height. This model estimates $\alpha = 4$, the Junge subrange, of the volume concentration is

SC524.25FR

TABLE 3-4

PROCESSES AFFECTING EVOLUTION OF AEROSOLS IN A
UNIT VOLUME OF LOWER ATMOSPHERE

-
1. Growth or change in particles by homogeneous or heterogeneous chemical reactions of gases on the surface of particles.
 2. Change in particles by attachment and adsorption of trace gases and vapors to aerosol particles.
 3. Net change by collision between particles undergoing Brownian motion or differential gravitational settling.
 4. Net change by collision between particles in the presence of turbulence in the suspending gas.
 5. Gain or loss in concentration by diffusion or convection from neighboring air volumes.
 6. Loss by gravitational settling.
 7. Removal at the earth's surface on obstacles by impaction, interception, Brownian motion, and turbulent diffusion.
 8. Loss or modification by rainout in clouds.
 9. Loss by washout under clouds.
-

SC524.25FR

constant with height.

Friedlander⁽⁷⁾ also proposed a coagulation subrange of the spectrum, in the extreme of sub-micron particles. Smoluchowski's model for coagulation predicts a value of $\alpha = 5/2$ in the coagulation subrange. Coagulation should dominate the lower portion of the particle spectrum in a region that is not expected to be strongly influenced by local sources of sub-micron particles, or by growth processes. This is best exemplified by the data at Goldstone. Indeed, there may be an extended range of $\alpha = 5/2$ at this location, as indicated in Figure 3-3. It is interesting that the case in Pomona, late in the day, also displays an extended sub-micron range with $\alpha \approx 5/2$.

4. PARTICLE DENSITY

The particle densities for most sites on which the mobile lab was operated during 1972 have been calculated from the following equation:

$$\rho_p = \frac{MT}{WAA + R220 + R245} \quad (3-3)$$

where ρ_p = particle density, gm/cm³

WAA = volume concentration of aerosol from the Whitby aerosol analyzer, $\mu\text{m}^3/\text{cm}^3$

R220 = volume concentration of aerosol from the Royco 220, $\mu\text{m}^3/\text{cm}^3$

R245 = volume concentration of aerosol from the Royco 245, $\mu\text{m}^3/\text{cm}^3$

MT = mass concentration of aerosol from total filter, $\mu\text{g}/\text{m}^3$

The particle density is a function of relative humidity. Since the temperature inside the mobile lab was usually different from the ambient outside temperature, the data obtained with the different instruments were obtained at different relative humidities.

The total filter sampled aerosol was not at the outside relative humidity (RH). From a heat transfer analysis the temperature of the sample stream

SC524.25FR

can be estimated at the total filter and a RH can be calculated. The mass concentration obtained from the total filter must be treated with caution since the total filter was equilibrated at 45% RH at the AIHL before being weighed. Thus, mass concentrations obtained from the total filter for time periods when the RH was high may be erroneous.

The WAA ionizer was operated with dry compressed air and the clean air was at inside ambient conditions of T and RH. The ratio of clean air to the sample air flow was 14:1. Therefore, the humidity at which the WAA sampled and measured the aerosol size distribution is unknown, but is probably close to that inside the trailer.

The performance of the Royco 220 optical particle counter (OPC), has been discussed in the preliminary report on the aerosol size distribution mismatch (see Appendix C). It is believed that the temperature of the sample stream in the view volume of the OPC was about the same as the inside temperature of the mobile lab.

The Royco 245 OPC was operated outside of the mobile lab. The aerosol was at the outside ambient relative humidity.

The graph in Figure 3-8 of the calculated particle density vs. RH for the several sites suggests that with the exception of Goldstone, the density may be a fairly strong function of RH, and the aerosols in most locations are quite hygroscopic. Furthermore, the dry particle densities of about 2.1 to 2.5 gm/cm³ are reasonable. During recent conversations with Hänel in Germany, he states that he has obtained dry particle densities of 2.1 to 3.5, and thinks that our values are a little low. Because of the uncertain effect of the temperature change between inside and outside of the trailer, it is possible that our densities are perhaps 30% low.

5. LIGHT SCATTERING AND SMOG

It has been known for some time that visibility reduction is primarily a function of light scattering from aerosols in the atmosphere. The principal measure adopted in this study to characterize light scattering is b_{scat} , the extinction coefficient for light scattered by particles.

SC524.25FR

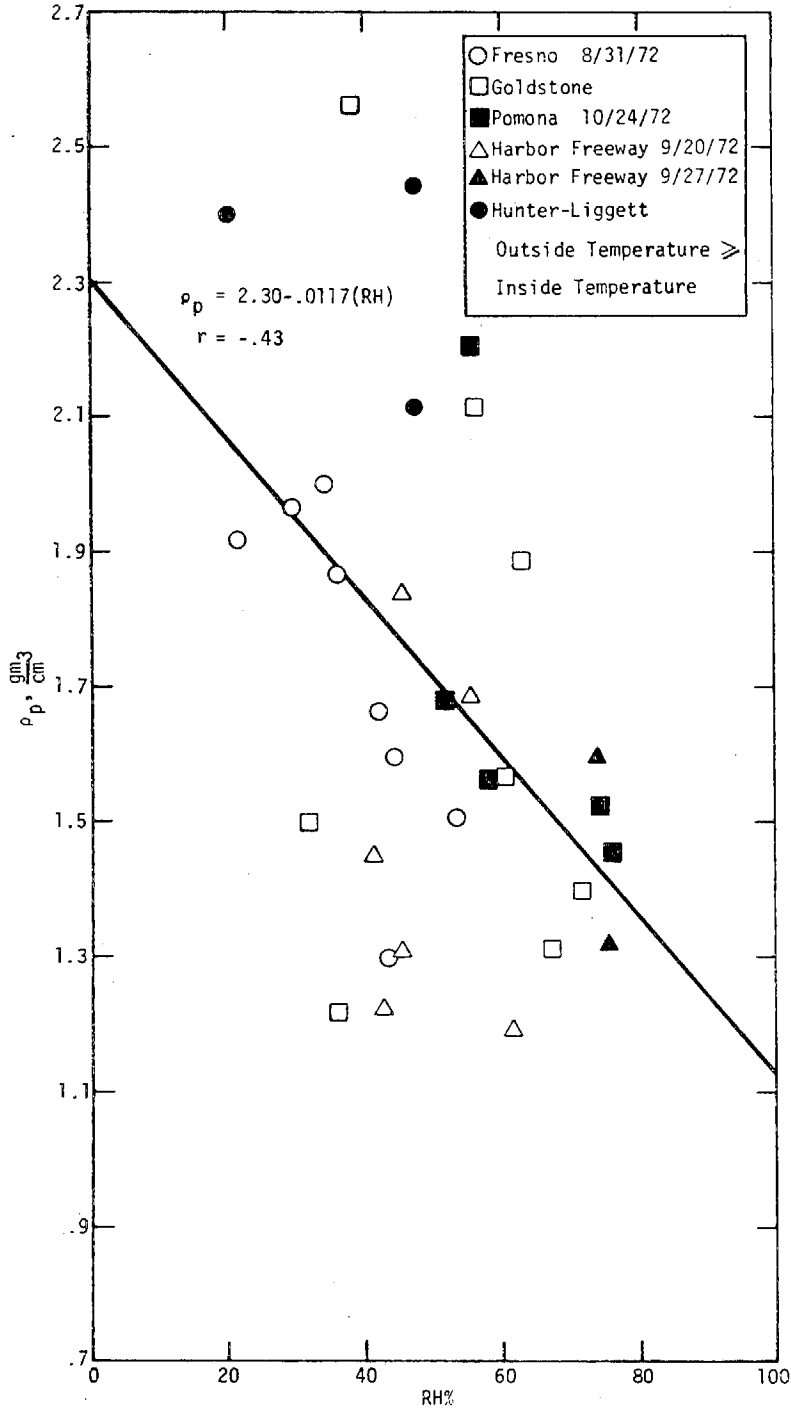


Figure 3-8. Variation in Apparent Particle Density With Relative Humidity

SC524.25FR

The visibility standard of the State of California, applicable whenever the relative humidity is $\leq 70\%$, requires that an observer be able to distinguish a prominent black object viewed against the horizon sky at a distance of ten miles. Physiological research has shown that he will be able to do so when the contrast between the light intensities I_1 , from the direction of the object, and I_2 , from the direction of the unobstructed horizon, exceeds some minimum value:

$$c = (I_2 - I_1)/I_2 \geq c_{\min} \quad (3-4)$$

In a horizontally uniform atmosphere, one can show that

$$c = \exp(-b_{\text{ext}}x), \quad (3-5)$$

where b_{ext} is the atmospheric extinction coefficient and x is the distance to the object. In this situation, the visibility standard can be interpreted as a standard for b_{ext} :

$$b_{\text{ext}} \leq (10 \text{ mi})^{-1} (-\log_e c_{\min}) \quad (3-6)$$

In the Los Angeles atmosphere, nearly all extinction of visible light is due to scattering by aerosols, and the aerosol scattering coefficient, b_{scat} , can be substituted for the extinction coefficient b_{ext} in Equation (3-6). The contrast threshold is often taken to be $c_{\min} = 0.02$, in which case the visibility standard corresponds approximately to an aerosol scattering standard:

$$b_{\text{scat}} \leq 2.5 \times 10^{-4} \text{ m}^{-1} \quad (3-7)$$

Relation of b_{scat} to Mass Concentration

The scattering due to a given mass concentration of aerosol depends on the size, shape, and composition of the aerosol particles. If the particles are uniform, homogeneous spheres of diameter D_p , density ρ , and refractive index m , then the ratio of aerosol scattering coefficient to aerosol mass concentration is given by⁽⁹⁾:

$$\begin{aligned} b_{\text{scat}}/\text{MASS} &= G(D_p) \\ &= (3/2\rho D_p) \int K(\pi D_p/\lambda, m) f(\lambda) d(\lambda), \end{aligned} \quad (3-8)$$

SC524.25FR

where K is the Mie scattering efficiency and $f(\lambda)$ is the normalized wavelength distribution of solar radiation. The function $G(D_p)$ plotted in Figure 3-9 peaks sharply when particle diameters are near the wavelengths of visible light.

Ambient aerosols are broadly distributed with respect to particle size, and $b_{\text{scat}}/\text{MASS}$ for the aerosol is obtained by averaging:

$$b_{\text{scat}}/\text{MASS} = \int G(D_p) \text{mass}(D_p) dD_p,$$

where $G(D_p)$ is the ratio for a monodisperse aerosol, given in Equation (3-8), and $\text{mass}(D_p)$ is the normalized aerosol mass distribution. It is found empirically that this ratio has a fairly narrow distribution for ambient Los Angeles aerosols. The approximate proportionality between b_{scat} and MASS for 60 two-hour samples taken by the mobile van during the 1973 expedition, is illustrated in Figure 3-10. The average $b_{\text{scat}}/\text{MASS}$ for these samples was 0.032, with a standard deviation of 0.009:

$$b_{\text{scat}}/\text{MASS} = 0.032 \pm 0.009. \quad (3-10)$$

For comparison, Charlson *et al.* (10) found a strong mode in the range $b_{\text{scat}}/\text{MASS} = 0.028 \pm 0.034$ for 52 samples taken at Altadena in December 1968.

Expression (3-10) is not a physical law, but simply a statistical statement about the aerosols sampled by the mobile van in 1973. It is not a priori applicable to different locations, different seasons, or different levels of emissions. However, Charlson and his coworkers have accumulated an impressive body of evidence supporting the overall stability for ambient aerosols of the approximate relationship expressed in (3-10), and it has proven useful in applications because of the complexity of the exact relationship between aerosol light scattering and composition.

Relation of b_{scat} to Sub-micron Volume

The theoretical relationship between the light scattering coefficient and particle diameter given in Equation (3-8) also can be recast to give b_{scat} in terms of particle surface concentration or to particle volume concentration. In fact, the light scattering coefficient should be a better indicator of such parameters than of mass concentration, wherein a density

SC524.25FR

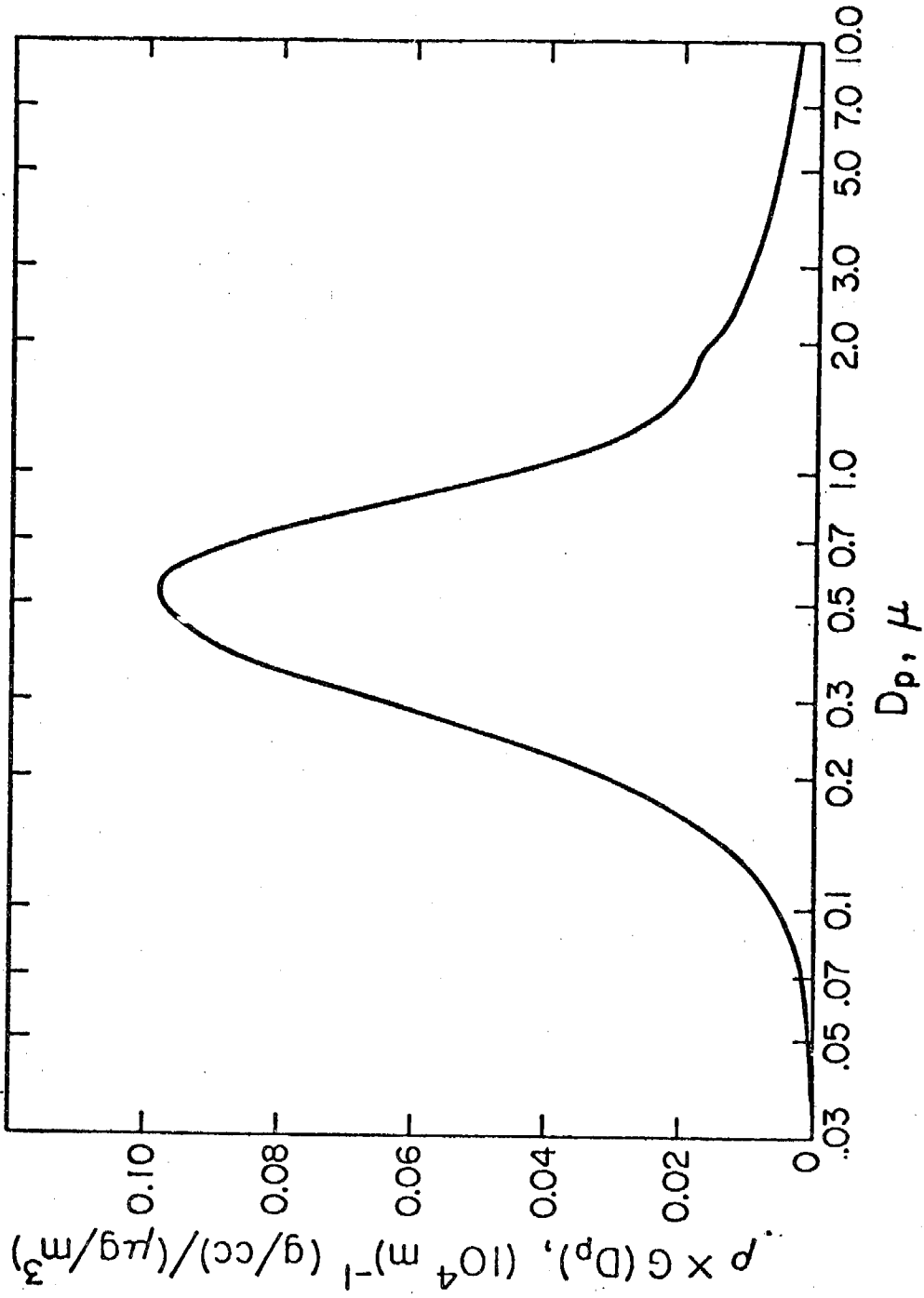


Figure 3-9. Ratio of Light Scattering Coefficient to Mass Concentration for Uniform Spherical Particles of Unit Density, Refractive Index 1.5, and Diameter D_p

SC524.25FR

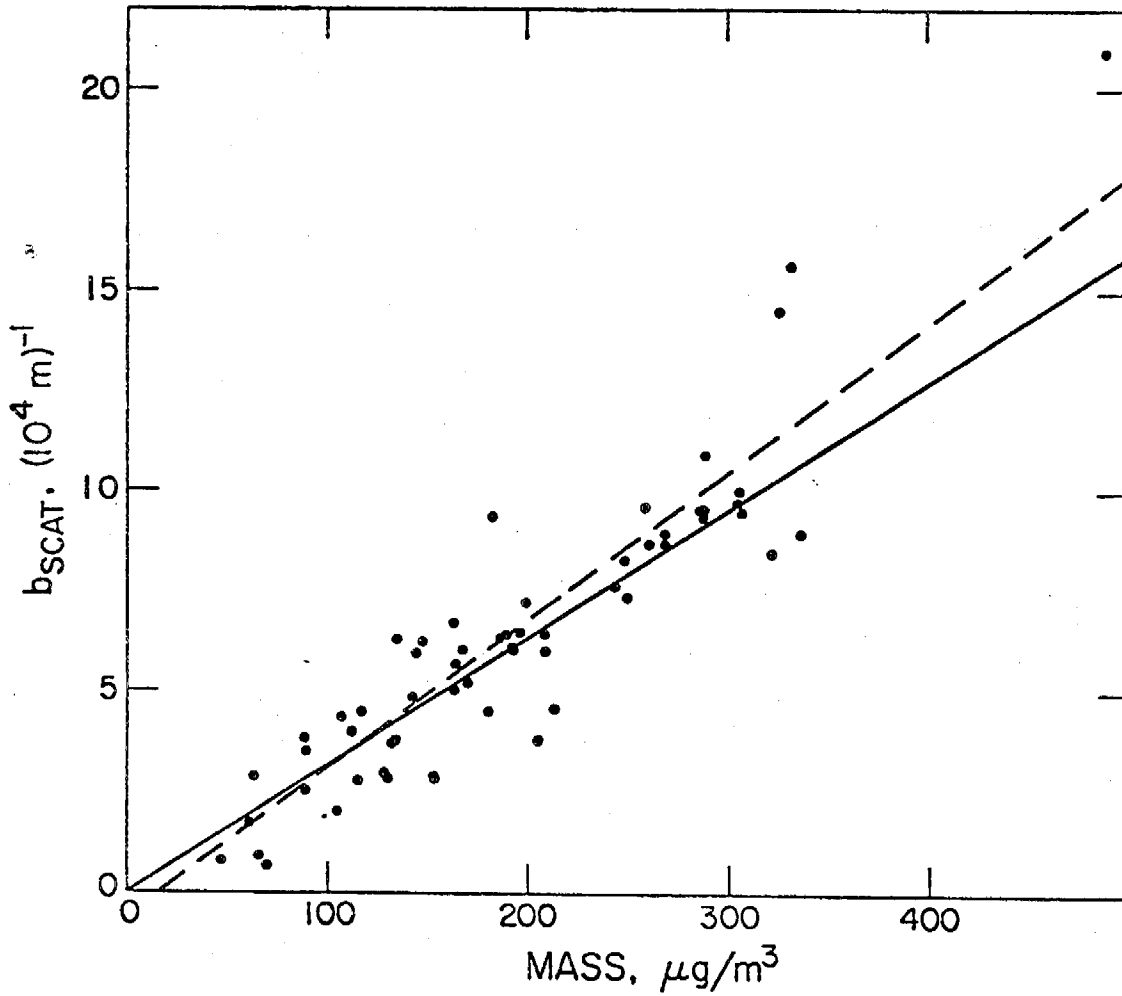


Figure 3-10. Correlation of Light Scattering Coefficient With Aerosol Mass Concentration in 60 Two-Hour Samples at Mobile Van Sites. Solid Line Shows Average Ratio $b_{\text{scat}}/\text{MASS}$. Dashed Line Shows Linear Regression of b_{scat} on Mass.

SC524.25FR

variation provides an added degree of freedom.

Analysis of the 1973 ACHEX data indeed shows that a useful relationship exists between b_{scat} and the particle volume between 0.1 μm and 1.0 μm diameter, as Figure 3-9 might suggest. Shown in Figure 3-11 are correlations between b_{scat} and the total volume, the volume $< 1.0 \mu\text{m}$ and the volume between 0.1 μm and 1.0 μm diameter. The best correlation is found for the last case.

The relation between light scattering, visibility, and the sub-micron aerosol volume was strikingly revealed in a sequence of data obtained on September 25, 1973 at Rubidoux. During this episode, the winds were reversed so that a dry, northeast flow prevented heavily polluted air from moving over the mobile laboratory most of the day. However, late in the afternoon, the wind shifted to blow from the west for a period so that a smog "front" moved over the trailer. When the clean air was present, the visibility at the trailer exceeded 20 km. However, when the polluted air penetrated the area, the visibility decreased to less than 3 km.

The size distributions characterizing the two air masses seen on September 28 are shown in Figure 3-12. The striking difference in particle volume between 0.1 μm and 1.0 μm diameter corresponding to a b_{scat} change of $\sim 3.4 \times 10^{-4} \text{m}^{-1}$ is indicated. At the same time, essentially no change was observed in the volume fraction for particles larger than 1.0 μm diameter.

Using a least squares fit of the two-hour averages for V3 vs. b_{scat} from the 1973 data (daytime only), a high correlation coefficient is obtained ($r = 0.944$); however, from Equation 3-11, it is seen that for vanishing b_{scat} , V3 is still $13.1 \mu\text{m}^3/\text{cm}^3$.

$$V3 = 13.1 + 7.58 \times 10^4 b_{\text{scat}} \quad (3-11)$$

Because of the large intercept, a parabola was fitted to the data and the following equation was obtained:

$$b_{\text{scat}} \times 10^4 = 0.038 + 0.081 V3 + 0.00026 (V3)^2 \quad (3-12)$$

This relation may be more useful than (3-11) to indicate the general correlation of scattering coefficient with aerosol volume. Such an empirical

SC524.25FR

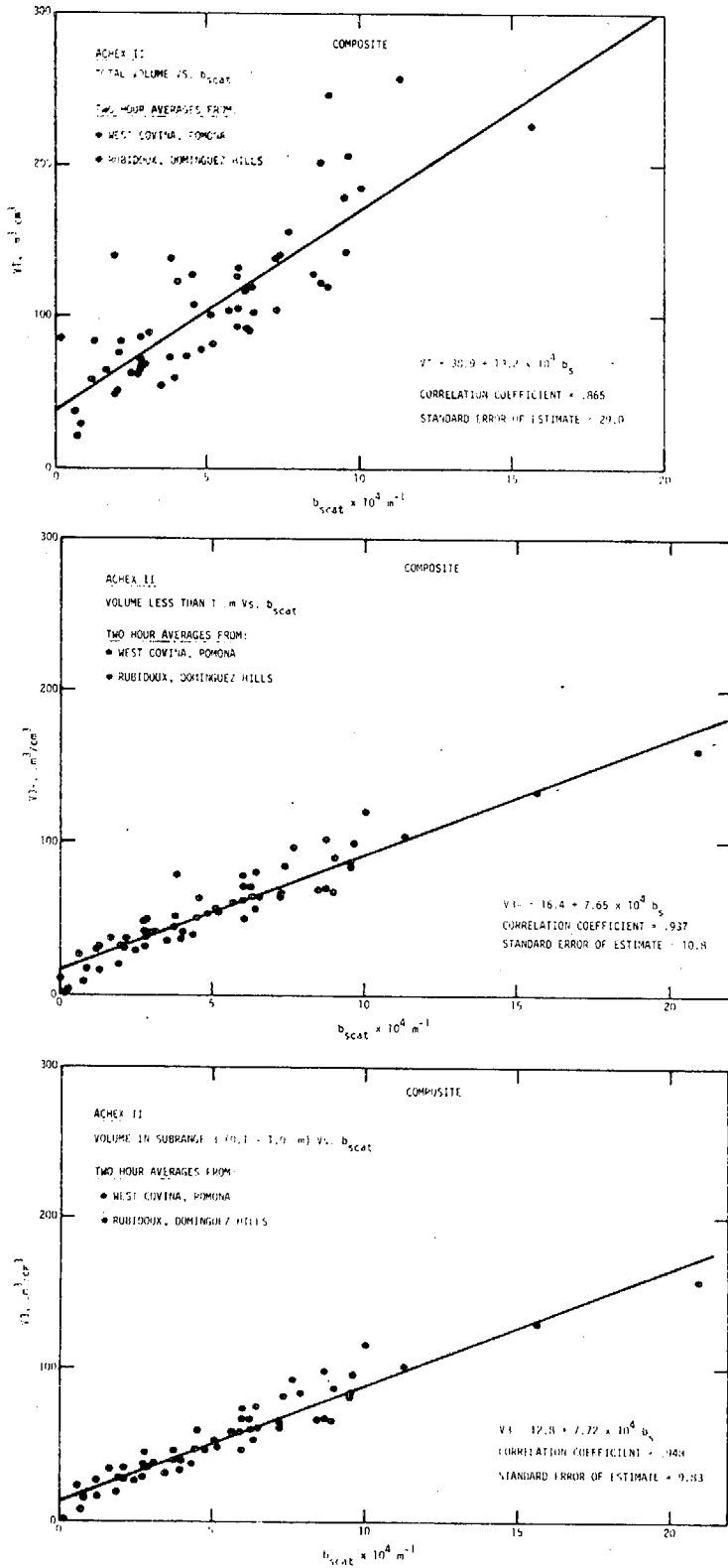


Figure 3-11. Correlations Between b_{scat} and the Aerosol Volume in Different Size Ranges

SC524.25FR

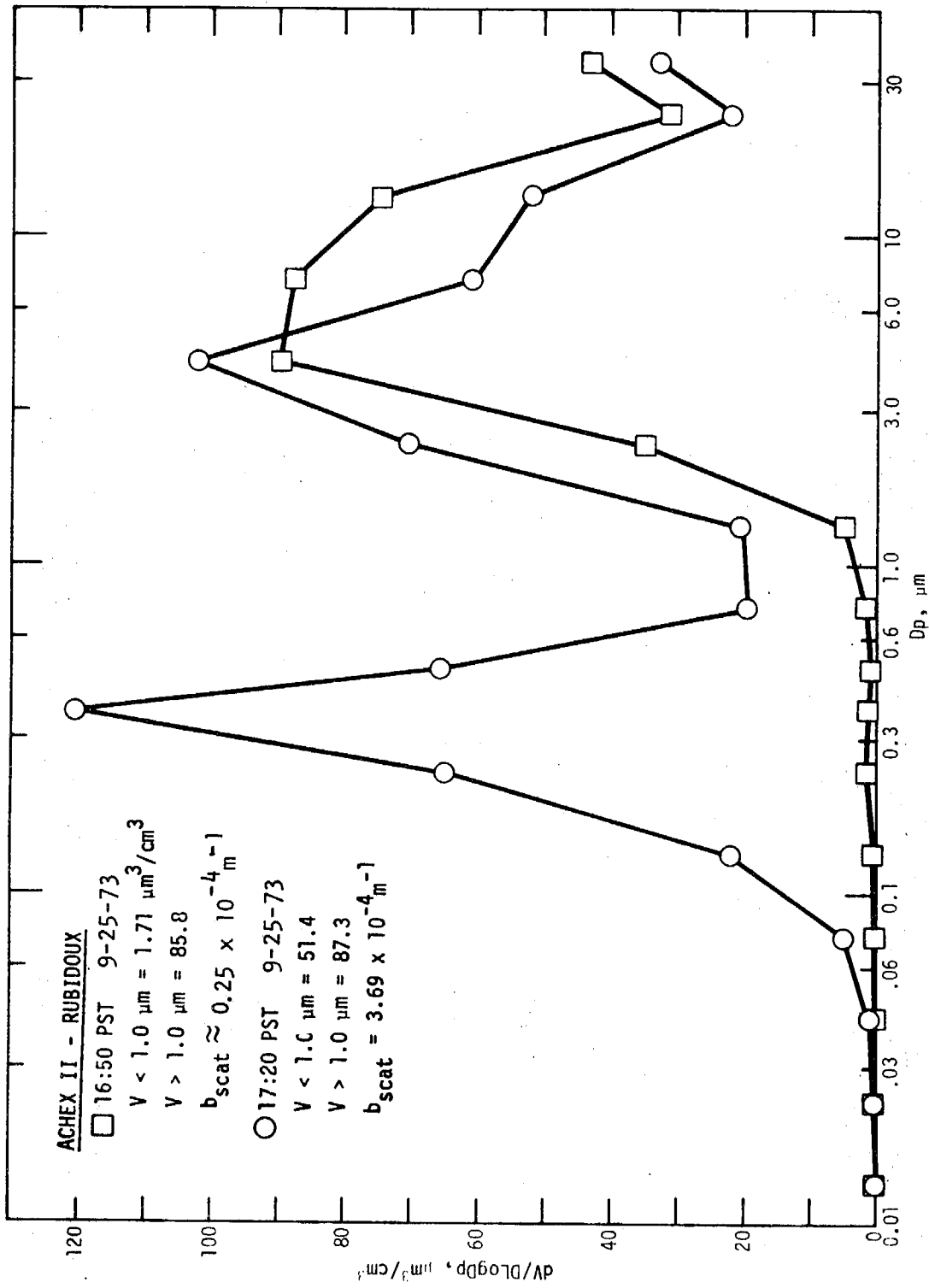


Figure 3-12. Particle Size Distributions Before and After the Arrival of Smog

SC524.25FR

relation should be examined carefully for its limitations prior to its widespread application. Graecan et al. ⁽¹¹⁾ have examined such relationships in more detail. In their work, the scattering coefficient due to aerosol particles, b_{sp} , is used. The broad band nephelometer used in the ARB mobile lab was adjusted to give a reading of $0.23 \times 10^{-4} m^{-1}$ while sampling clean air in order to account for Rayleigh air scattering. For the present work b_{sp} was used which is defined as

$$b_{sp} = b_{scat} - 0.23 \times 10^{-4} m^{-1}$$

b_{scat} is the value obtained directly from the nephelometer.

V3- ($D_p \leq 1 \mu m$) is probably the most useful measure of submicron aerosol volume since size segregating instruments, if incorporated into future air monitoring networks, will probably not distinguish between V2 ($0.01 \mu m \leq D_p \leq 0.1 \mu m$) and V3 ($0.1 \mu m \leq D_p \leq 1 \mu m$). However, since the nephelometer responds primarily to particles in the optical sub-range $0.2 \mu m \leq D_p \leq 2 \mu m$, ⁽¹²⁾ our studies have included both V3- and V3 for comparison.

A limitation of the Graecan et al. work is the use of averaged runs. Most particle and nephelometer data are collected during ten-minute intervals when, hopefully, conditions such as wind direction remain stable. The temptation to use the two-hour averages (12 ten-minute runs) is particularly strong as an order of magnitude reduction in the number of points considered is achieved. However, the penalty may outweigh the convenience in some instances. For example, the two-hour average from 1600 - 1800 on September 25, 1973 at Rubidoux (Run #582) contains at least two 10-minute runs which bear no resemblance to each other and should not be averaged (see Figure 3.12).

Additional statistical error is introduced by weighting averages equally regardless of the time period.

Figure 3.13 is a plot of b_{sp} vs. V3- for ACHEX I and other data. The data points are plotted on log-log paper to get more resolution than Figure 3.11B provides at low values of b_{sp} and V3-. The format of the plot was chosen based on discussions between Whitby and Charlson. The three lines $K = 9, 14,$ and 20 are used in the following equation:

SC524.25FR

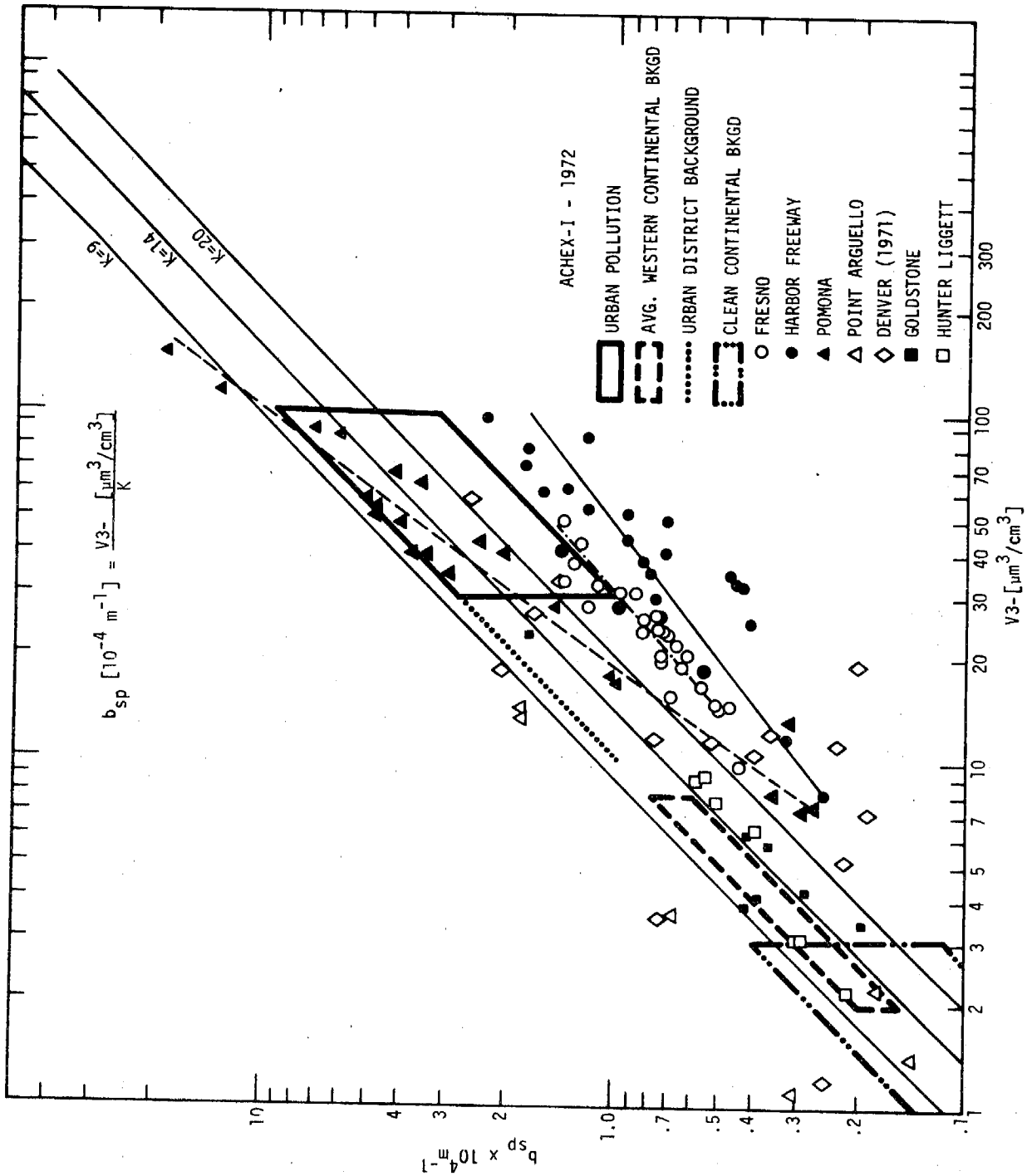


Figure 3-13. Extinction Due to the Aerosol as a Function of V3-

SC524.25FR

$$b_{sp} \times 10^4 [m^{-1}] = V3- [\mu m^3/cm^3]/K \quad (3-13)$$

The value $K = 9$ is the lowest value suggested by Charlson and also the value used by Covert in his thesis for a geometric standard deviation $\sigma_g = 2$, index of refraction $m = 1.5$, and white light. The value $K = 20$ is thought to be the upper limit that is possible based on the data reviewed by Charlson and Covert.

From Figure 3-13, it is seen that the Goldstone and Hunter Liggett data fall within the suggested correlation band ($9 \leq K \leq 20$). Fresno and Harbor Freeway data fall below and to the right of the central part of the band, with a composite slope nearly parallel to the correlation band. The most striking plot is the one of Pomona data. Whereas the other sites have volumes lying within one decade or less, the Pomona volumes cover nearly one and one half decades spanning all of the points recorded for Harbor Freeway, Fresno, and Hunter Liggett. Another feature of the Pomona plot is that data points lie both above and below the correlation band, having a composite slope greater than one. The Pomona correlation coefficients for $\ln b_{sp}$ vs. $\ln V3-$, $\ln b_{sp}$ vs. $\ln V3$, and b_{sp} vs. $V3$ are, moreover, the highest found for any of the sites, 0.983, 0.987, and 0.951, respectively (see Table 3.5).

An inspection of the data and the log book revealed that:

- 1) Pomona
 - a. 10/5/72, Runs 86 - 96.

Runs 86 - 88

Only five b_{scat} values were recorded for Run 86 and no Royco 220 counts were recorded for all three runs. Therefore these runs should be discarded.

Run 89

Only three WAA, Royco 220, and Royco 245 ten minute averages were recorded.

Runs 92 - 96

All these runs have a lower b_{scat} than expected. Run 96 is consistent with Runs 92 - 95. For Run 96, there is some volume in V2 and CNC, CO, HCT, and NO are all high indicating fresh aerosol

SC524.25FR

 TABLE 3-5
 CORRELATION COEFFICIENTS FOR b_{sp} VERSUS V3 OR V3-

<u>Site</u>	<u>Allowable Averages at Site</u>	<u>averaging period, hours</u>	<u>$\ln b_{sp}$ vs V3-</u>	<u>b_{sp} vs V3-</u>	<u>$\ln b_{sp}$ vs V3</u>	<u>b_{sp} vs V3</u>
Pomona (1972)	20	2	.983		.987	.951
Pomona (less last 4 points)	16	2			.953	
Goldstone	11	3 - 14				
Fresno	24	2	.925	.906	.938	
Point Arguello	6	2 - 4				
Hunter Liggett	4	6				
Harbor Freeway	25	1 - 2	.856	.874		
Total ACHEX I	106	1 - 14				.839
West Covina	25	2 - 6				
Pomona (1973)	18	2 - 5	.877	.91		
Rubidoux	24	2 - 5				
Dominguez Hills	18	2 - 5				.839
Total ACHEX II (2-hr. averages)	59	2				.944
Denver (1971)	14	20 min. - 13 hrs.				
St. Louis						
1st intensive	19	2	.86			
2nd intensive						
3rd intensive	22	1	.713			
4th intensive	33	1	.66			
5th intensive	30	1				
6th intensive	26	1				

SC524.25FR

below the optical range. In Pomona it was discovered that the glass window between the nephelometer viewing volume and the light source had loosened causing a serious leak. It is speculated that this may have happened when the trailer was being towed from the Hunter Liggett site, as the road was very rough and traversed a dry river bed. The leak was fixed at Pomona after the intensive on October 5, 1972 and before October 16, 1972. Therefore Runs 86 - 96 should be used with caution.

- b. 10/24/72, Runs 74 - 85.

Runs 74 - 85

During Run 74, visibility was reduced by fog. During the afternoon the greatest amount of photochemical activity during ACHEX I was monitored. These runs are typical of urban pollution.

- 2) Harbor Freeway

- a. 9/19/72, Runs 49 - 61.

All data points from the Harbor Freeway lie below the expected correlation. The slope is the same as the expected correlation. The location of the data on the plot is expected for data taken with the wind from the freeway. For this case (Runs 54, 56 - 60), the volume of the aerosol from the freeway (about $17.1 \mu\text{m}^3/\text{cm}^3$ at rush hour) is below the optical scattering range. Note that Run 54 was taken with the wind from the freeway at the rush hour and is a data point among the farthest from the expected correlation. Runs 49, 50, and 51 were obtained during the evening hours with the wind from the general city area.

- b. 9/27/72, Runs 62 - 73.

Run 62

The wind was from the freeway; note the data point.

Runs 63 - 65

The wind was opposite the freeway at night. There is a much better correlation than for Run 62.

Runs 66 - 67

The wind was opposite the freeway but there was increased

SC524.25FR

anthropogenic activity as people were driving to work.

Runs 68 - 73

The wind was from the freeway. For Runs 70 - 72, b_{scat} is much lower than the other runs. Log book notes visibility ~ 20 miles at 16:00. At 12:00 the log book notes show visibility low to the east but better to the west.

Consider the following:

<u>Run</u>	<u>V2/V3</u>
68	0.174
69	0.317
70	0.600
71	0.584
72	0.814
73	0.609

As expected, Runs 70 - 72 with relatively high V2/V3 lie farther below the expected correlation. Run 73 is somewhat higher than 70 - 72, but still below Runs 68 and 69. For both episodes at the Harbor Freeway the b_{scat} values may be lower than the actual value due to a leak in the nephelometer discussed in relation to the Pomona data.

- 3) Fresno
8/31/72, Runs 10 - 21.
All data points appear to be valid. University of Washington nephelometer data are being sent to verify the data for this site.
- 4) Goldstone, Runs 46 and 47.
Runs 46 and 47 each contain only three 10 minute runs. Note data point "I" for aged aerosol. This is a good example of urban district background.
- 5) Hunter Liggett
All data points appear valid.
- 6) Point Arguello
The accuracy of data from this site is difficult to analyze. The background classifications proposed by Whitby are also shown

SC524.25FR

on Figure 3-13 and presented in Table 3-6. The areas marked off on Figure 3-13 are just one way of interpreting Table 3-6. The collection and analysis of additional data may lead to modification of Table 3-6.

Figure 3-14 is a plot of b_{sp} vs. V_3 . The correlation coefficient for b_{sp} vs. V_3 is 0.839 with all averages equally weighted.

To explain the large variation of K ($V_3 - b_{sp}$) for the 1972 Pomona data, an investigation of the optical scattering response of the integrating nephelometer was begun. The theoretical response of a spectral nephelometer ($\lambda = 550$ nm) to a white aerosol with refractive index 1.50 as a function of mass mean radius and geometric standard deviation was numerically calculated by Ensor and is shown in Figure 3-15. This relation exhibits a minimum at a mass mean radius of $0.27 \mu\text{m}$ ($\text{MMD} = 0.54 \mu\text{m}$) with a K value of $10 \mu\text{m}^3 - \text{m}/\text{cm}^3$ for a logarithmic normal distribution with $\sigma_g = 1$. Below a $\text{MMD} = 0.4 \mu\text{m}$, K values increase rapidly to reach a value of 40 at $\text{MMD} = 0.2 \mu\text{m}$.

To obtain a comparison between observed K and volume mean diameters and the theoretical ones, it was necessary to assume a particle density and transform Figure 3-15 to a plot of K vs. DGV_3 . Particle density was assumed to be unity and the abscissa of Figure 3-15 was converted to the abscissa of Figure 3-16 by the following relation:

$$\text{DGV}_3 = 2 \times \text{mass mean radius} \quad (3-14)$$

K values were calculated using the relation

$$K = V_3 [\mu\text{m}^3/\text{cm}^3]/b_{sp} \times 10^4 [\text{m}^{-1}]. \quad (3-15)$$

DGV_3 was calculated by finding the geometric mean of the volume frequency data at each point (DV vs. D_{pi})* in the range $0.133 \mu\text{m} \leq D_{pi} \leq 0.75 \mu\text{m}$. Preliminary work shows that including data at smaller D_{pi} 's does not change DGV_3 , but does increase σ_g . Including data at larger D_{pi} 's cause an increase in the value of DGV_3 , due in some part to contributions from the upper volume mode. In later work, it may be possible to separate the

* D_{pi} is the particle diameter at the midpoint of a particle size range measured by an instrument.

SC524.25FR

TABLE 3-6

 CATEGORIES OF AMBIENT AIR ENVIRONMENTS AND NUMERICAL VALUES
 FOR THEIR PARAMETRIC DESCRIPTION

<u>Aerosol Category</u>	<u>Aitken Nuclei NT, no./cm</u>	<u>Total Volume VT, $\mu\text{m}^3/\text{cm}^3$</u>	<u>Submicron Volume V3- $\mu\text{m}^3/\text{cm}^3$</u>	<u>Scattering Coefficient b_{scat}, $\text{m}^{-1} \times 10^5$</u>	<u>Approx. U.S. Area \times Time</u>
Clean Continental Background	50-500	2-10	.5-3	.2-4	1/4
Average Western Continental Background	2K-5K	10-40	2-8	2-6	1/2
Urban District Background	5K-10K	20-60	10-30	10-30	1/4
Oceanic Background	200-400			1-2	
Urban Pollution	100K-1000K	100-300	30-100	10-100	

SC524.25FR

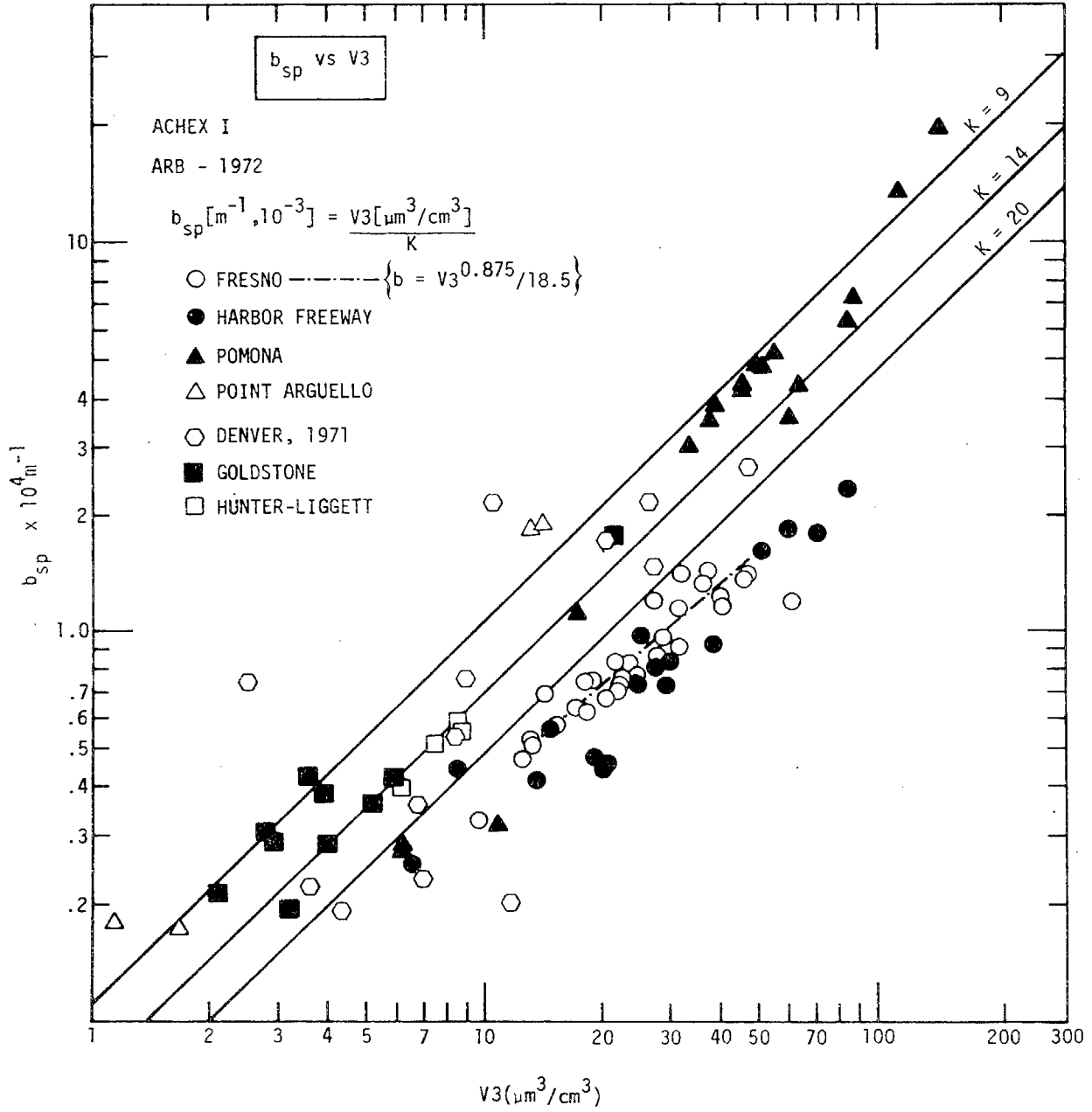


Figure 3-14. Correlation of b_{sp} vs. $V3$ for ACHEX-1 Data.

SC524.25FR

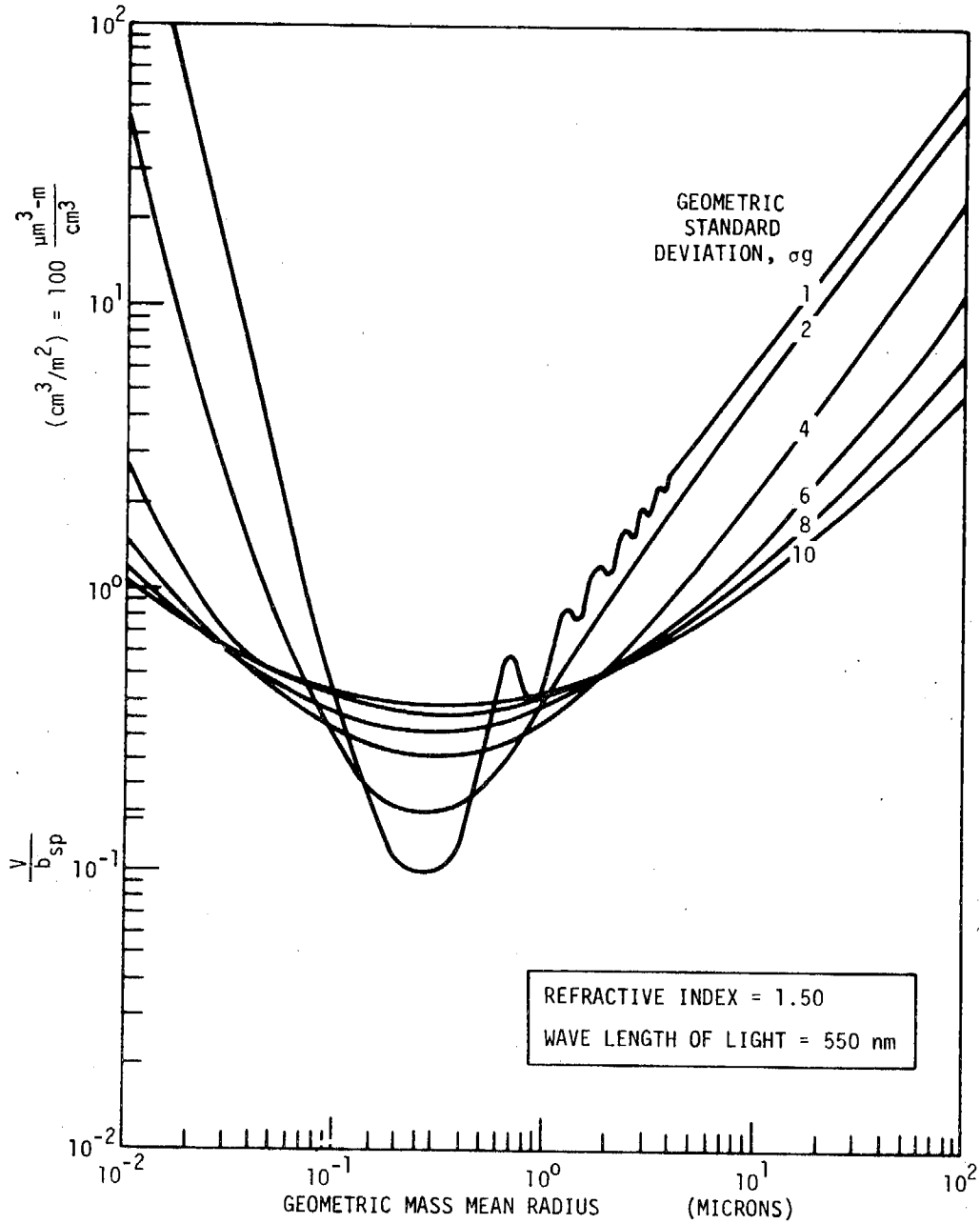


Figure 3-15. Parameter K as a Function of the Log-Normal Size Distribution Parameters for a White Aerosol.

SC524.25FR

upper and lower modes of the volume distribution by fitting the data to a function which is the sum of two log-normal functions. If such a separation of modes were possible, the true volume mean diameter (and σ_g) of the lower mode could be obtained.

On the basis of the preliminary work, the trend of increasing K values with decreasing DGV3 is strongly confirmed by the Pomona data in Figure 3-16. The slope of the Pomona data in Figure 3-13 cannot be explained solely on the basis of the correlation of K with DGV3, however. There is another mechanism responsible for the observed decrease of DGV3 with decreasing V3.

It is apparent from the Pomona plot (Figure 3-16) that the lowest K values are obtained for DGV3 in the neighborhood of 0.4 μm . K ranges from 10 to 20 $\mu\text{m}^3 - \text{m}/\text{cm}^3$ when DGV3 is between 0.3 μm and 0.4 μm . Higher K values are obtained for DGV3 < 0.3 μm . Figure 3-17 is the plot of K vs. DGV3 for the Harbor Freeway. DGV3's are grouped below 0.3 μm . Corresponding K values are well above 20 $\mu\text{m}^3 - \text{m}/\text{cm}^3$. Fresno data show DGV3's in the range 0.3 μm to 0.35 μm and K values grouped between 20 and 30 $\mu\text{m}^3 - \text{m}/\text{cm}^3$. Thus, deviations from the suggested correlation band of b_{scat} vs. V3 can be related to shifts by the mean volume diameter to higher or lower sizes.

The adequacy of the theoretical curve shown in Figure 3-15 for describing the response of the broad band nephelometer to atmospheric aerosols is questionable in some details, but shows promise as the basis for a useful continuous measurement of the submicron aerosol fraction. Later work may include modifying Ensor's program to account for the broad band light scattering and several refractive indices.

B. CHEMICAL PROPERTIES

The chemical composition of aerosols sampled in California is rather complicated. Traces of a wide variety of materials are found in the airborne particles. These components are distributed in different ways according to particle size that reflects to their origins.

1. CHEMICAL COMPOSITION

The complexity of the chemistry of aerosol samples is illustrated in the data listed in Table 3-7. Results of this are similar for most urban and non-urban samples in which the components, water soluble

SC524.25FR

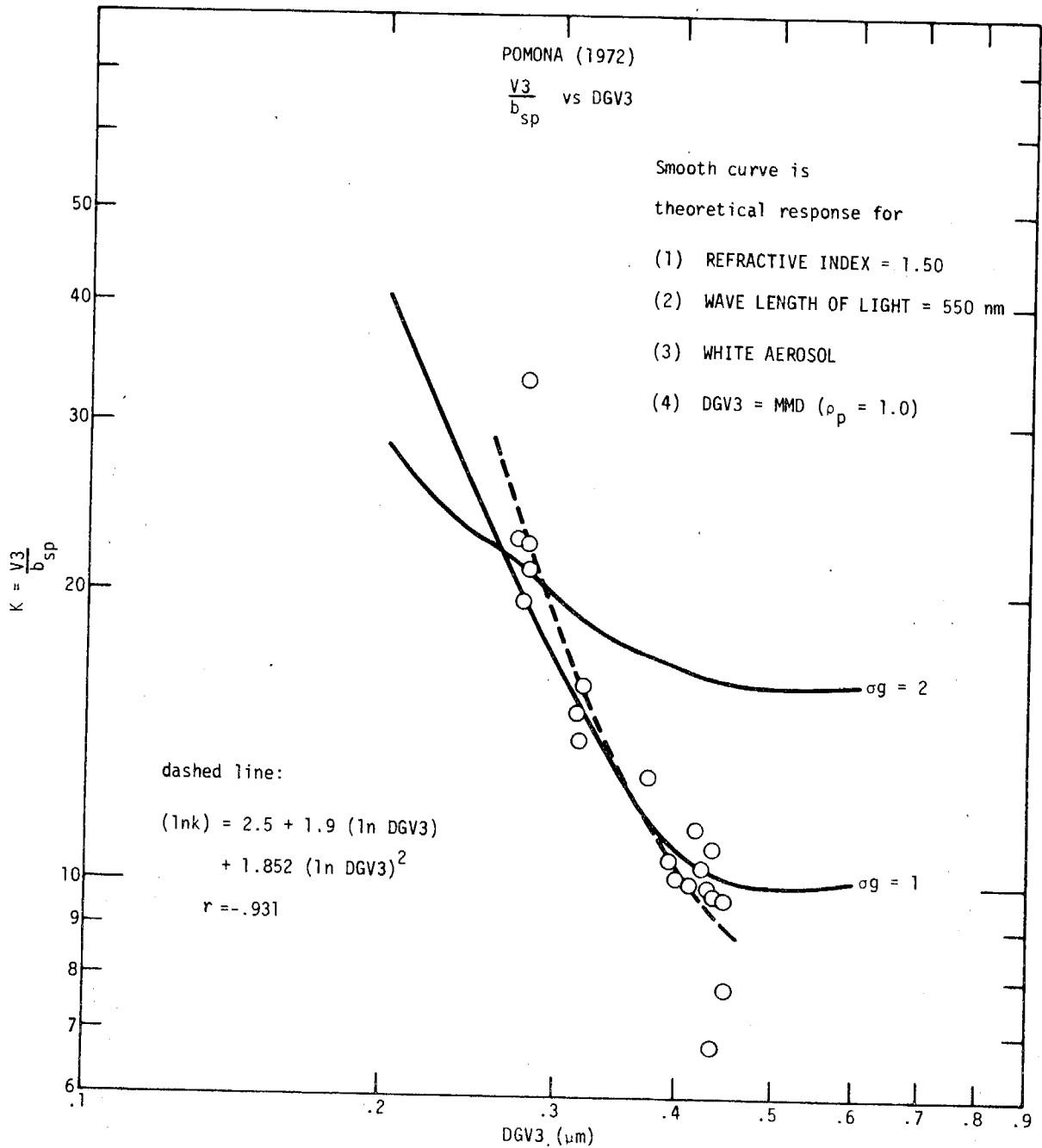


Figure 3-16. Variation in V_3/b_{sp} vs. DGV3 for the Pomona Data in 1972.

SC524.25FR

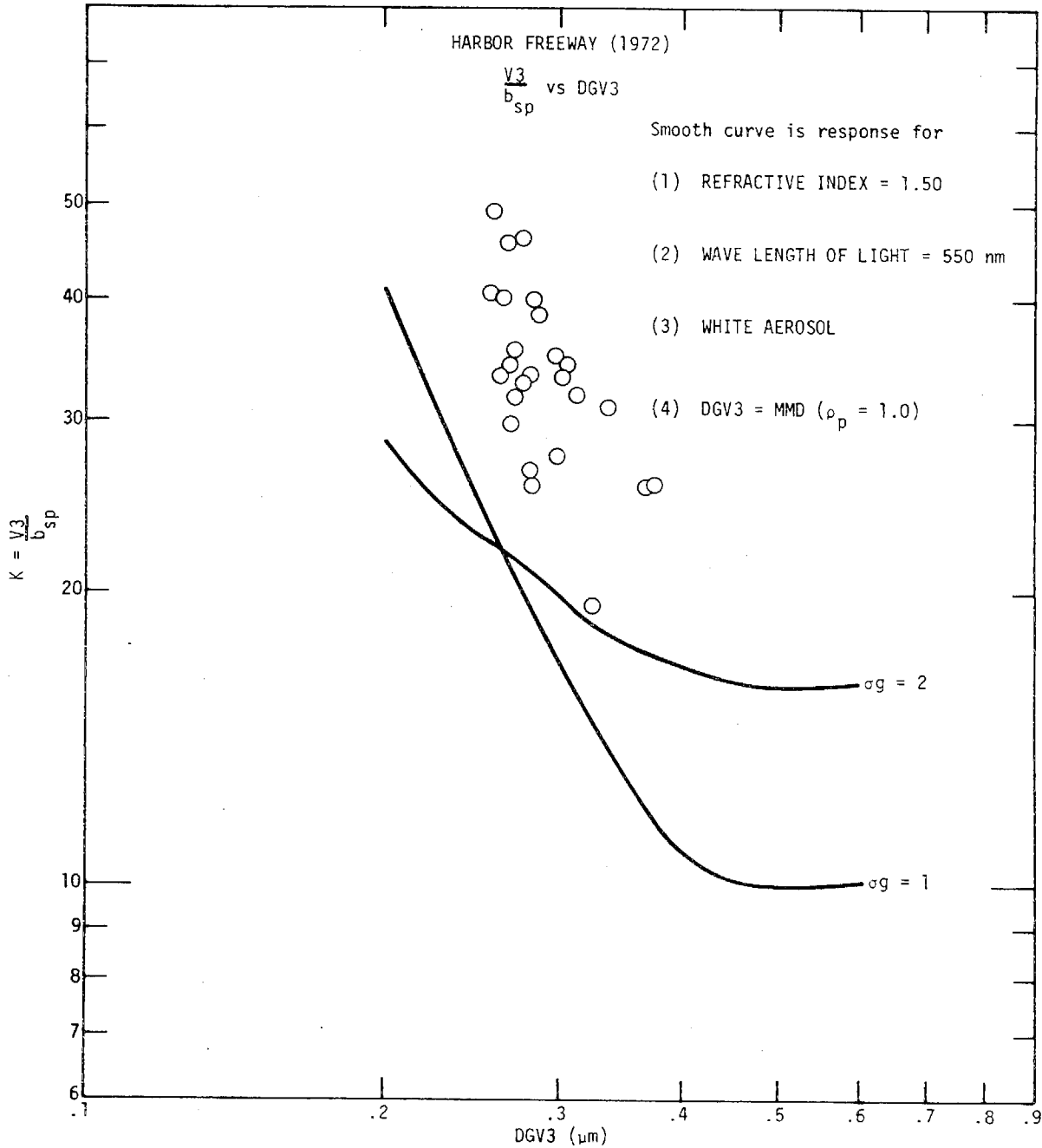


Figure 3-17. Variation of $V3/b_{sp}$ vs. DGV3 for the Harbor Freeway Data.

SC524.25FR

TABLE 3-7

CHEMICAL COMPOSITION OF FILTER COLLECTED AEROSOL SAMPLES

Constituent	Weight Percent			
	Non-Urban		Urban	
	Pacific Coast* Offshore	Desert ⁺	Fresno	Pomona
Al	2.8	2.4	2.4	0.99
Si	5.0	5.2	6.3	2.2
Na	3.6	0.71	0.40	1.1
Cl	9.9	0.32	0.19	0.51
K	1.3	0.39	0.33	0.24
Ca	1.9	2.1	0.47	1.0
Ti	0.15	0.13	0.09	0.11
V	N.D.	0.004	N.D.	0.008
Cr	0.02	N.D.	0.00528	0.013
Mn	0.04	0.028	0.025	0.025
Fe	1.6	1.4	1.03	0.86
Cu	0.6	0.028	0.0058	0.014
Zn	0.2	0.035	0.055	0.13
Br	0.2	0.059	0.098	0.36
Pb	0.4	0.017	0.42	1.6
I	-	-	-	-
SO ₄ ⁼	17.5	2.8	2.0	10.6
NO ₃ ⁻	5.7	3.5	3.8	20.2
NH ₄ ⁺	2.2	1.7	1.5	9.1
Non Carb C	3.0	N.D.	8.25 ⁺⁺	40.0 ⁺⁺
Total (µg/m ³)	30	42.4	207	180

* Average of 20 samples at San Nicolas Island (13)

⁺ Single 24 hour sample at Goldstone

⁺⁺ Estimated as 5 × cyclohexane extractable organics

SC524.25FR

sulfate, nitrate, and non-carbonate carbon, with ammonium (and water) make up a significant fraction of the total particulate mass collected. To date, comprehensive chemical analyses of aerosol samples have not provided complete identification of the total mass of aerosol.

An improvement in mass balance can be achieved assuming that NO_3^- is NH_4NO_3 , $\text{SO}_4^{=}$ is NH_4HSO_4 , and the organic carbon is 1.2 (non-volatile carbon + volatile carbon + pyrolyzable carbon)* or total elemental carbon measured by the AIHL method; Si is contained as 20% of soil dust, and Pb is present as PbBrCl . With such easily defensible assumptions, the material balance for aerosol samples on total filters is improved substantially, as shown for the 1973 mobile laboratory data in Table 3-8. Here, 60% to 80% of the aerosol mass can be accounted for. If scale factors for organic carbon are employed to account for oxygen and hydrogen, and liquid water is considered at an approximate fraction of 10% of the mass, further improvements in the mass balance can be achieved. Such considerations are discussed in more detail in Chapter 10.

Several averages and range of constituents that are potentially important to air quality are listed in Tables 3-1 and 3-2 for the ACHEX. These data indicate that the South Coast Basin showed the highest levels of total mass concentration, sulfates, nitrates, and lead during the study. Extreme values of $71 \mu\text{g}/\text{m}^3$ of sulfate over a two-hour period were observed at Rubidoux. At the same location, an extreme value of $247 \mu\text{g}/\text{m}^3$ of nitrate was found. Lead concentrations were somewhat higher in the South Coast Basin than encountered elsewhere.

The twenty-four hour average sulfate and nitrate concentrations were similar to those reported in the National Air Surveillance Network (NASN) data. Some annual average values for the Los Angeles area are shown for comparison in Table 3-9. The 1968 NASN data⁽¹⁴⁾ show larger annual averaged sulfate in the west part of the city than we experienced, but otherwise the results are remarkably similar. Thus, it is concluded that

* Correction factor based on intercomparison between AIHL total carbon method and DuPont thermal analyzer method; it does not include organic oxygen or hydrogen.

SC524.25FR

TABLE 3-8
SUMMATION OF TOTAL FILTER CONSTITUENTS

1. West Covina	Time	C	NO ₃	S	Si	Pb	HC	NH ₄ NO ₃	NH ₄ HSO ₄	Soil Dust	PbBrCl	Total	Mass	(Total Mass)
TB	2300	*18.8	10.0	11.1	6.0	4.4	20.7	13.0	40.0	30.0	6.6	110.3	167	.66
	0330	10.3	17.4	5.2	3.3	3.4	11.3	22.6	18.7	16.5	5.1	74.2	117	.63
	0700	19.7	32.2	6.9	4.9	4.9	21.7	41.9	24.8	24.5	7.4	120.3	164	.73
	0900	25.0	29.6	11.6	6.7	6.7	27.5	38.5	41.8	33.5	10.0	151.3	243	.62
	1100	33.5	25.9	15.6	7.5	3.8	36.9	33.7	56.2	37.5	5.7	170.0	258	.66
	1300	47.6	12.0	15.2	11.1	3.9	52.4	15.6	54.7	55.5	5.9	184.1	268	.69
	1500	49.3	7.2	24.8	15.2	4.0	54.2	9.4	89.3	76.0	6.0	284.9	305	.77
	1700	33.3	8.4	17.6	14.0	3.3	36.6	10.9	63.4	70.0	5.0	185.9	208	.89
	1930	21.1	7.2	12.5	8.0	3.7	23.2	9.4	45.0	40.0	5.6	123.2	163	.76
	TC	0200	(9.2)	11.6	5.5	5.8	2.9	(10.1)	15.1	19.8	29.0	4.4	78.4	129
0630		(16.3)	20.1	8.6	5.6	4.2	(17.9)	26.1	31.0	28.0	6.3	109.3	189	.58
0900		(29.9)	50.2	12.1	8.5	7.4	(32.9)	65.3	43.6	42.5	11.1	195.4	286	.68
1100		(31.6)	36.7	15.2	11.1	5.1	(34.8)	47.7	54.7	55.5	7.7	200.4	287	.70
1300		(38.6)	17.3	13.5	13.5	4.4	(42.5)	22.5	48.6	67.5	6.6	187.7	304	.62
1500		(29.0)	8.4	14.1	13.1	3.2	(31.9)	10.9	50.8	65.5	4.8	163.9	248	.66
TD	0630	(14.9)	20.8	2.2	10.1	7.4	(16.4)	27.0	7.9	50.5	11.1	112.9	150	.75
	0900	(15.2)	36.1	8.2	9.9	3.9	(16.7)	46.9	29.5	49.5	5.9	148.5	193	.77
	1100	(13.0)	34.0	10.5	4.4	3.0	(14.3)	44.2	37.8	22.0	4.5	122.8	186	.66
	1300	(11.2)	14.1	7.6	6.8	2.2	(12.3)	18.3	27.4	34.0	3.3	95.3	170	.56
	1500	(9.0)	10.0	8.2	11.0	1.8	(9.9)	13.0	29.5	55.0	2.7	110.1	153	.72
	1700	(5.9)	12.1	7.5	5.4	1.8	(6.5)	15.7	27.0	27.0	2.7	78.9	105	.75
2. Riverside/Rubidoux	VH 0100	(6.2)	23.3	1.9	4.0	1.3	(6.8)	30.3	6.8	20.0	2.0	65.9	97.2	.68
	0530	(5.9)	19.2	2.0	2.6	1.8	(7.6)	25.0	7.2	13.0	2.7	55.5	87.8	.63
	0900	(19.2)	74.3	5.5	17.3	2.5	(21.1)	96.6	19.8	86.5	3.8	227.8	321	.71
	1100	(14.0)	76.0	6.4	10.3	1.4	(15.4)	98.8	23.0	51.5	2.1	190.8	268	.71
	1300	(15.0)	48.5	5.3	10.2	1.5	(16.5)	63.1	19.1	51.0	2.3	152.0	260	.58
	1500	(16.2)	73.5	7.6	14.2	2.3	(17.8)	95.6	27.4	71.0	3.5	215.3	287	.75
	1700	(17.8)	63.6	11.0	8.8	1.9	(19.6)	82.7	39.6	44.0	2.9	188.6	306	.62
	1900	(19.4)	66.8	10.4	11.0	2.2	(21.3)	86.8	37.4	55.0	3.3	203.8	288	.71
2130	(23.7)	81.8	8.4	20.5	2.3	(26.1)	106.3	30.2	102.5	3.5	268.6	325	.83	

SC524.25FR

TABLE 3-8

SUMMATION OF TOTAL FILTER CONSTITUENTS (Continued)

Time	C	NO ₃ ⁻	S	SI	Pb	HC	NH ₄ NO ₃	NH ₄ H ₂ SO ₄	Soil		PbBrCl	Total	Mass	(Total Mass)
									Dust	Dust				
2. Riverside/Rubidoux (continued)														
V1 0100	(9.2)	71.1	4.1	4.5	1.7	(10.1)	92.4	14.8	22.5	2.6	142.4	202	.70	
0530	(8.8)	54.0	3.0	3.9	2.3	(9.7)	70.2	10.8	19.5	3.5	113.7	182	.62	
0900	(18.3)	93.0	11.9	8.2	2.8	(20.1)	120.9	42.8	41.0	4.2	229.0	331	.69	
1100	(24.3)	149.0	17.3	27.8	2.7	(26.7)	193.7	62.3	139.0	4.1	425.8	489	.87	
1300	(32.9)	24.7	11.3	48.1	1.7	(36.2)	32.1	40.7	240.5	2.6	352.1	467	.75	
1500	(22.0)	66.1	8.7	29.0	2.1	(24.2)	85.9	31.3	145.0	3.2	289.6	336	.86	
1700	(7.2)	31.9	5.5	11.0	1.1	(7.9)	41.5	19.8	55.0	1.7	125.9	180	.70	
1900	(9.6)	37.6	5.4	9.8	1.5	(10.6)	48.9	19.4	49.0	2.3	130.2	192	.68	
2100	(9.9)	43.4	4.3	10.5	1.6	(10.9)	56.4	15.5	52.5	2.4	137.7	163	.84	
3. Dominguez Hills														
WK 2300	(5.8)	16.1	5.2	2.9	1.8	(6.4)	20.9	18.7	14.5	2.7	63.2	98.4	.64	
0330	(8.3)	7.8	10.4	3.7	1.1	(9.1)	10.1	37.4	18.5	1.7	76.8	119	.65	
0700	(8.6)	8.4	16.6	2.5	2.5	(9.5)	10.9	59.8	12.5	3.8	96.5	144	.67	
0900	(11.3)	6.0	15.1	2.0	2.0	(12.4)	7.8	54.4	10.0	3.0	87.6	147	.60	
1100	(14.2)	2.6	14.3	2.1	1.3	(15.6)	3.4	51.5	10.5	2.0	83.0	134	.62	
1300	(12.8)	4.4	13.5	2.4	0.9	(14.1)	5.7	48.6	12.0	1.4	81.8	142	.58	
1500	(7.7)	5.0	11.8	3.0	0.9	(8.5)	6.5	42.5	15.0	1.4	73.9	112	.66	
1700	(5.3)	3.7	8.3	1.4	1.0	(5.8)	4.8	29.9	7.0	1.5	49.0	89.0	.55	
1930	(3.7)	2.7	7.3	1.0	1.0	(4.1)	3.5	26.3	5.0	1.5	40.4	62.9	.64	
WL 2300	(9.2)	5.8	< 1.2	2.4	4.3	(10.1)	7.5	-	12.0	6.5	36.1	64.9	.56	
0330	(17.0)	7.3	< 1.2	3.5	6.0	(18.7)	9.5	-	17.5	9.0	54.7	104	.53	
0700	(34.4)	9.2	< 3.0	10.5	12.5	(37.8)	12.0	-	52.5	18.8	121	205	.59	
0900	(28.2)	27.3	< 2.1	7.4	6.1	(31.0)	35.5	-	37.0	9.2	113	213	.53	
1100	(18.4)	24.2	3.6	6.0	3.6	(20.2)	31.5	13.0	30.0	5.4	100	152	.66	
1300	(7.0)	7.7	4.4	1.2	1.1	(7.7)	10.0	15.8	6.0	1.7	41.2	70.1	.59	
1500	(6.0)	12.3	2.5	0.9	1.2	(6.6)	16.0	9.0	4.5	1.8	37.9	66.1	.57	
1700	(4.0)	6.8	1.4	1.0	1.3	(4.4)	8.8	5.0	5.0	2.0	25.2	46.7	.54	
1930	(5.5)	11.0	1.6	1.3	1.9	(6.1)	14.3	5.8	6.5	2.9	35.6	60.9	.58	

*Total Carbon (CEL); () Total Carbon 1.2 (CPR + CNV + CVL)

SC524.25FR

TABLE 3-9

NASN NETWORK DATA FOR NITRATE AND SULFATE
 IN THE SOUTH COAST BASIN FOR 1968
 (ANNUAL 24-HR AVERAGE VALUES)^{a,b}

<u>Sampling Location</u>	<u>SO₄⁼</u>		<u>NO₃⁻</u>	
	<u>µg/m³</u>	<u>% of Mass</u>	<u>µg/m³</u>	<u>% of Mass</u>
Long Beach	12.7	11.1	5.7	5.0
Los Angeles	10.2	7.9	7.7	6.0
Ontario	9.0	7.8	9.1	7.9
Riverside	8.3	7.2	10.2	8.8

^aFrom reference 14

^bData based on geometric mean of 26 24-hour sampling periods

SC524.25FR

the data obtained in the ACHEX are reasonably representative of long-term conditions in the South Coast Basin, even though we sought cases where smog was heavier than "average".

2. SIZE DISTRIBUTION

The distribution of constituents with respect to particle size is an important factor in the makeup of the aerosols. The ACHEX data were useful in showing in detail distinct differences between material in certain particle size ranges. This is illustrated in the curves shown in Figure 3-18 for sulfate and nitrate. In all locations, sulfate was concentrated in particles smaller than $1 \mu\text{m}$; sulfate generally was found in the submicron particles smaller than nitrate, except for the Rubidoux area. This is indicated in the tabulations of particle mean diameter listed in Table 3-10. Note in Figure 3-18 that the nitrate concentration is lower than sulfate except on the east side of the Basin at Rubidoux.

It is not possible to account for the amount of sulfate and nitrate in aerosol samples from contributions of known primary sources. Therefore, the ions are attributed to secondary production processes in the atmosphere involving the oxidation of SO_2 and NO_x .

Similar distributions for the fuel combustion related elements Pb and Nickel are shown in Figure 3-19. Again these are concentrated in the submicron fraction of the aerosol. Similarly, the data from the total filters and the after filters indicated that most of the carbon in the aerosols was found in the fraction less than $0.5 \mu\text{m}$ in diameter. This conclusion agrees with the earlier results of Mueller et al. (15).

Estimates of primary emissions of carbon in Los Angeles air cannot account for more than a small fraction of the carbon in the ambient aerosol. Therefore, most of this material is deduced to be derived from atmospheric reactions (see also Chapter X).

In contrast to the primary combustion (Pb, V, C) and secondary aerosol constituents (SO_4^{2-} , NO_3^- , C), the natural and quasi-natural process dominated elements such as Na, Si, and Al and Fe were found largely in the super-micron particle portion. Such distributions are illustrated for these elements in Figure 3-20.

SC524.25FR

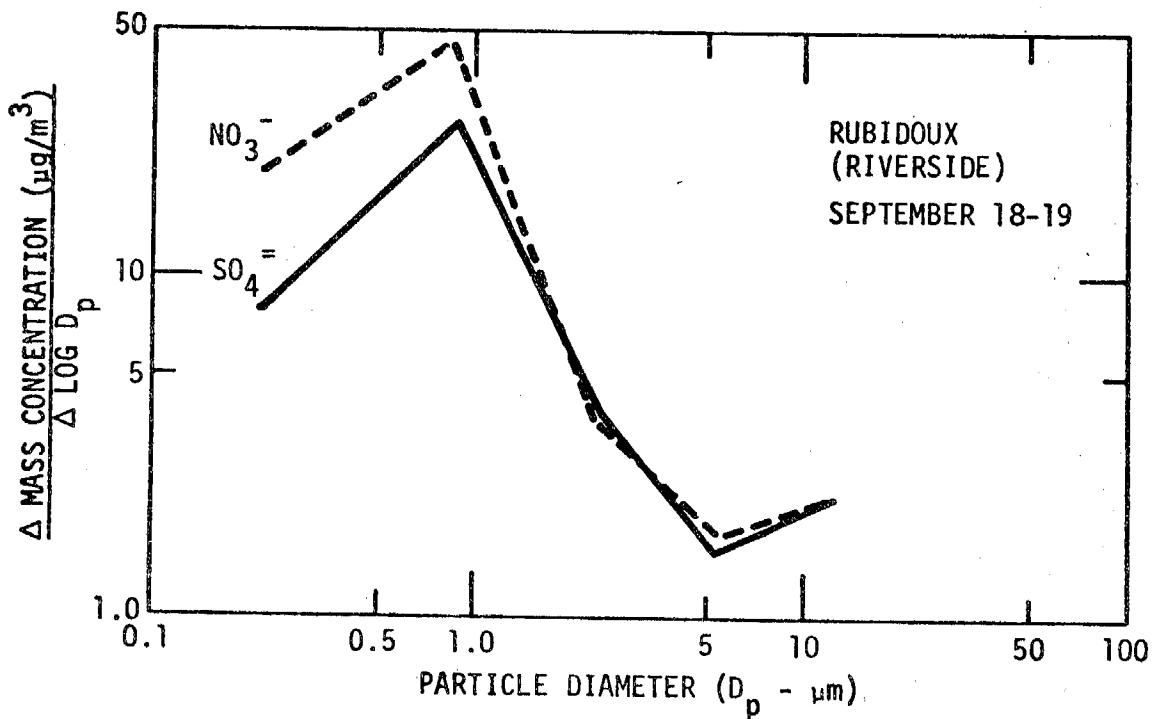
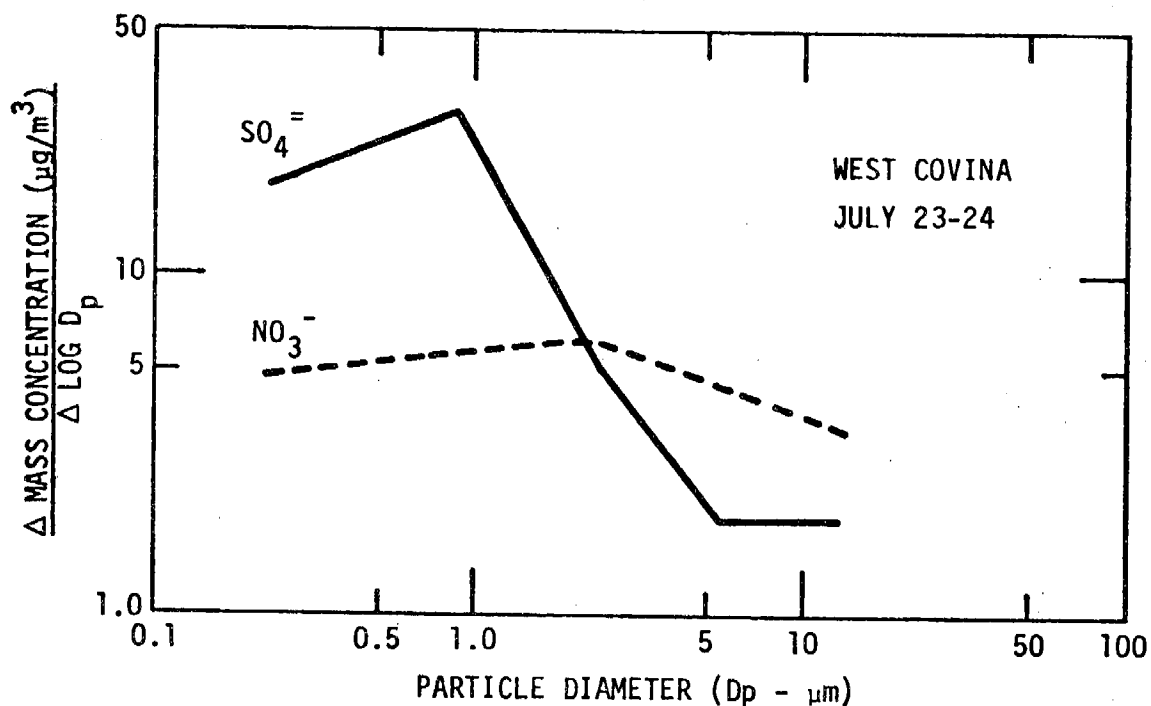


Figure 3-18. Mass Distributions of $\text{SO}_4^{=}$ and NO_3^- with Particle Size

SC524.25FR

TABLE 3-10

 MASS MEDIAN PARTICLE DIAMETER
 SOUTH COAST AIR BASIN, 1973^{a)}

<u>Sampling Location</u>	<u>Nitrate (μm)</u>	<u>Sulfate (μm)</u>
Dominguez Hills		
Oct 4-5	1.64	0.43
Oct 10-11	0.72	0.42
West Covina		
July 23-24	1.13	0.34
July 26 ^{b)}	0.62	< 0.22
Pomona		
Aug 16-17	0.68	0.39
Rubidoux		
Sept 5-6	0.33	0.33
Sept 18-19	0.34	0.43

^{a)} Except as noted based on 24-hour average size distributions obtained with the 5-stage Lundgren Impactor.

^{b)} 13-hour average, 0500-1800 hours.

SC524.25FR

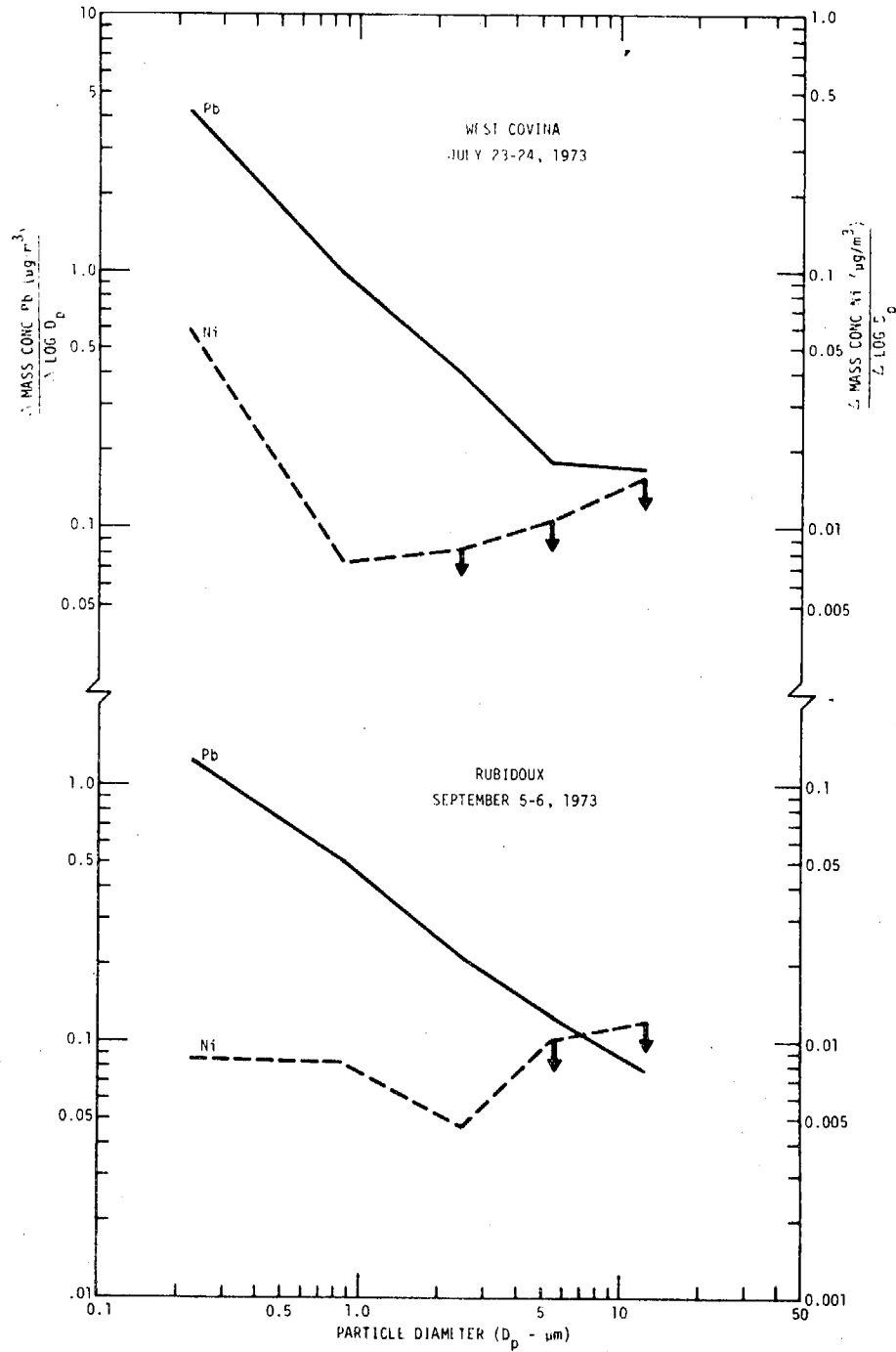


Figure 3-19. Mass Distributions of Ni and Pb with Particle Size.
When the Ni concentration was not detectable, the limit
of detectability was plotted with a downward arrow.

SC524.25FR

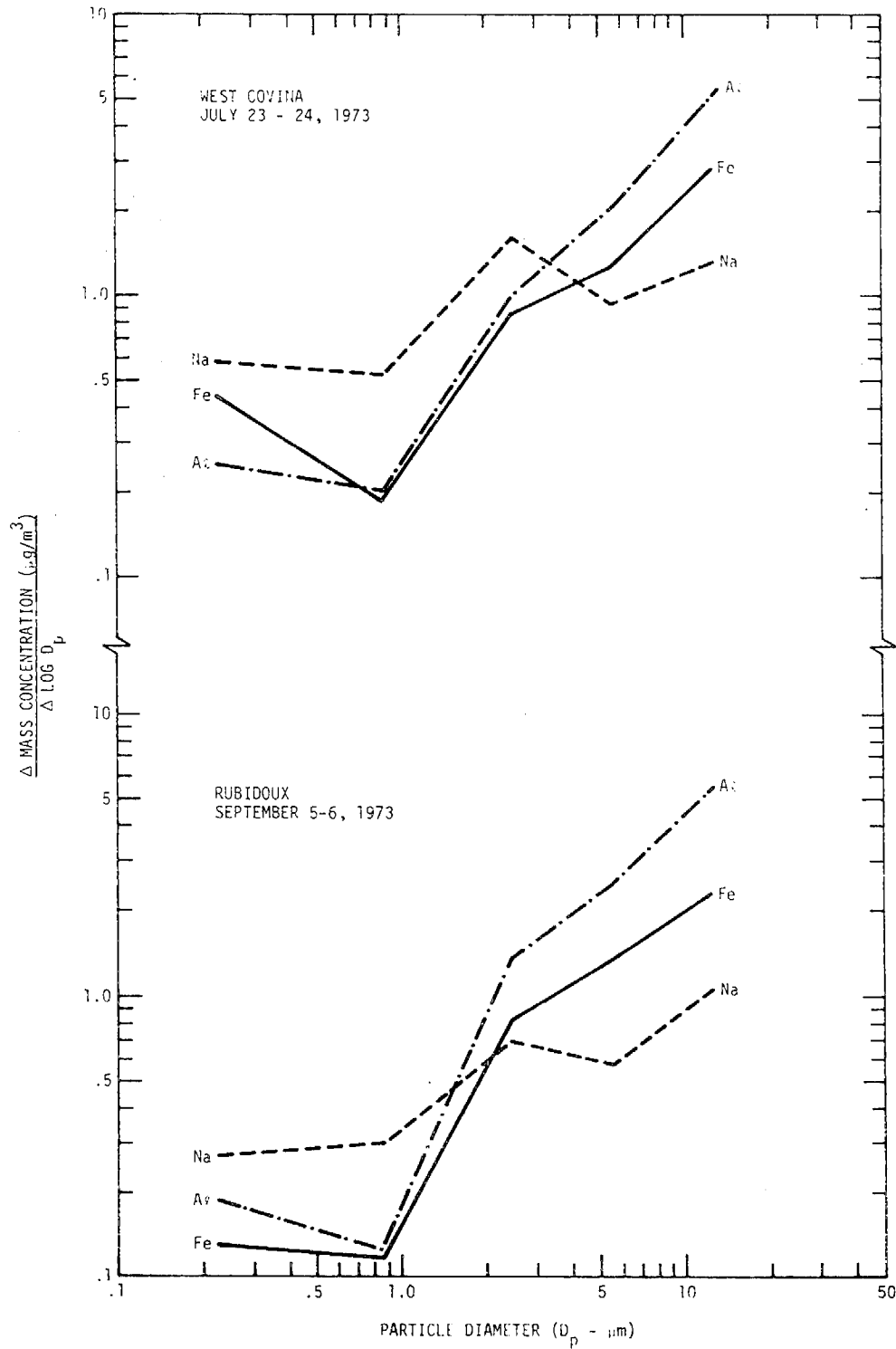


Figure 3-20. Mass Distributions of Na, Al, and Fe with Particle Size.

SC524.25FR

The data for distribution of chemical elements illustrated in Figures 3-18 through 3-20 supply the hypothesis proposed in Figure 2-1 on the basis of sketchy results obtained previously. In particular, for aerosol samples in California, at least, there is substantial evidence confirming the principal anthropogenic and secondary aerosol contribution to the submicron fraction. The natural source materials such as sea salt and wind blown dust, as traced by Na and Al for example, are heavily concentrated in the large particle fraction.

3. LIQUID WATER CONTENT

Results derived by several means have shown the importance of liquid water in aerosol behavior. The water filter results indicated that the liquid water content of filter collected material over a period of 24 hours ranged from zero at the desert site of Goldstone to more than 30% of the mass. Estimates of water content based on assumptions of the chemical nature of the urban aerosol show a range of water content of the order of 10% or greater for filter collected material equilibrated to air at 50% relative humidity or less. The humidified nephelometry results by the University of Washington showed considerable evidence of hygroscopic nature of California aerosols and their rapid equilibration with water vapor.

The results taken from the microwave waterometer provided important information about the changes in liquid water content with daily buildup of aerosol mass concentration. Such results are well illustrated in Figures 7-19 through 7-22 where semi-continuous mass concentration observations are shown with change in liquid water content. Even with a decrease in the relative humidity, the liquid water content closely follows the buildup and decrease in mass concentration. The question of the importance of liquid water is discussed in more detail in Chapter IX.

4. ROLE OF AMMONIA

Traces of ammonia are present in the atmosphere in quantities sufficient to neutralize strong acids in the aerosol for many cases (for example, see the ACHEX data in Volume III). The hypothesis that sulfate and nitrate are

SC524.25FR

largely present as ammonium salts in California was tested for several cases of ACHEX. The calculations are shown in Table 3-11. For these calculations, it was assumed that NO_3^- and $\text{SO}_4^{=}$ are present as NH_4NO_3 and $(\text{NH}_4)_2\text{SO}_4$. The results for the 24-hour high volume filter samples suggest that, on the average, 85% of these anions can be accounted for in terms of ammonium salts. By assuming ammonium acid sulfate, the balance could be improved. Indeed, the assumption that $\text{SO}_4^{=}$ and NO_3^- are present as NH_4NO_3 and NH_4HSO_4 provides the framework for much of the subsequent discussion of aerosol behavior. The proportion of apparent ammonium salts present is not, however, readily predictable from the gas phase NH_3 levels. Table 3-12 includes 24-hour average NH_3 values calculated from samples collected for 2 or 4-hour periods. In addition the corresponding $\text{SO}_4^{=}$ and NO_3^- levels are given together with the calculated concentration of NH_3 needed to just neutralize the sulfate and nitrate assumed to be present as the acids. The ratio of observed to calculated minimum NH_3 was always ≥ 1 but displayed no apparent correlation with the proportion of ammonium salts shown in Table 3-11. This may reflect the significance of cations other than H^+ and NH_4^+ (e.g., Na^+).

5. SOURCE DOMINATED AND RECEPTOR CHEMISTRY

The sampling devoted to establishing differences between areas far from major sources and those dominated by nearby emissions was useful in making some distinctions between regions. The results, for example, taken at the Harbor Freeway can be compared with one another for the contribution of motor vehicle exhaust vs. the receptor mixture at the same site by examining data corresponding to wind blowing from the freeway vs. wind blowing towards the freeway. Such results are shown in Table 3-13. Qualitatively, the influence of auto exhaust is evident in the lead halides and reduced sulfur. However, taking the difference between the two cases for other constituents reveals an uncertain influence of the fresh freeway emissions on the general aerosol burden in the downtown area, despite the fact that auto exhaust is known to contain traces of several of the materials listed. Thus, the development of an auto exhaust aerosol contribution requires further consideration than simple comparisons shown in Table 3-13. Such an analysis

SC524.25FR

TABLE 3-11

 COMPARISON OF THEORETICAL AND EXPERIMENTAL AMMONIUM VALUES
 AT URBAN SITES (a)

	No. of Samples	Expected NH_4^+ Based on NO_3^- and SO_4^{2-} Present (b)	Observed NH_4^+ As % of Expected
Harbor Freeway	2	4.0	103
Pasadena	6	4.0	82
West Covina	4	10.3	76
Pomona - 1972	5	8.9	94
Pomona - 1973	2	6.6	75
Riverside	7	7.9	93
Rubidoux	3	15.5	73
Dominguez Hills	2	7.9	62
Pt. Arguello	1	2.7	131
Goldstone	1	0.9	79
Hunter Liggett	1	1.9	125
S.F. Airport	1	1.0	71
Richmond	2	1.7	59
Fresno	2	3.6	106
San Jose	7	3.0	78
AVERAGE		6.2	85

^aAnalyses on hi-vol samples collected on Whatman-41 filters.

^bAssuming the composition $(\text{NH}_4)_2\text{SO}_4$ and NH_4NO_3 .

The units are $\mu\text{g}/\text{m}^3$.

SC524.25FR

TABLE 3-12

 AMMONIA CONCENTRATIONS vs OBSERVED NH_4^+ AT NONURBAN SITES
 ($\mu\text{g}/\text{m}^3$)

<u>Site</u>	<u>NH_3</u>	<u>$\text{SO}_4^{=}$</u>	<u>NO_3^-</u>	<u>NH_4^+</u>	<u>Calc.^a NH_3</u>	<u>Obs. NH_3/ Calc. NH_3</u>	<u>Obs. NH_4^+ (As % of Expected)</u>
Pt. Arguello	9.7±2.8	6.5	0.99	0.36	2.57	3.8	131
Goldstone	4.6±0.9	1.20	1.50	0.71	0.84	5.5	79
Fresno	15.6±4.7	3.59	7.67	3.8	3.37	4.6	106

^aThe concentration of NH_3 just required to neutralize $\text{SO}_4^{=}$ and NO_3^- assuming their presence as H_2SO_4 and HNO_3 .

SC524.25FR

TABLE 3-13

 AFTER FILTER CHEMISTRY FOR SAMPLES OBTAINED
 NEAR THE HARBOR FREEWAY SEPTEMBER 20, 1972
 ($\mu\text{g}/\text{m}^3$)

<u>Species</u>	<u>Auto Exhaust Dominated</u>	<u>Mid-Town Mixed Aerosol</u>
	0500-0700 PST	0700-0900 PST
Al	0.0334 \pm 0.0099	- \pm -
Br	6.32 \pm 0.14	1.65 \pm 0.070
Ca	0.097 \pm 0.024	0.174 \pm 0.023
Cl	3.19 \pm 0.10	0.963 \pm 0.061
Fe	0.112 \pm 0.005	0.235 \pm 0.009
Na	0.136 \pm 0.032	0.168 \pm 0.0276
Pb	13.3 \pm 0.5	5.75 \pm 0.23
V	0.00712 \pm 0.00712	0.00821 \pm 0.00031
Zn	0.094	0.109 \pm 0.004
S ⁺	1.20 \pm 0.3	1.63 \pm 0.30
S ⁻	1.50 \pm 0.3	0.48 \pm 0.09
C	- -	26.4 \pm 4.0
Mass	68.6 \pm 7.6	58.4 \pm 6.4

 *Based on total filter (silver membrane)

SC524.25FR

TABLE 3-14

OVERALL AVERAGED ANALYSIS FOR CHEMICAL
 CONSTITUENTS OF SAN NICOLAS ISLAND AEROSOL
 (BASIS 30 $\mu\text{g}/\text{m}^3$ OF PARTICLE CONCENTRATION)

<u>Constituent</u>	<u>Percent by weight^a</u>	
Al	2.8	($\pm 50\%$)
Si	5.0	($\pm 50\%$)
Na	3.6	($\pm 5\%$)
P	N.D. ^b	
Cl	9.9	($\pm 10\%$)
K	1.3	($\pm 25\%$)
Ca	1.9	($\pm 25\%$)
Ti	0.15	($\pm 20\%$)
V	N.D.	
Cr	0.02	($\pm 20\%$)
Mn	.04	($\pm 20\%$)
Fe	1.6	($\pm 20\%$)
Cu	0.6	($\pm 20\%$)
Zn	0.2	($\pm 20\%$)
Br	0.2	($\pm 20\%$)
Pb	0.4	($\pm 20\%$)
I	N.D.	
SO ₄ ⁼	17.5	($\pm 10\%$)
NO ₃ ⁻	5.7	($\pm 10\%$)
NH ₄ ⁺	2.2	($\pm 10\%$)
Total organics accounted for	53.1	
Cyclohexane soluble (organics)		20 ($\pm 10\%$)
Non-carbonate carbon	3.0	
Sum of constituents	56.1	
Total ash content (TAC)	74.6	
Loss on ignition (100-TAC)	25.4	

^aPercentage in parentheses is error estimated by analyst; x-ray fluorescence for α -particle excitation only.

^bN.D. is less than minimum detectable concentration.

SC524.25FR

is given in Chapter X.

By similar arguments, the impact of groups of stationary sources potentially can be examined using the data taken at Dominguez Hills. Shown in Table 3-15 are three illustrative cases corresponding periods of markedly different wind directions. Toward the south of the sampling site were chemical works mixed with refineries further distant. To the west is a large refinery complex and a major freeway. To the northeast is the general urban mix of Los Angeles, with a nearby oil field. The data tabulated show, as in Table 3-13, that the variations between samples transported from different wind directions are relatively small. As expected, such elements as vanadium and nickel appear to be larger in concentration from the stationary source dominated areas. Considerably more ground level sulfate was observed from the chemical plant to the south than from the west. However, the reverse was apparently true in the case for nitrate. For unknown reasons, there is significantly more iodine from the south than from the west. The lead concentration is significantly higher in air drifting in from the northeast, as was the total mass concentration. Yet the sulfate concentration was surprisingly low.

There are marked differences between the freeway aerosols sampled in 1972 and the Dominguez Hills material, particularly in Al, Ca, Fe, Na, and V.

The complexity of the data taken at such source dominated sites is difficult to interpret, and it is necessary to continue to rely heavily on emission inventory data to understand the origins of such material.

From the results cited for illustration, it is not surprising that receptor sites "see" an aerosol that represents an extremely complex mixture of airborne particles that will vary from time to time, depending on transport and atmospheric chemistry. The interpretation of such data in terms of sources requires considerable insight into the aerometric conditions of an air basin, which is discussed in more detail in Chapter X.

C. AEROSOL BACKGROUND

An important factor in the development of control strategy for

SC524.25FR

TABLE 3-15
TOTAL FILTER CHEMICAL ANALYSIS OF SELECTED CASES
AT DOMINGUEZ HILLS (in $\mu\text{g}/\text{m}^3$)

Species	South Wind (WK)	West Wind (WL)	(Variable) North/ Northeast Wind (WL/WK)
	1000-1200 PST	1200-1400 PST	0100-0600 PST
Na	2.42±0.113	1.20±0.097	-
Mg	N.D.	N.D.	-
Al	1.50±0.063	0.521±0.035	1.2±0.6
Si	2.1±0.5	1.2±0.6	3.5±1.2
Cl	0.156±0.053	0.30±0.056	-
K	0.355±0.063	0.22±0.068	0.547±0.035
Ca	1.18±0.49	0.569±0.273	1.16±0.06
Ti	0.126±0.49	0.0811±0.0298	0.165±0.042
V	0.0592±0.0018	0.0487±0.0018	tr
Cr	tr	tr	0.015±0.004
Mn	0.0267±0.0017	0.0145±0.0013	0.043±0.003
Fe	1.01±0.04	0.561±0.022	1.57±0.06
Ni	0.047±0.003	0.080±0.004	0.022±0.002
Cu	0.021±0.003	0.013±0.003	0.029±0.002
Zn	0.142±0.006	0.099±0.004	0.200±0.008
Br	0.154±0.0044	1.78±0.0051	2.16±0.09
Pd	tr	N.D.	-
I	0.0142±0.00096	0.0059±0.00066	-
Ba	0.0540±0.0111	tr	-
Hg	tr	tr	N.D.
Pb	1.28±0.05	1.13±0.050	6.03±0.24
NO ₃	3.58±0.358	1.72	7.31±0.73
SO ₄	50.3±5.03	11.8	2.33±0.23
C*	14.1	-	-
Mass	142±1.57	66.1	205±1.5

* Based on sum of CPR + CNV + CVL

SC524.25FR

California air basins is the aerosol background. The effective background may be sufficiently large in many cases to be a major fraction of the overall aerosol burden.

The "background" is somewhat difficult to define because it represents a combination of material coming from natural sources such as marine aerosol from evaporated sea water droplets, wind blown soil dust, and aged aerosol from many distant origins mixed with fresh material.

Part of the ACHEX was designed to provide some information about all three of these components. The desert background has been studied by considering the phenomenology of the Goldstone results in 1972. The discussion of this study is given in Appendix A.

The distinction between an urban aerosol and a background aerosol of simple origins such as a marine aerosol can be illustrated well in results obtained from the analysis of samples taken at San Nicolas Island in 1970. San Nicolas Island (SNI) is located a distance of 120 km almost directly west of Los Angeles and represents a useful background station for air entering the South Coast Basin.

Shown in Figure 3-21 is a bar diagram of the concentration of several species found in the San Nicolas aerosol compared with calculated values for the Los Angeles background given by Miller *et al.*⁽¹⁶⁾ and made up exclusively of sea salt and soil dust. There is agreement between the SNI data and the estimated background for only some constituents. Notable departures are found between sulfate and nitrate, as well as copper. In the latter case, the Cu at SNI values are believed to be far too high from contamination by aerosols generated in the hi-vol motor. In any case, one can see the striking differences between the Pasadena/urban aerosol and the SNI material.

The SNI aerosol composition represents a useful point of departure for defining an aged aerosol background for Southern California, where the marine air normally influences much of the Los Angeles Basin. A useful average value of this background aerosol concentration is $30 \mu\text{g}/\text{m}^3$. For such an example, the average composition is listed in Table 3-14.

It is expected that the background aerosol will tend to change in its

SC524.25FR

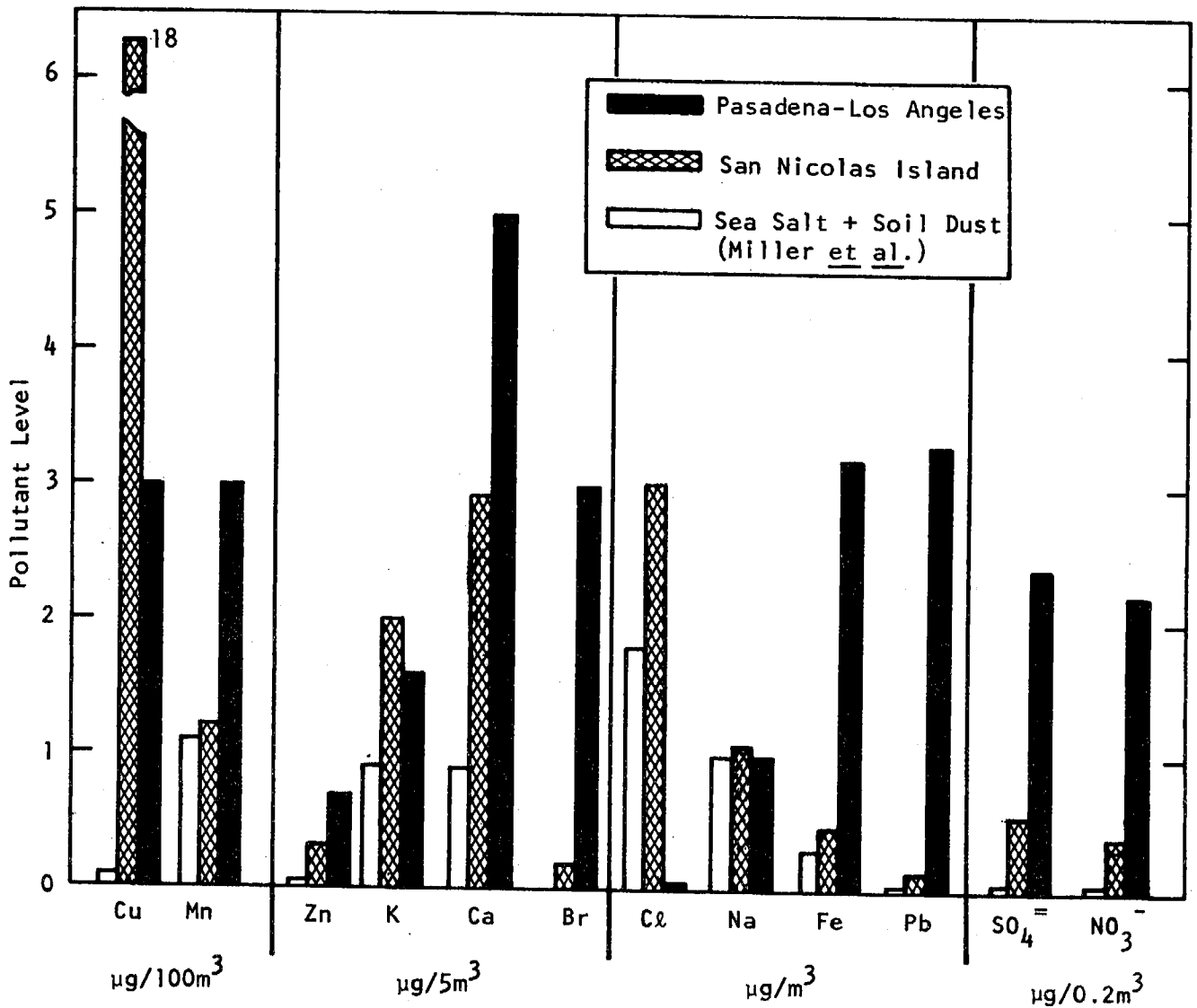


Figure 3-21. Comparison Between Trace Material Concentration in the Los Angeles Atmosphere and the Offshore Background on San Nicolas Island. Data for Average Concentrations in Pasadena Were Based on Results in 1969 Reported by Miller et al. (16), except for SO₄⁼ and NO₃⁻ Which Were Average Values from the National Air Surveillance Network.

SC524.25FR

chemical character eastward away from the ocean. This appears to be the case, as indicated by examination of some of the ACHEX chemistry. For example, it was found that a general depletion in sodium away from the sea was accompanied by a substantial increase in aluminum inland. The contribution of material of continental origins high in K and Ca relative to sea water also shows a systematic shift with distance from the ocean. These effects are illustrated in Figures 3-22 and 3-23, where the Ca/Na and K/Na ratios are plotted for the 1972 ACHEX data. Both of these ratios increase with distance from the ocean, with an approach toward the ratios expected for crustal rock.

Since there is a clear heterogeneity in the character of the background aerosol, with the exception of the secondary constituents, it appears that the most suitable definition for this material remains in terms of that attributed to sea salt (sodium tracer) and soil dust (silicon or aluminum tracer).

Perhaps most important to the development of control strategy for the South Coast Basin is the establishment of the background for sulfate, nitrate, and organic carbon. From the comparison in Figure 3-21, these contributions to the background are important by mass to the urban aerosol and should be defined as well as possible for existing measurements.

A recent survey by Trijonis⁽¹⁷⁾ has summarized the present knowledge of background sulfate, nitrate, and organic (solvent extractable) carbon. His tabulation is given in Table 3-16. These results show the widest variations in sulfate, but nitrate and organic carbon are similar for a number of marine dominated and desert sites. The high values of sulfate found in earlier data of Halzunt are believed to be non-representative of present conditions and are discounted here.

On the basis of the available data, it is recommended that the following values be used for the secondary background in $\mu\text{g}/\text{m}^3$:

	<u>Estimated Range</u>	<u>Adopted Value</u>
Total mass concentration	20 - 30	30
Sulfate (water soluble)	3 - 5	4
Nitrate (water soluble)	1 - 3	2
Organics (solvent extractable)	3 - 5	4

SC524.25FR

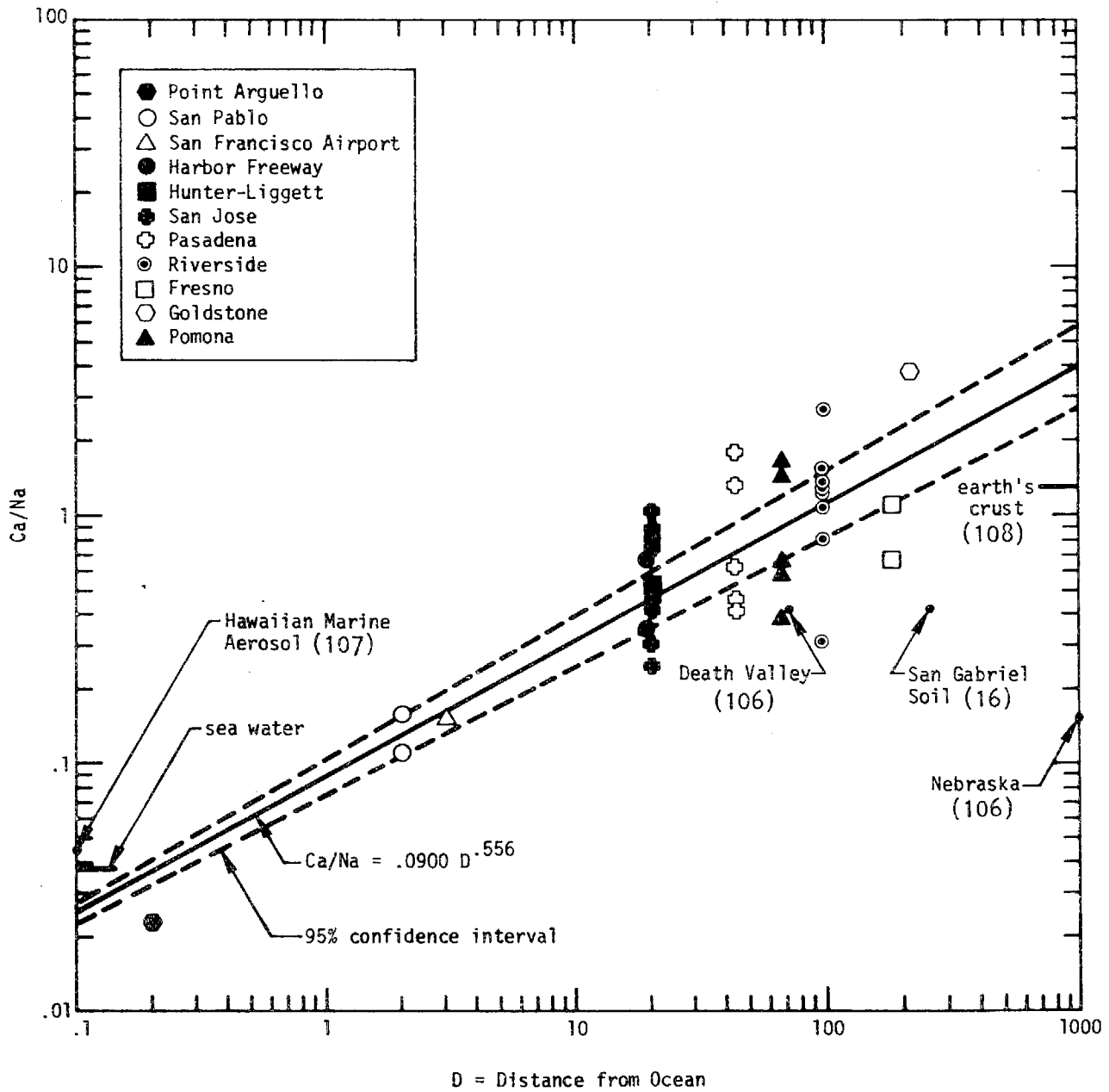


Figure 3-22. Variation in the Cu/Na Ratio with Distance from the Ocean. References are in parentheses.

SC524.25FR

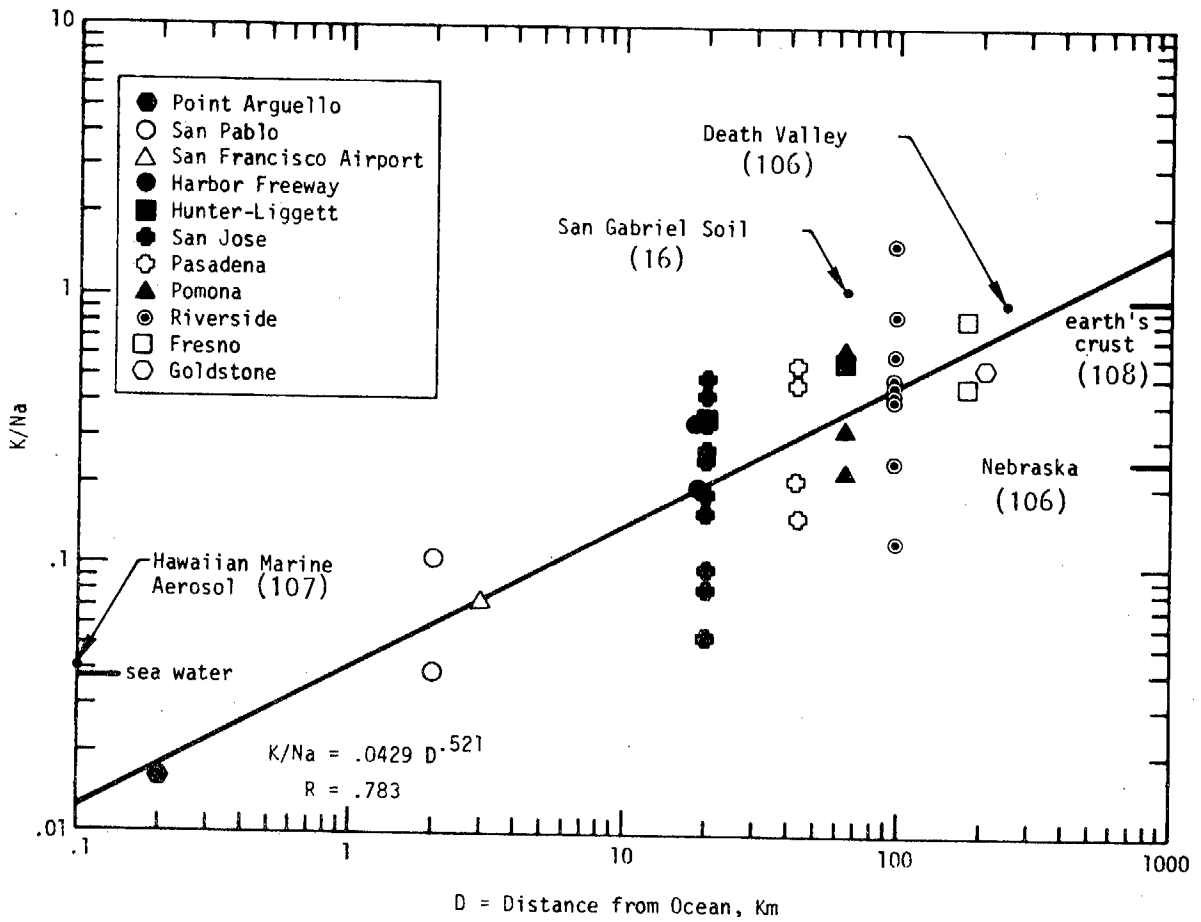


Figure 3-23. Variation in the K/Na Ratio with Distance From the Ocean.

SC524.25FR

TABLE 3-16

 SUSPENDED PARTICULATE MEASUREMENTS
 AT NONURBAN CALIFORNIA LOCATIONS
 (FROM TRIJONIS, REFERENCE 17)

Location	Date Source (Reference)	Number of Samples	Average Suspended Particulates ($\mu\text{g}/\text{m}^3$)			
			Total	SO_4	NO_3	Organics
MARINE ENVIRONMENT						
Crescent City (Lighthouse)	9	24	184	13.2	2.3	5.5 ^b
S.E. Farallon Island (Lighthouse)	9	46	184	13.8	1.0	4.1 ^b
Point Pedras Blancos (Lighthouse)	9	28	291	18.6	2.2	2.5 ^b
San Nicolas Island (150 meter elevation)	9	9	69	8.4	2.0	3.6 ^b
San Nicolas Island (200 meter elevation)	8	22	30	5.3	1.7	0.6 ^c
Point Reyes (USCG Station)	10	1	129	6.2	0.4	4.5 ^c
Point Arguello (USCG Station)	10	1	185	6.5	1.0	3.3 ^c
Trinidad (Lighthouse)	11	49	44	2.4	0.4	2.5 ^b
DESERT ENVIRONMENT						
Amboy	5	140	31*	3.3*	2.2*	3.4* ^b
Kramer Jct.	5	142	46*	4.5*	4.0*	3.5* ^b
29 Palms	5	145	61*	5.7*	3.6*	4.2* ^b
Needles	5	141	38*	3.3*	2.4*	4.1* ^b
Baker	5	141	44*	3.8*	2.8*	4.1* ^b
Goldstone	10	2	46	1.7	1.6	4.0 ^c

* Geometric Means

^b Extracted with Benzene^c Extracted with Cyclohexane

SC524.25FR

IV. PATTERNS OF DAILY CHANGE IN AEROMETRIC PARAMETERS

A number of the features of aerosol behavior are seen best by considering the diurnal patterns of change that took place during key episodes which were investigated. The purpose of this section is to provide a description of the highlights of several runs to establish the ground work for a detailed discussion of the elements of the secondary production mechanisms. First, a review is given of the episodes chosen to be of high priority interest in 1972, then a description of several 1973 cases is given.

A. SELECTED EPISODES FROM THE 1972 PROGRAM

1. POMONA - OCTOBER 24 AND 25, 1972

This particular episode was chosen for specially detailed examination, because it was the day with the highest oxidant levels observed during the fall of 1972 in the South Coast Basin; and, at the same time, it was the day that the highest extinction coefficient values were measured. The period is also of interest because it was the day that the MRI Aircraft program was making measurements, and the Metronics tracer study was underway. In general, the meteorology of the day has been discussed in Volume III, Section VI, but one important feature of the wind is of interest from the standpoint of the mobile laboratory results. There was a wind shift in the early morning on this day. Between 0800 and 0900, the winds were from the southeast. Later, about 1030, the wind shifted to bring air from the west-southwest sector into the Los Angeles County Fairgrounds. In general, the winds on that day were quite light at the surface, about 5 to 7 km/hr.

The aerometric data for pollutant gases for Pomona on October 24 are shown in Figure 4-1. Early in the morning, accompanying the southeast winds, the CO, total hydrocarbon, methane, and NO levels were relatively high, and all reached a minimum value about the time the wind shifted around to the west. NO₂ measured on this day was high in the morning hours when the wind was from the southeast; it then showed a minimum with the wind shift; and later, a second maximum, in the new air coming from the west. The data indicate that the air coming from the southeast was probably polluted by early morning vehicle traffic on the San Bernardino Freeway, just a couple of miles

SC524.25FR

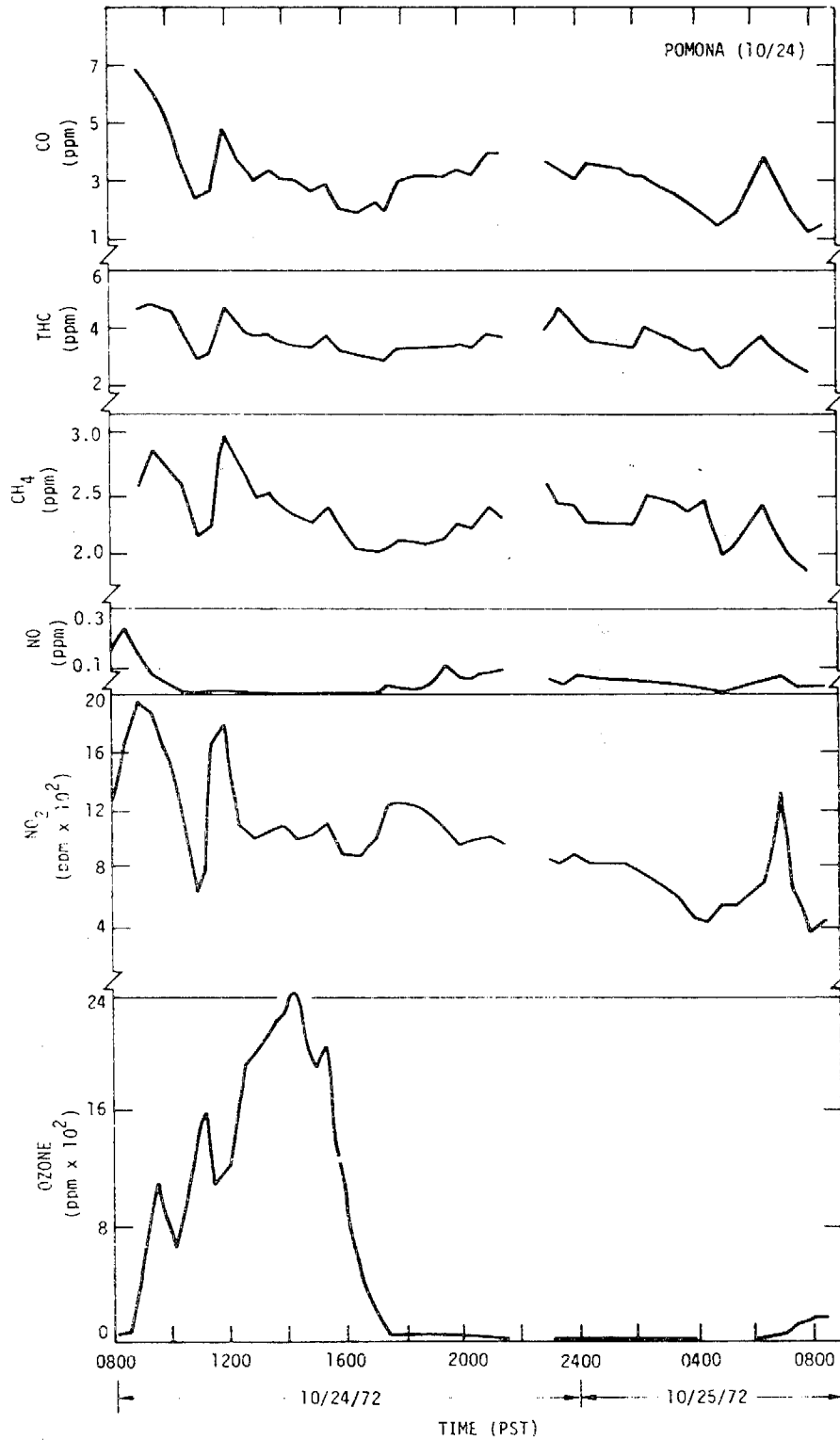


Figure 4-1. Diurnal Patterns of Pollutant Gases Taken at Pomona on October 24-25, 1972 (Sheet 1 of 2)

SC524.25FR

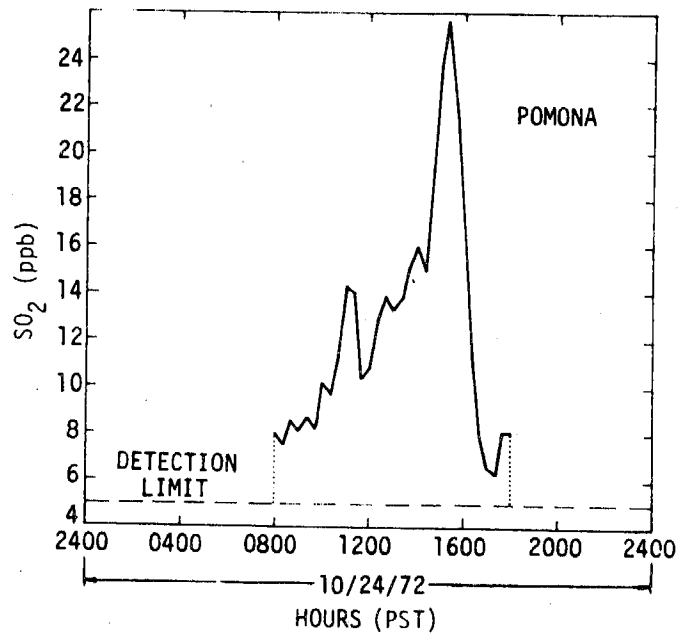


Figure 4-1. Diurnal Patterns of Pollutant Gases Taken at Pomona on October 24-25, 1972 (Sheet 2 of 2)

SC524.25FR

south of the site. With the wind shift in the early morning hours, the ozone level systematically increased to a maximum value of 0.24 ppm at 1400 PST. The early morning hours were accompanied by rather high humidity. During the later portion of the day, the air became drier, with an accompanying decrease in relative humidity. The mirrors in the dewpoint hygrometers in both the mobile laboratory and the University of Washington van were later found to be pitted. Therefore, the relative humidity measurements accompanying the data are not considered to be quantitatively accurate; however, qualitatively, the changes noted should be useful. The relative humidity results are expected to be systematically low by 10% or more.

In Figure 4-2, the diurnal changes in aerosol parameters for the October 24 period in Pomona are shown. Aitken nuclei population showed an early morning maximum of $\sim 1.6 \times 10^5$ particles/cc, gradually dropping off to a minimum in midmorning, with a second series of maxima late in the day, probably related to local traffic or other combustion sources. Perhaps the most interesting feature of this episode is the very strong increase in early morning of the integral scattering parameter, b_{scat} , followed by a systematic drop later in the day. This was accompanied by a maximum in the total surface area concentration and the volume fraction of aerosols. The maximum in the large aerosol particles in the aerosol distribution, as reflected by these parameters, accompanied the maximum in NO_2 level, but was not correlated at all with the maximum ozone concentration during the day. Despite the fact that there was a significant amount of photochemical activity during this day, the growth in the large aerosols, presumably from chemical transformations, was uncorrelated in time with ozone. It is in contrast to the "simple" picture obtained in Pasadena in 1969, where photochemical aerosol was characterized by a maximum in b_{scat} accompanying the maximum in oxidant level at midday.

The diurnal curves for the chemical species are shown in Figure 4-3. As at the Harbor Freeway, lead and bromine correspond well during the day. The total mass of aerosol on the after filter shows a maximum that is broad during morning and midday followed by a decrease in late afternoon. In this case, in a pattern similar to the development of the light scattering coefficient,

SC524.25FR

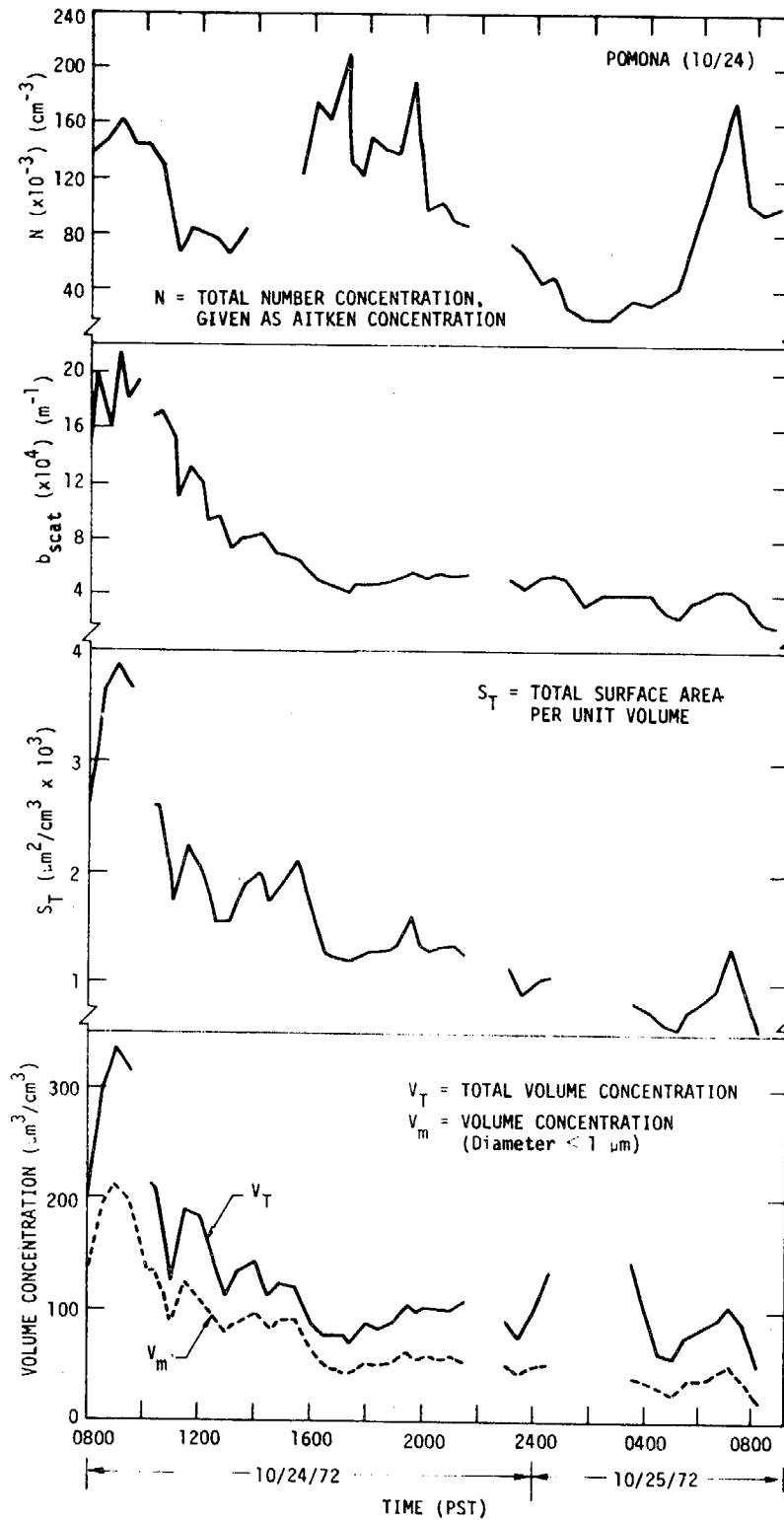


Figure 4-2. Diurnal Patterns of Aerosol Parameters Taken at Pomona on October 24-25, 1972

SC524.25FR

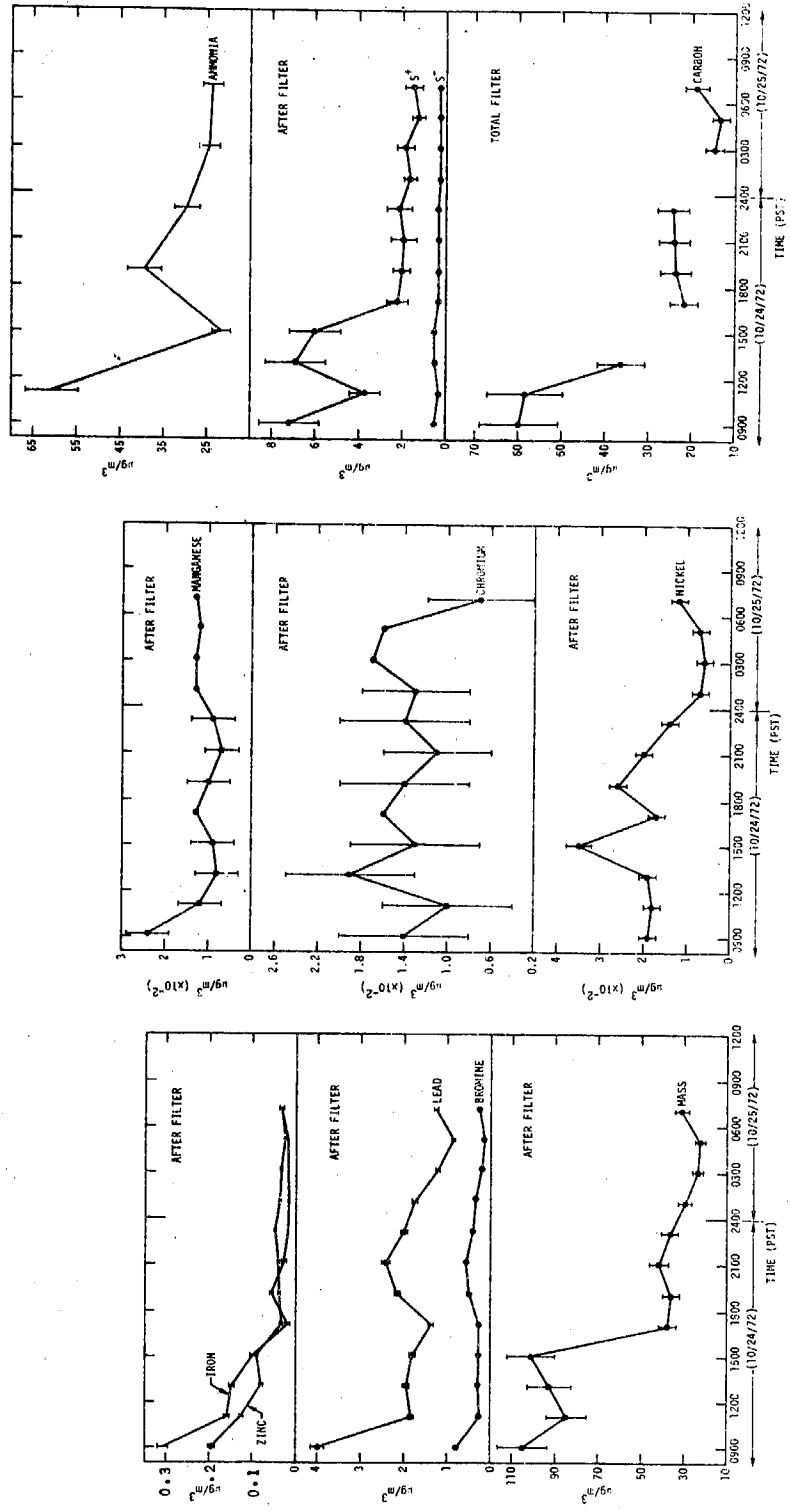


Figure 4-3. Diurnal Patterns of Chemical Species for Pomona - October 24-25, 1972

SC524.25FR

b_{scat} , lead, as well as the after filter mass, are high in the early morning on October 24 and decrease to a low level during the day. As with mass, the Pb and Br decrease to a lower level during the day, but there is a second maximum in lead and bromine by late in the afternoon. The lead and bromine are high along with high CO and NO in early morning. Later, with the wind shift, these elements are observed to decrease. On the other hand, the zinc and iron show high concentration in the morning with the total mass, and decrease to a low level during the day. The oxidized sulfur and reduced sulfur are also shown in Figure 4-3. The oxidized sulfur levels, in contrast to the Harbor Freeway, are considerably higher than those for the reduced sulfur. In the early morning, there is a high concentration in oxidized sulfur, decreasing in the morning, but returning to a second maximum in the midafternoon. The decrease is associated with the behavior of some of the trace gases, like CO, NO, and NO₂.

The total carbon measurement for Pomona showed a morning maximum, but interestingly enough, there is a general pattern of decrease in the afternoon to a low level by the end of the day. The ammonia diurnal pattern shows a morning maximum, and a later decrease in midafternoon, with a second peak developing in the evening hours. The correlation between ammonia and lead could indicate an automobile source for ammonia on this day. Of course, it is also possible that the ammonia was brought in from an area with a large cattle population (between Pomona and Los Angeles), with the same air mass that transports the aged aerosol from Los Angeles. A reinforcement of the correlation of ammonia concentrations with automobile exhaust products comes from a model constructed by BAAPCD. Based on data from the LAAPCD giving auto exhaust emissions of ammonia per gallons of gasoline consumed and a computer prediction of ambient concentrations based on source emissions, the BAAPCD has predicted ammonia levels in the Bay Area which are within a factor of 2 to 3 of those found in the present study (Levaggi, private communication). Thus, in areas where natural sources of ammonia are of reduced importance, auto exhaust may be an important source of the ammonia found.

SC524.25FR

2. SOUTH COAST BASIN - SEPTEMBER 20 AND 21, 1972

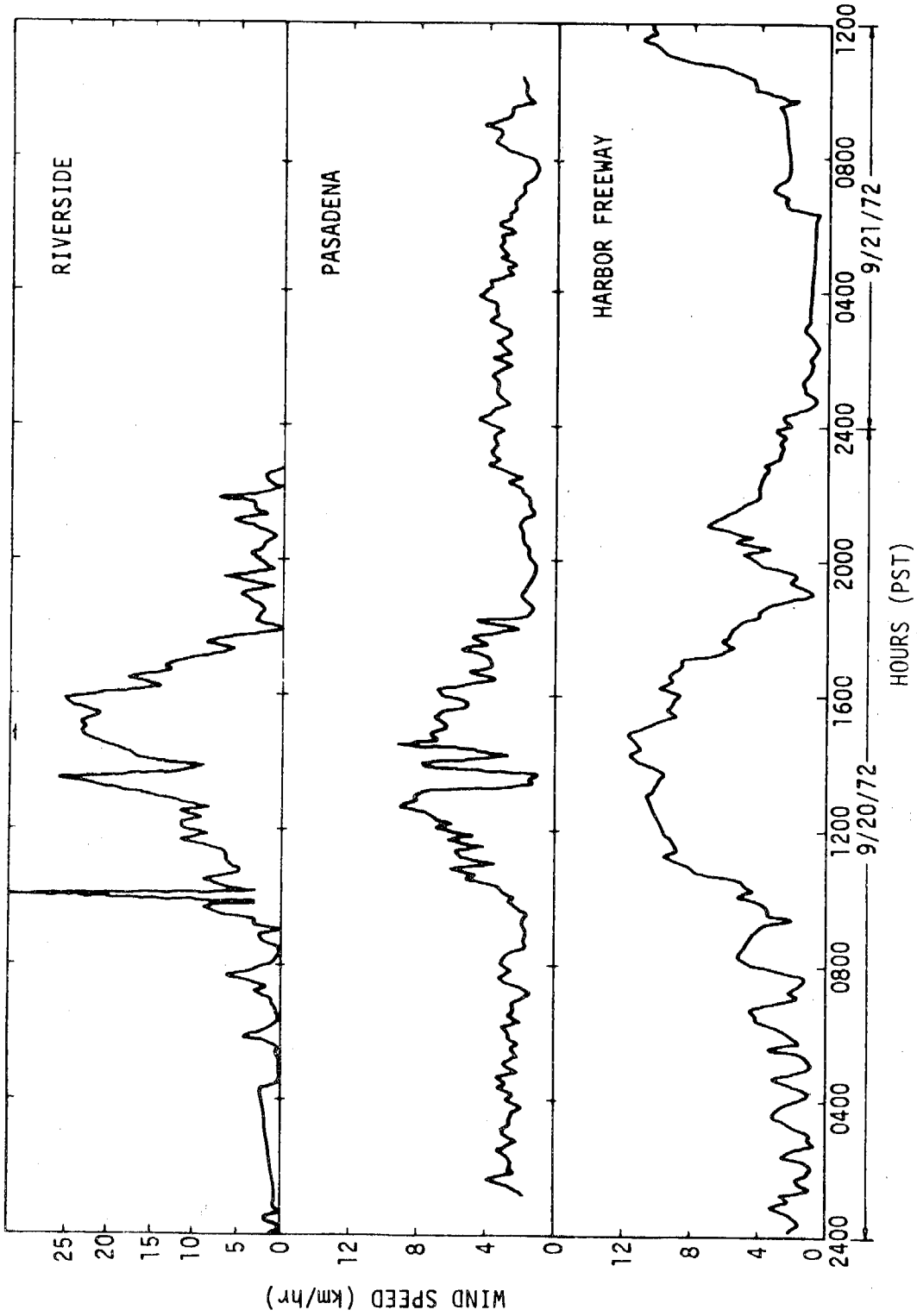
This episode was selected because it represented a case of rather dry air being present in the South Coast Basin, with a mild Santa Ana condition preventing a smog buildup in the eastern and northern part of the basin.

The measurements taken at the Harbor Freeway should reflect a strong contribution from automobile emissions, without the complicating effect of strong chemical transformations. This day was also of interest in that MRI and Metronics were conducting their respective experiments. The results taken at the Harbor Freeway were particularly interesting because of two periods: (1) between 0700 and 0900 and (2) an extended period during the midday, when the winds were blowing directly across the Harbor Freeway toward the trailer. There were one or two other conditions, when the wind reversed and blew more aged aerosol from downtown back across the trailer, giving an interesting and useful comparison of aerometric conditions. The diurnal plots for the Harbor Freeway, Pasadena, and Riverside for September 20, shown in Figure 4-4, a through k, represent 10-minute average data, as plotted directly from the computer output. The data indicate particularly high levels of NO and CO when the wind was blowing from the freeway. Also, the ratio of ethylene and acetylene was quite high at the Harbor Freeway; they were found to be essentially unity. Interestingly enough, this location showed the lowest oxidant maximum and ozone level observed during the program; the level observed here was even lower than for the background sites. Of course, this was probably due to the reaction of ozone - the scavenging of ozone by the high concentrations of NO from motor vehicle traffic. The results from Pasadena and Riverside on this day indicate systematically low levels of pollutant gases. There appears to be some correspondence between data from different sites for some of the pollutants, whereas, little correspondence is observed for some of the others. The aerosol measurements indicate that the day was quite clean.

The Aitken nuclei population at the various locations was of the order 10^4 to 10^5 particles/cc or lower. b_{scat} was in the range of $1 \times 10^{-4} \text{ m}^{-1}$, representing a day with quite high visibility.

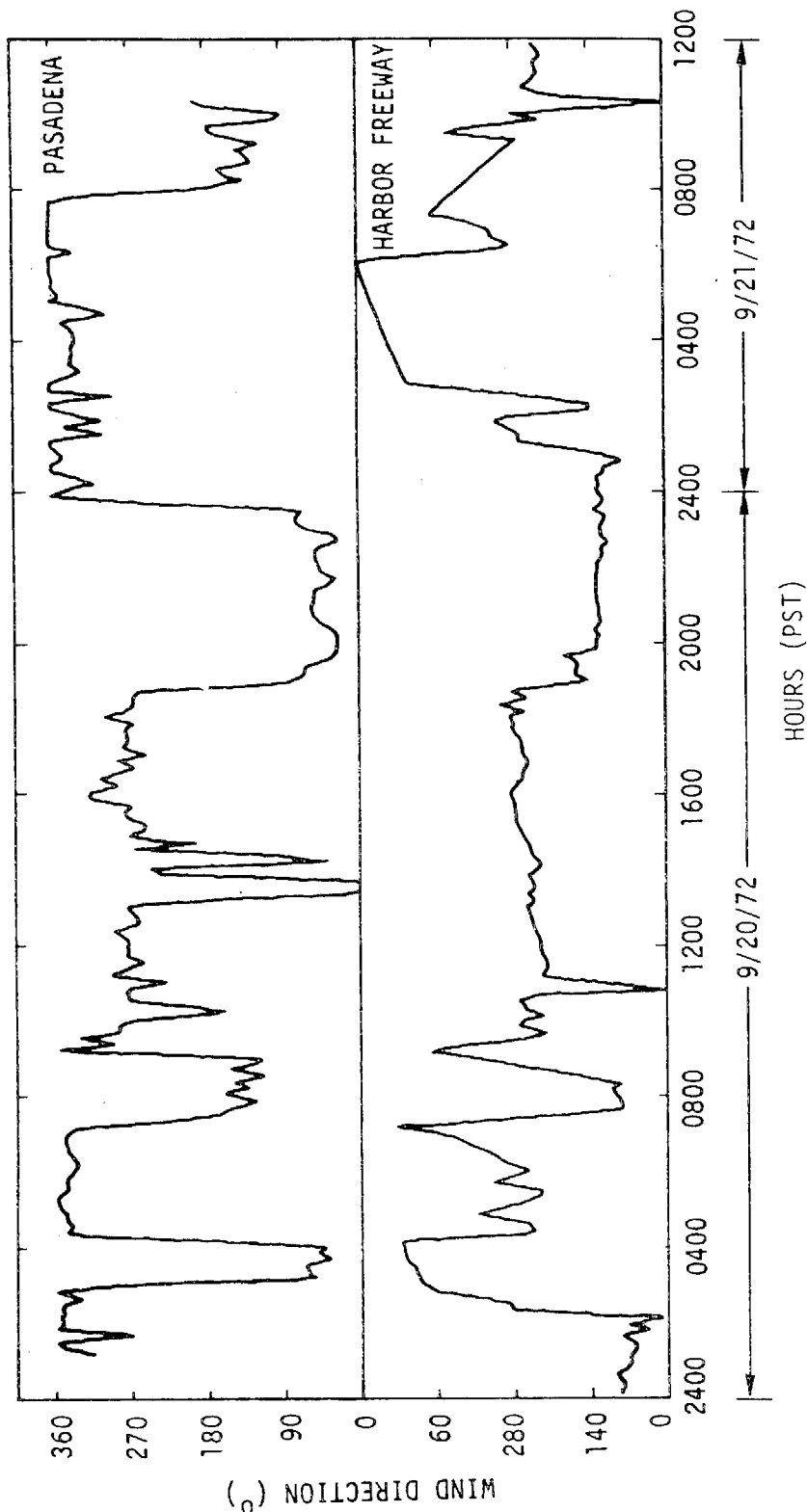
The SO_2 data measured by the Varian instrument on the trailer indicate very strong oscillations in SO_2 concentrations during the day, reaching the

SC524/25FR



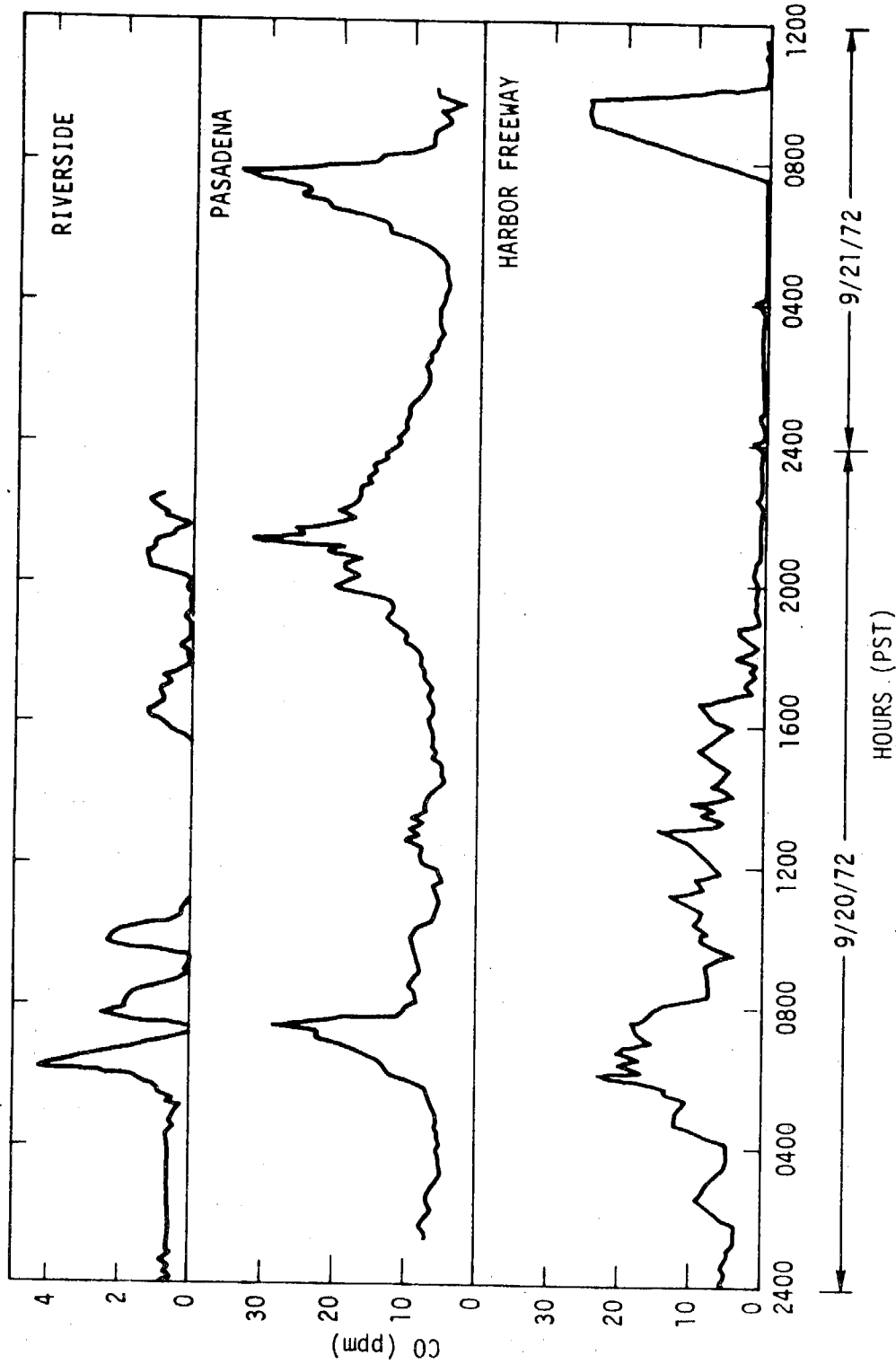
a. Wind Speed
Figure 4-4. Diurnal Patterns for Riverside, Pasadena, and Harbor Freeway
on September 20-21, 1972 (Sheet 1 of 11)

SC524.25FR



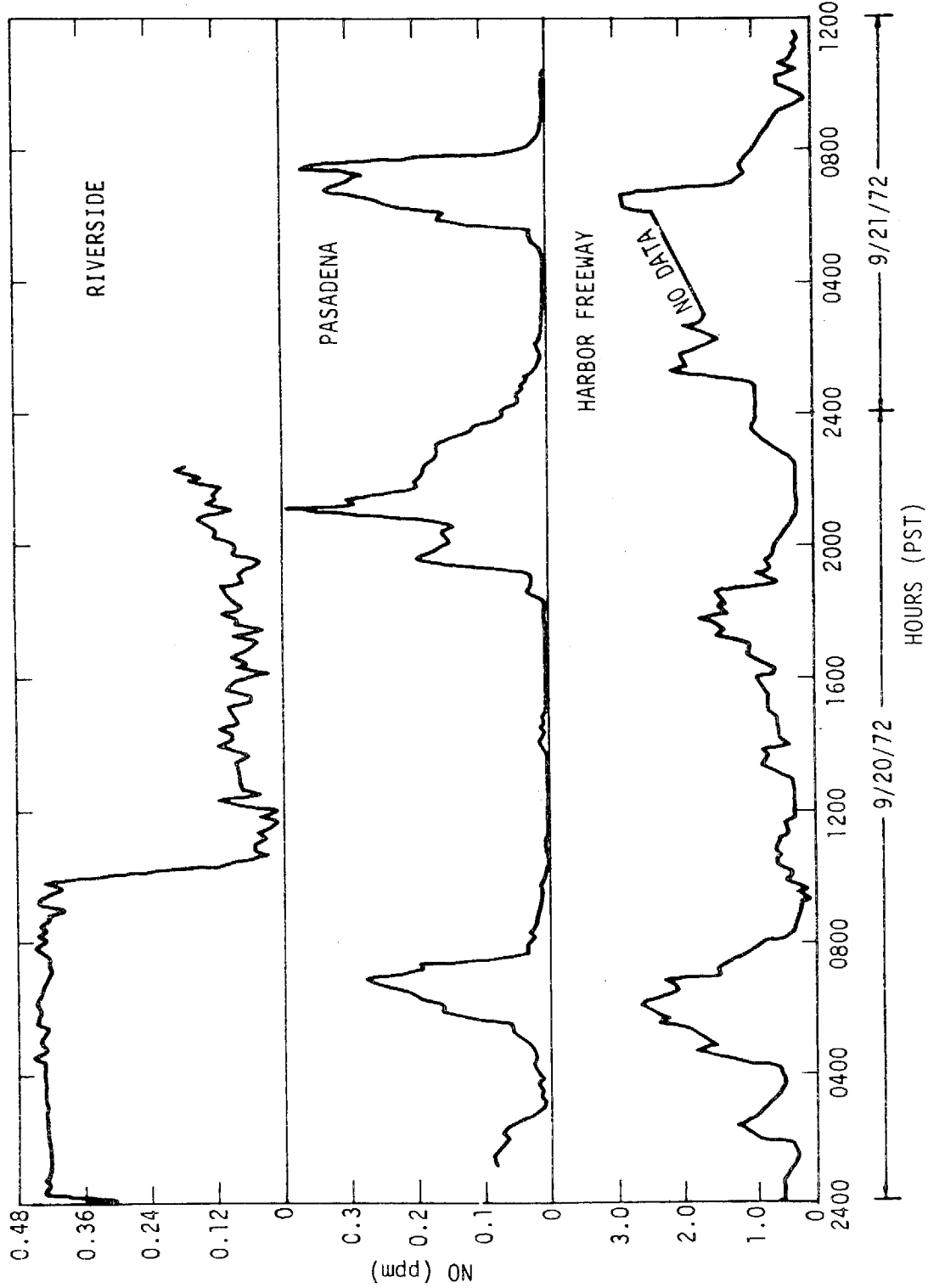
b. Wind Direction
Figure 4-4. Diurnal Patterns for Riverside, Pasadena, and Harbor Freeway
on September 20-21, 1972 (Sheet 2 of 11)

SC524.25FR



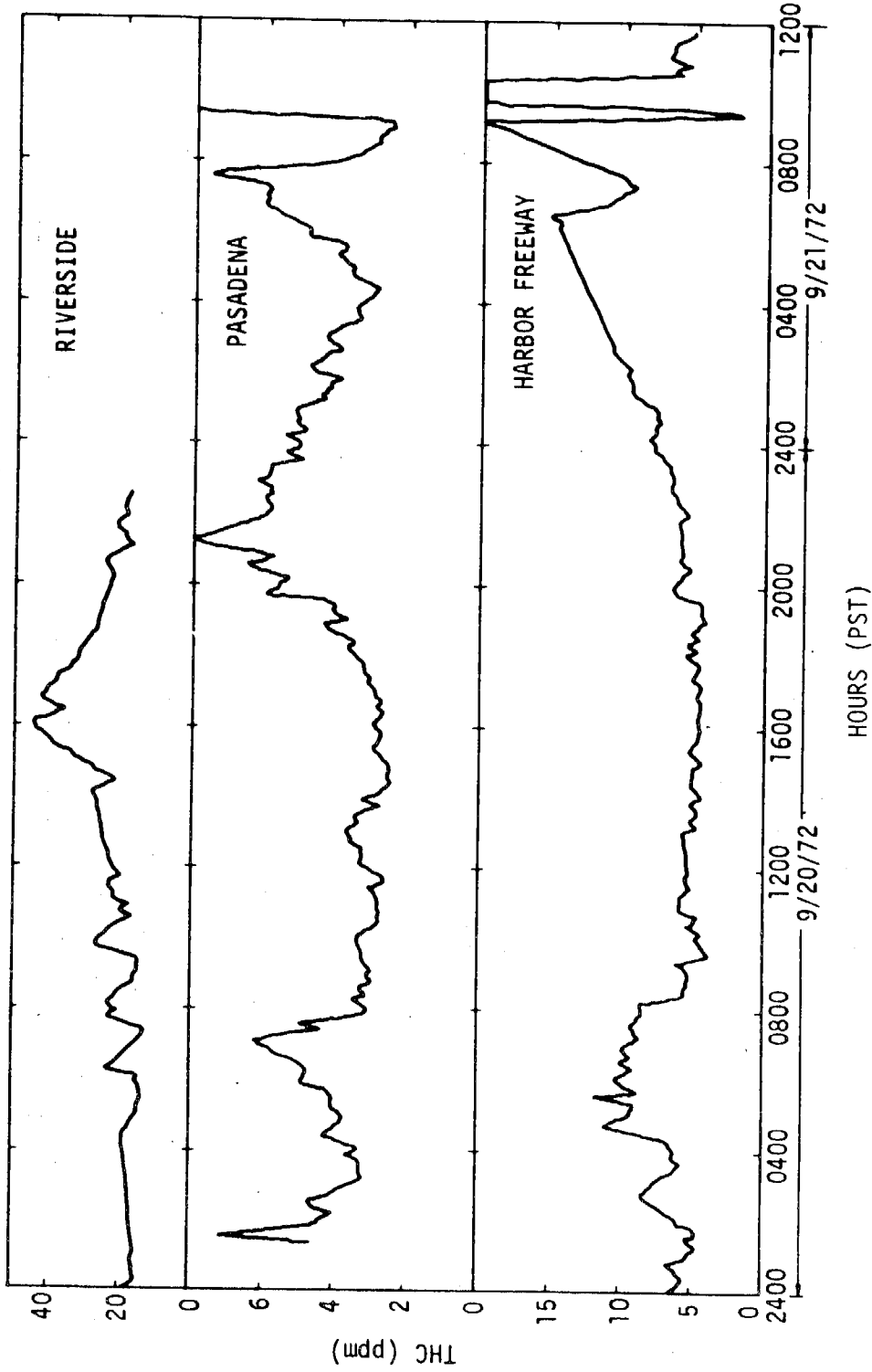
c. Carbon Monoxide
Figure 4-4. Diurnal Patterns for Riverside, Pasadena, and Harbor Freeway
on September 20-21, 1972 (Sheet 3 of 11)

SC524.25FR



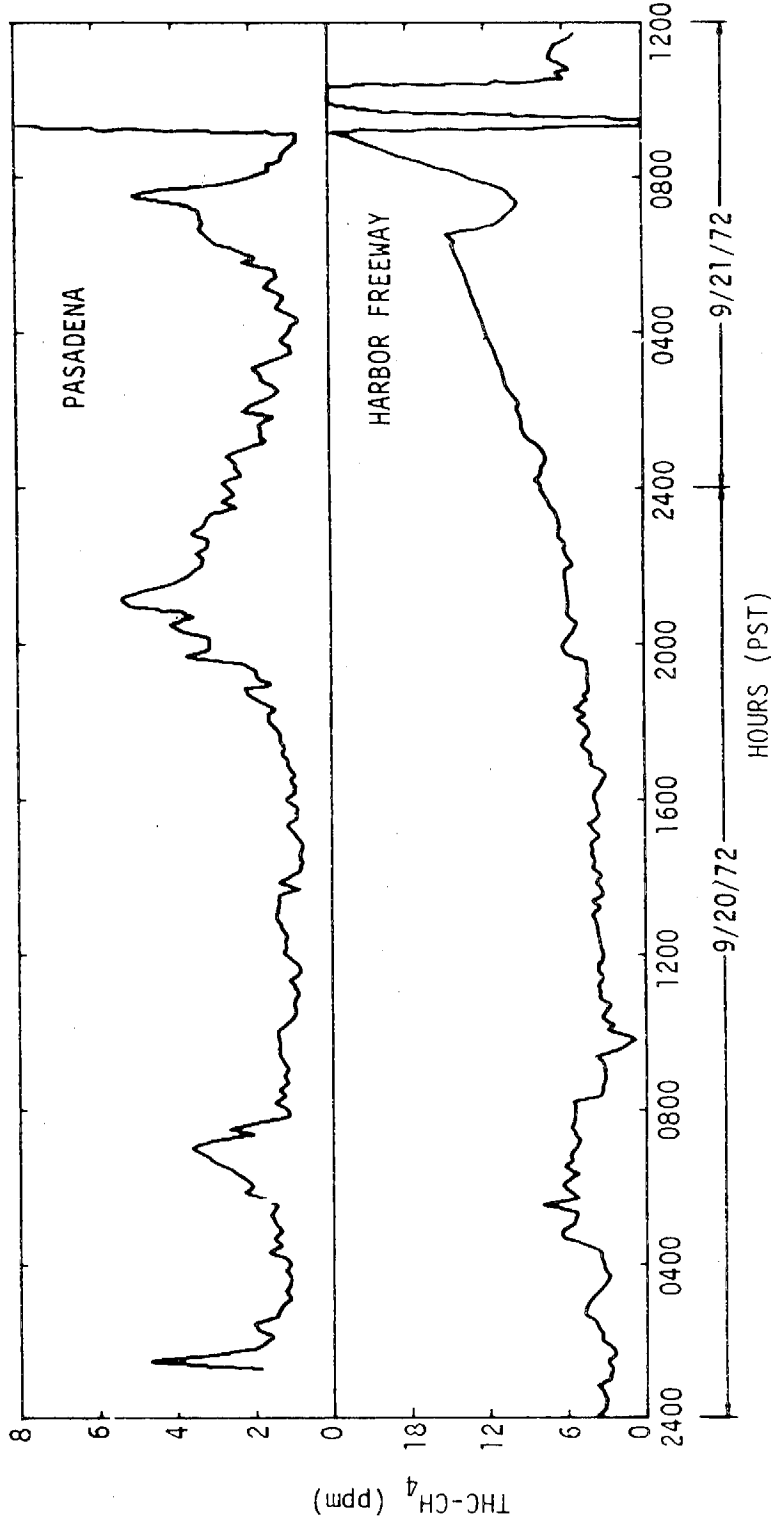
d. Nitric Oxide
Figure 4-4. Diurnal Patterns for Riverside, Pasadena, and Harbor Freeway
on September 20-21, 1972 (Sheet 4 of 11)

SC524.25FR



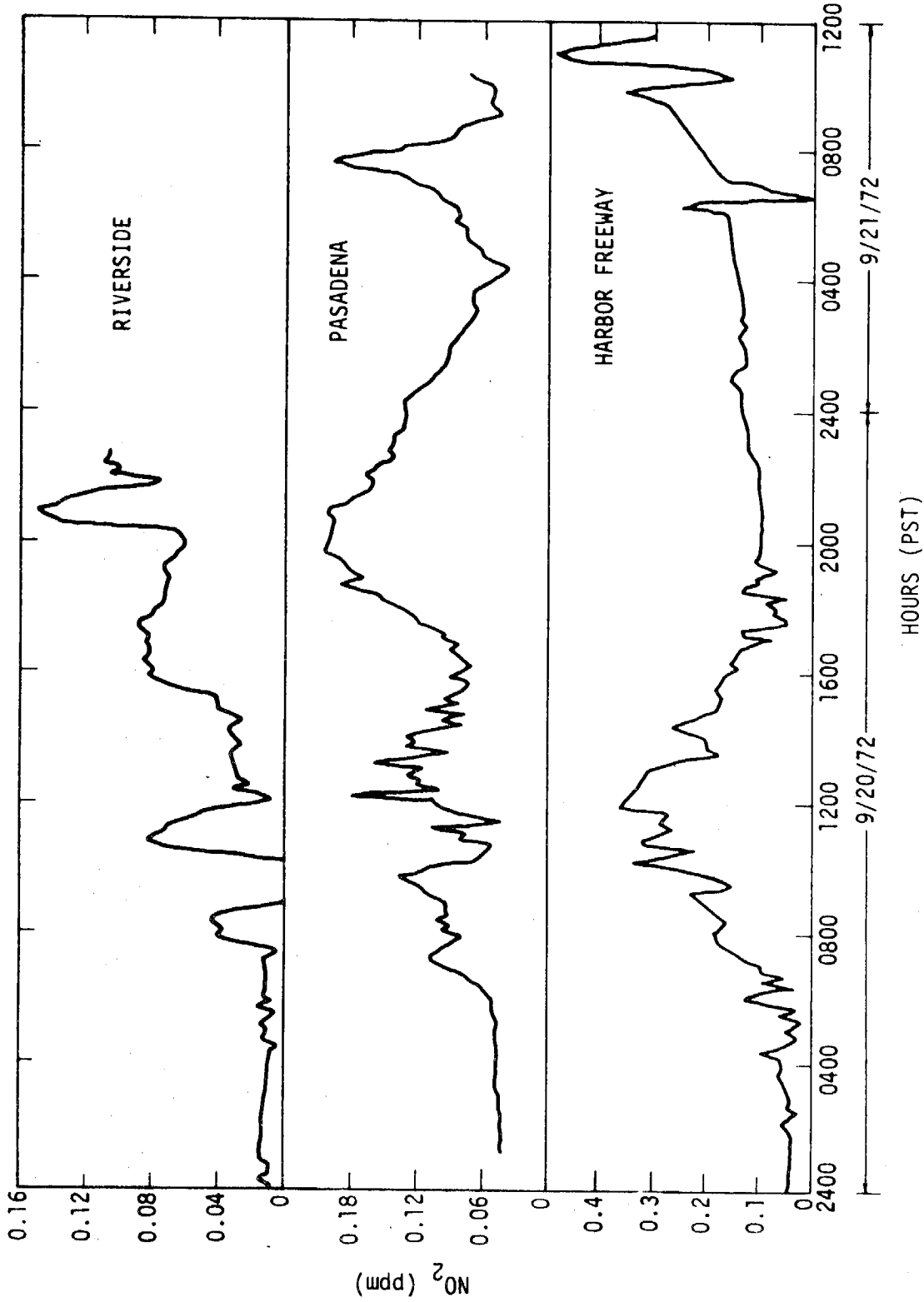
e. Total Hydrocarbons
Figure 4-4. Diurnal Patterns for Riverside, Pasadena, and Harbor Freeway
on September 20-21, 1972 (Sheet 5 of 11)

SC524.25FR



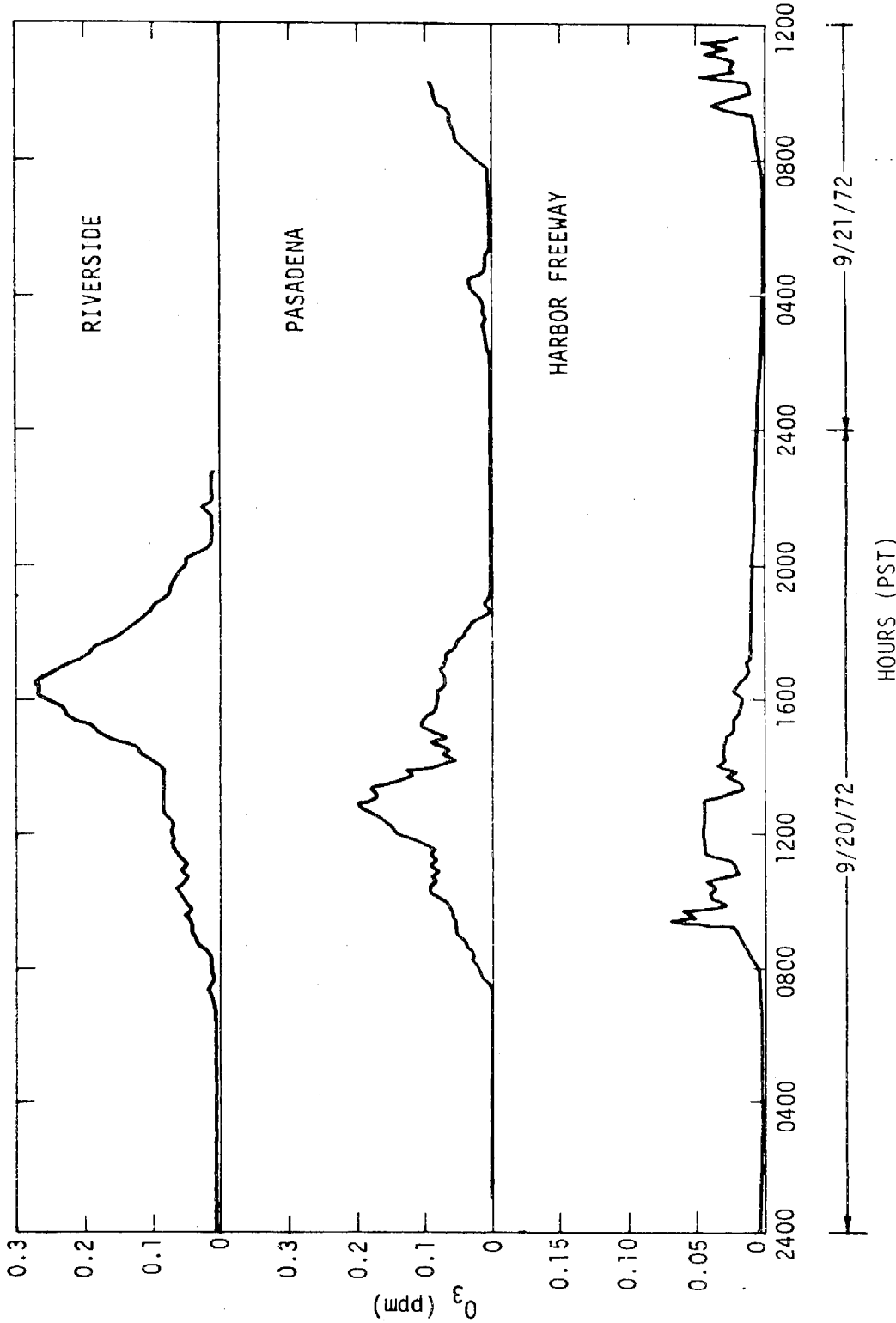
f. Total Hydrocarbons - Methane
Diurnal Patterns for Riverside, Pasadena, and Harbor Freeway
on September 20-21, 1972 (Sheet 6 of 11)

SC524.25FR



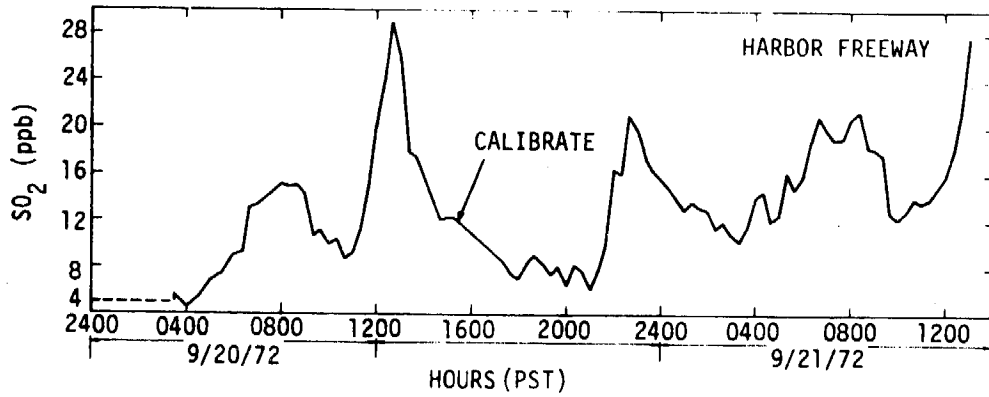
g. Nitrogen Dioxide
Figure 4-4. Diurnal Patterns for Riverside, Pasadena, and Harbor Freeway
on September 20-21, 1972 (Sheet 7 of 11)

SC524.25FR

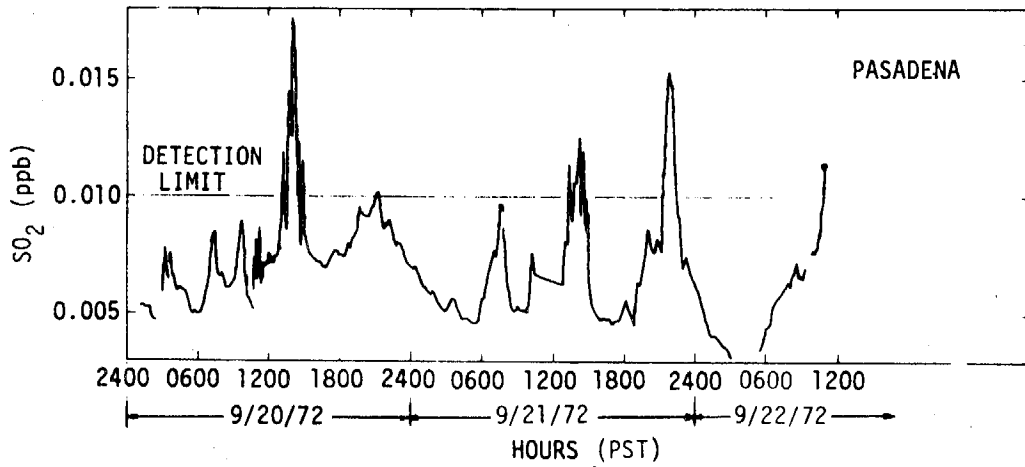


h. Ozone
Figure 4-4. Diurnal Patterns for Riverside, Pasadena, and Harbor Freeway
on September 20-21, 1972 (Sheet 8 of 11)

SC524.25FR



(1) Harbor Freeway



(2) Pasadena

i. Sulfur Dioxide

Figure 4-4. Diurnal Patterns for Riverside, Pasadena, and Harbor Freeway on September 20-21, 1972 (Sheet 9 of 11)

SC524.25FR

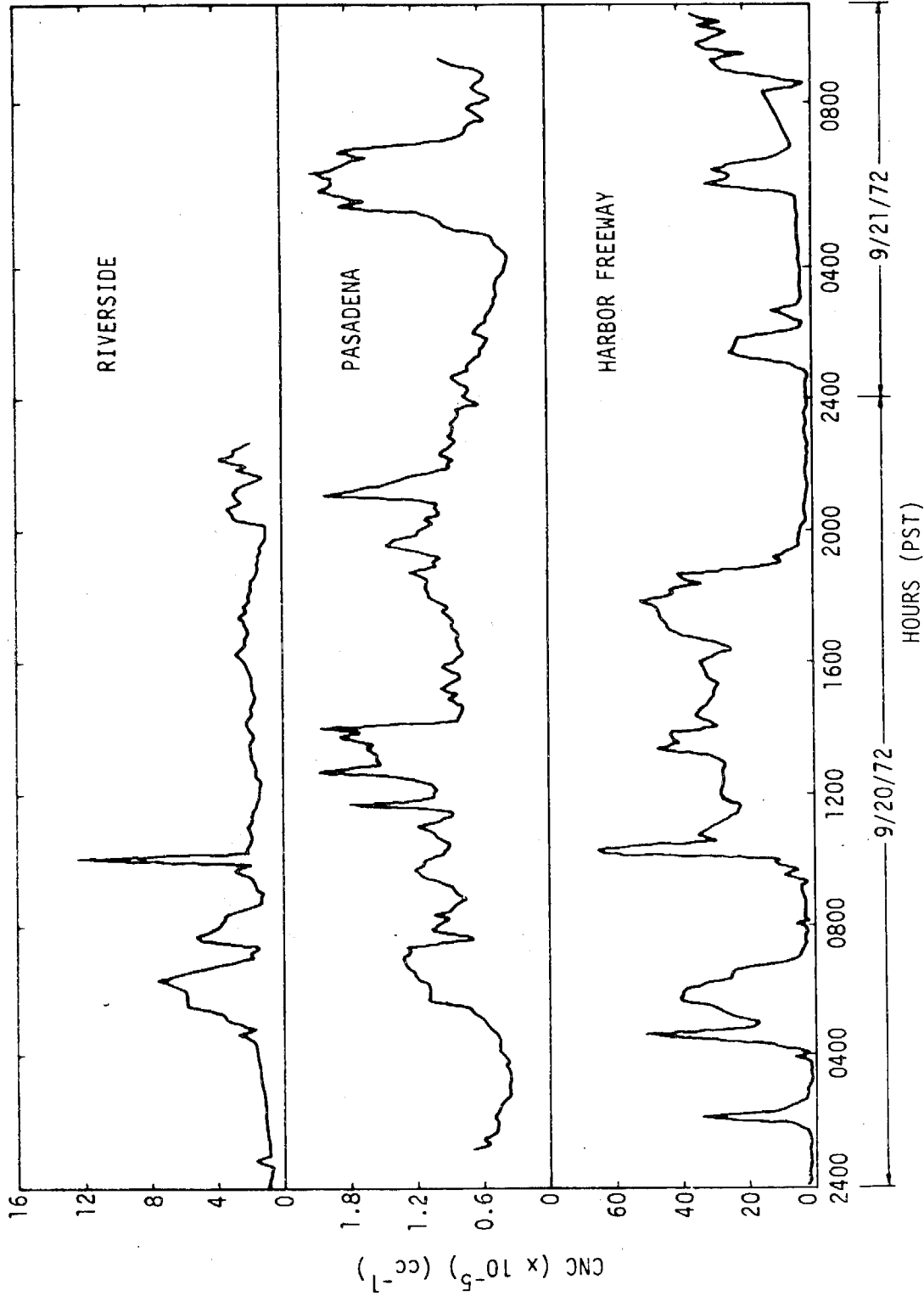
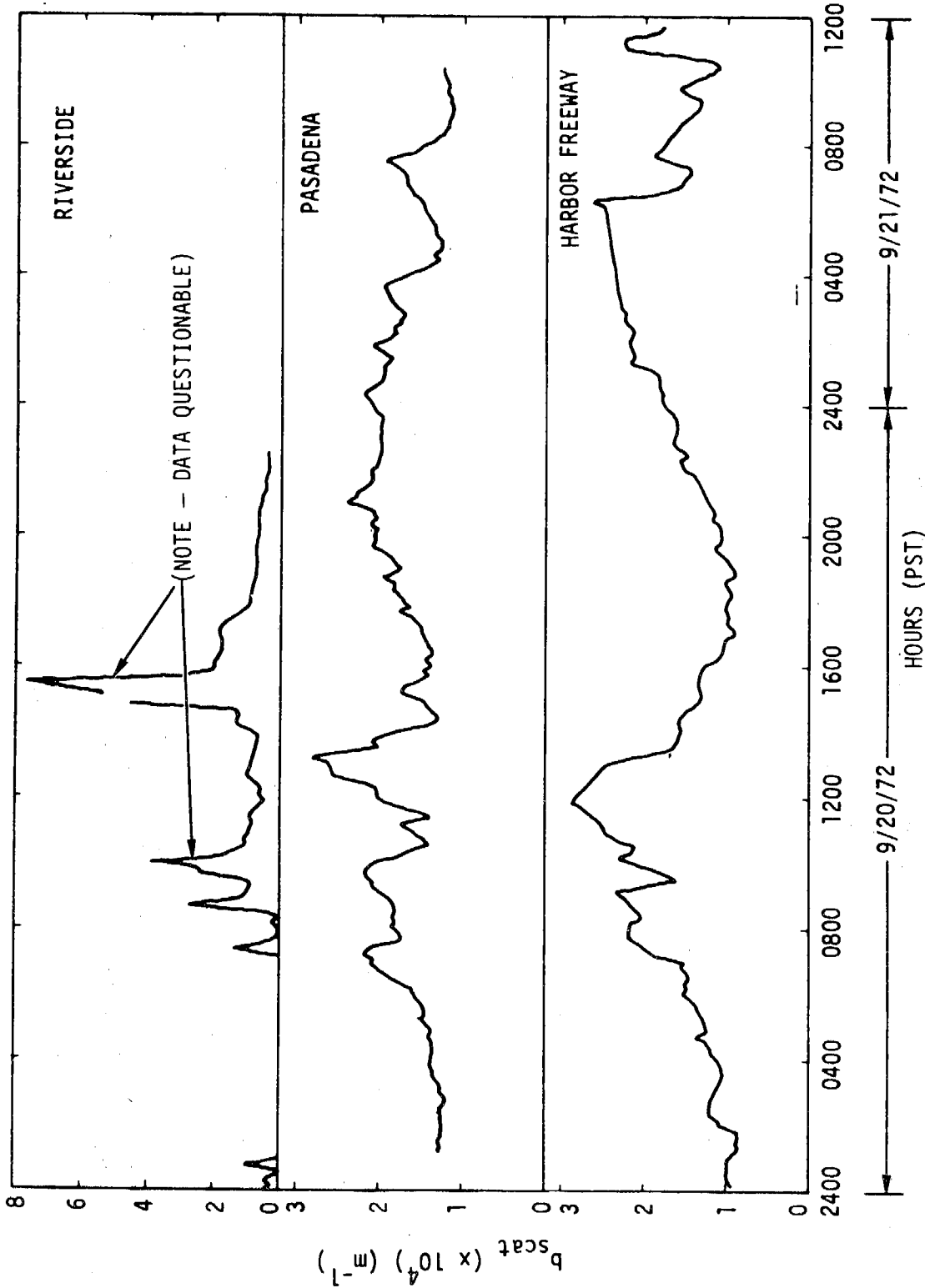


Figure 4-4. J. Condensation Nuclei Concentration Diurnal Patterns for Riverside, Pasadena, and Harbor Freeway on September 20-21, 1972 (Sheet 10 of 11)

SC524.25FR



k. Extinction Coefficient Due to Light Scattering
Figure 4-4. Diurnal Patterns for Riverside, Pasadena, and Harbor Freeway
on September 20-21, 1972 (Sheet 11 of 11)

SC524.25FR

highest concentration observed during our stay in the South Coast Basin (~ 0.12 to 0.13 ppm SO_2). In contrast, the SO_2 levels were below the limit of detectability at Riverside, and reached and exceeded the nominal detection limit at the Pasadena station only a few times during this day. In general during this period, one sees that the concentration of total sulfur in the atmosphere remained below or near 10 ppb away from areas dominated by local sources. The Varian chromatograph essentially measured no H_2S within the limits of detection at any of the locations in the South Coast Basin.

The diurnal plots of heavy elements, as measured by LBL x-ray fluorescence for the Harbor Freeway, Pasadena and Riverside, September 20, are shown in Figures 4-5 through 4-7. Samples of the inorganic fraction at the Harbor Freeway are shown in Figure 4-5A. In these data, there are very marked changes during the day in the filter-collected aerosols. In the case of the total filter (from the trailer) and the after filter (on the Lundgren impactors), the lead patterns show a very strong peak in early morning and in the evenings that is associated with the heaviest traffic during the day at the freeway. On the other hand, the zinc and iron show somewhat different behavior. In particular, the iron shows a midday peak.

The data are particularly useful when one considers wind patterns. It is of interest, for example, that the 0700 to 0900 period in the morning was a case where the wind was blowing from the freeway most of the time. During the midday, the wind was again blowing directly from the freeway; but there were cases before 0700 to 0900 and after 1800 where the wind shifted to come from the east or southeast.

In Figure 4-5B, the patterns of oxidized and reduced sulfur are shown along with oxidized and reduced nitrogen compounds. It can be seen in these data that there is a suggestion that reduced sulfur on the total filters is related to the automobile with a strong morning peak. There is little correspondence between the oxidized sulfur and the reduced sulfur. At the freeway, the particulate sulfur content was quite large, and interestingly enough, the reduced sulfur concentration through the morning and evening hours was approximately the same as the oxidized sulfur. In the case of the nitrogen compounds, the ESCA analysis indicates that the reduced nitrogen concentrations

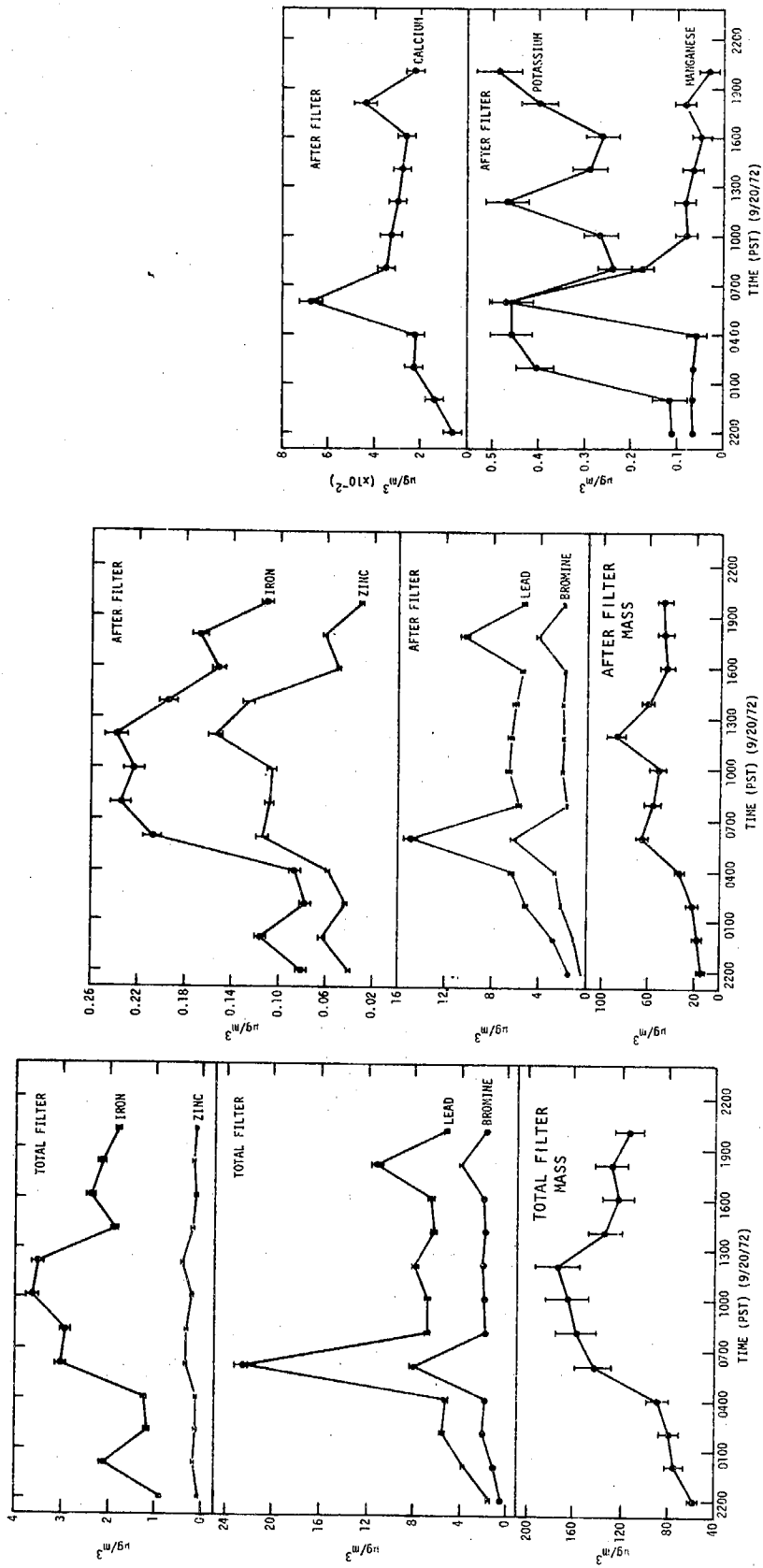


Figure 4-5A. Diurnal Patterns of Chemical Species (Inorganic Fraction) on September 19-20, 1972

SC524.25FR

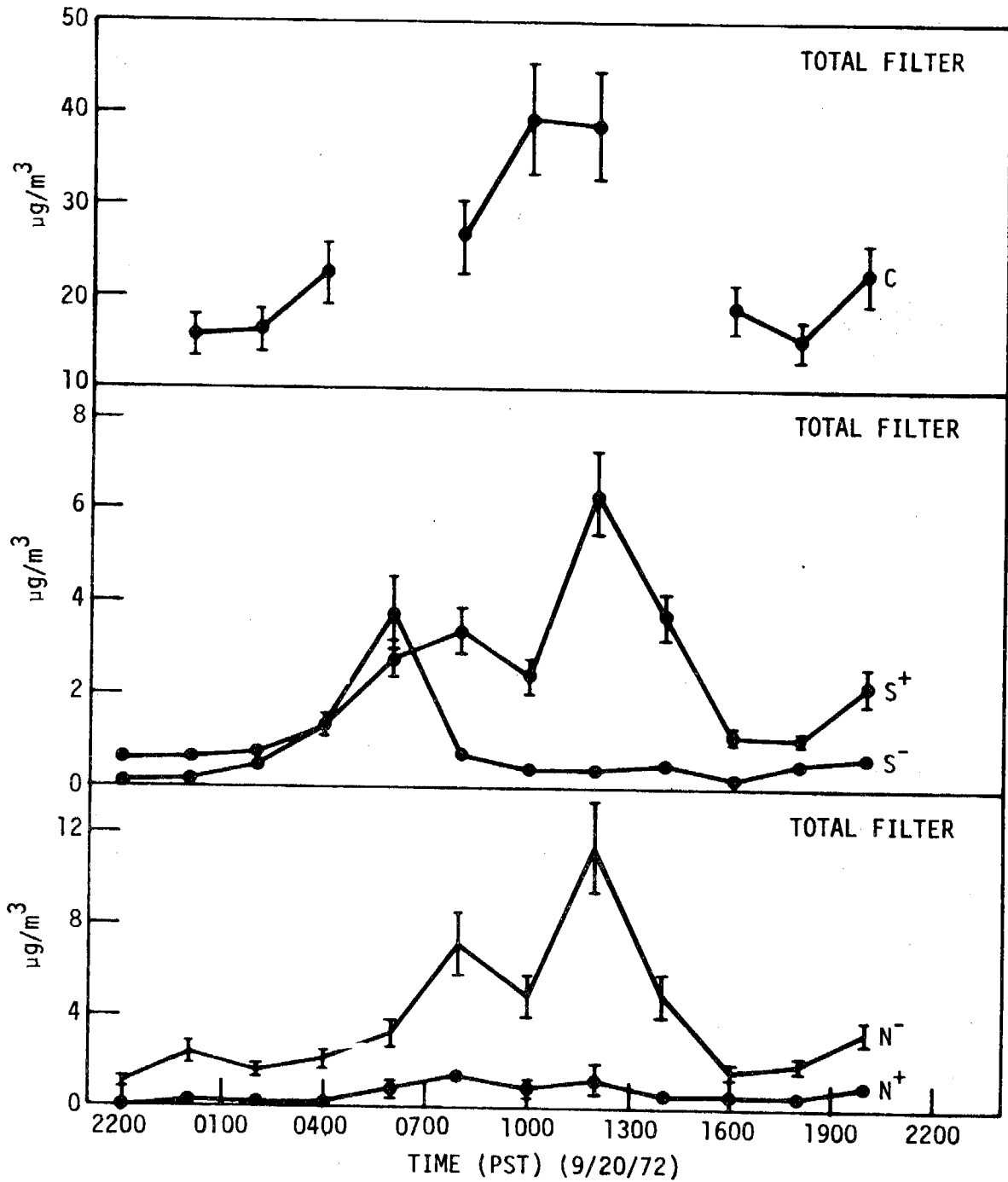


Figure 4-5B. Diurnal Patterns of Chemical Species (Carbon, and Oxidized and Reduced Sulfur and Nitrogen) for Harbor Freeway on September 19-20, 1972

SC524.25FR

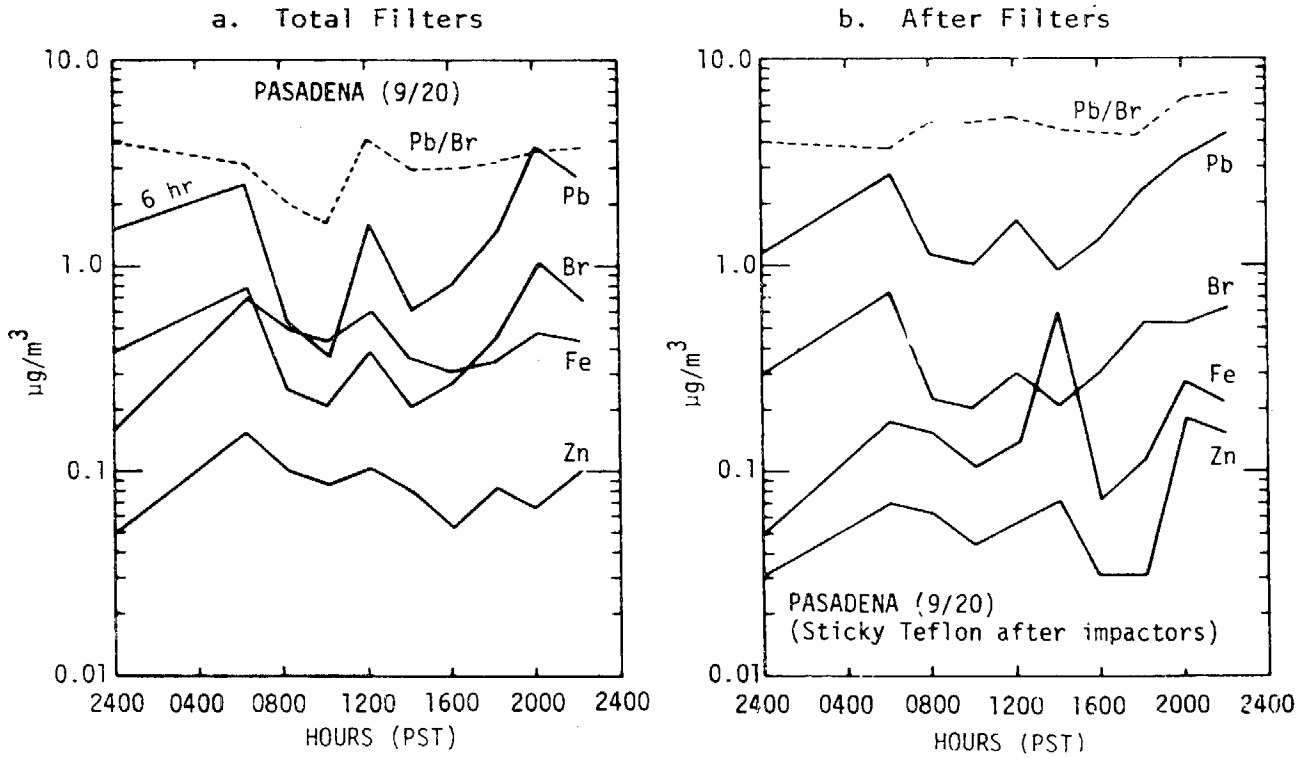


Figure 4-6. Diurnal Patterns of Heavy Elements for Pasadena - September 20, 1972

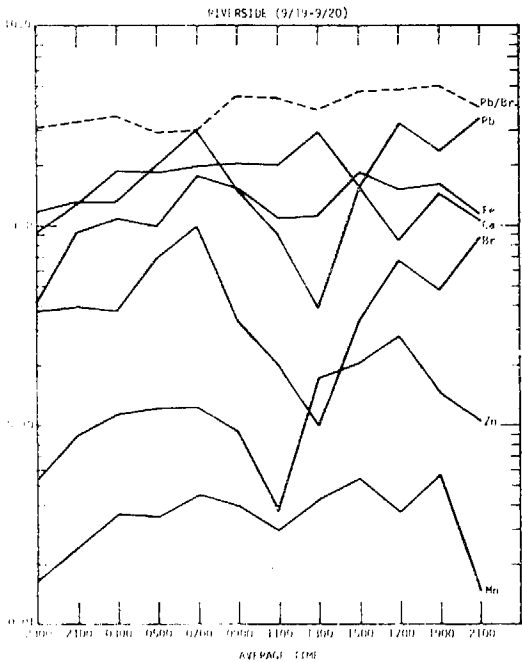


Figure 4-7. Diurnal Patterns of Heavy Elements for Riverside - September 19-20, 1972

SC524.25FR

were substantially higher at the freeway than the oxidized nitrogen content. This is particularly interesting in view of the early results that were taken in 1969 in Pasadena, where a somewhat similar pattern emerged.

Concentration of total carbon, as measured from the silver membrane filters, is shown in Figure 4-5B. There is the appearance of a midday maximum in total carbon. Comparison between the cyclohexane-extractable organic fraction and the amount of total carbon present in the aerosol, as measured by essentially a combustion technique, indicates an important difference in the data. That is, the total carbon contained in the aerosol at locations like the Harbor Freeway, as well as other locations in the South Coast Basin, shows substantially higher total carbon content than that measured by the cyclohexane extract. A similar pattern was found indirectly in the results taken in 1969 in Pasadena. The difference between the benzene solvent extract concentration from the NASN and the total carbon was not as great at that time.

A set of data for total filters and after filters in Pasadena for September 20 is indicated in Figure 4-6. In this case, the maximum lead concentrations are seen to be observed at night with a general decrease in the morning hours, followed by a weak maximum by midday. The bromine again follows the lead, and there appears to be some correlation between iron and zinc for the total filter. In the after filters a similar pattern is observed except that, in this case, the iron and zinc show less of a corresponding behavior to the lead and bromine combination.

At Riverside on September 20, the pattern of lead and bromine behavior shows a midday minimum, similar to that in Pasadena on this day (Figure 4-7). Similarly, the zinc and manganese curves show a pattern that corresponds reasonably well with lead and bromine; however, iron and calcium are somewhat different in their behavior, and their concentrations are significantly higher than those observed in Pasadena.

Nuclei Production and Motor Vehicles

The evaluation of the trace gas measurements at the Harbor Freeway as illustrated adds further complexity to the interpretation of aerosol data at this location. As an example, consider the observations of condensation (Aitken) nuclei concentration at the Freeway. During the midday on

SC524.25FR

September 20, the nuclei counts were observed to fluctuate but generally exceeded 10^6 particles/cm³. There is a body of evidence indicating that very high nuclei concentrations are attributable to "primary" emissions from combustion sources, including the automobile. During the midday on September 20, the wind was steady from the sector 220 to 260° (SW-W); but Burton⁽¹⁸⁾ has found that there is only a weak correlation between the condensation nuclei variation and the changes in acetylene concentration, a hydrocarbon gas identified principally with auto exhaust. This indicates that the very high nuclei populations at the Freeway were dominated at times by sources other than the auto traffic adjacent to the mobile laboratory.

It also is interesting that the exceedingly high nuclei concentrations accompany the high concentrations of SO₂ in midday that could not be explained by the local auto traffic patterns.

A survey of potential alternate sources for the Aitken nuclei suggests that they may come from a local stationary source or from advection of air masses polluted by heavy traffic further west, say, for example, earlier in the day at the San Diego Freeway, by aircraft emissions at Los Angeles International Airport, by emissions from the refinery-chemical plant complex at El Segundo, or by the Scattergood power plant complex at El Segundo.

Based on the west to southwest winds on September 20, ~ 3 to 3-1/2 hour would have been required to traverse the distance from El Segundo to the Harbor Freeway location. At Aitken nuclei concentrations of 7×10^6 particles/cm³, the thermal coagulation rate of particles is significant. Thus, primary emissions of particles would have to be unrealistically high at sources to the west to retain the concentrations observed at the Freeway. No local sources for nuclei have been identified immediately to the west of the Freeway site at this point. It then would appear that the alternate possibility that the nuclei are being produced in the advected polluted air mass by chemical transformations must be considered. This process of particle production was ruled out in Los Angeles earlier on the basis of experiments in Pasadena in 1969 [Husar et al.⁽⁶²⁾ and Hidy et al.⁽⁴¹⁾]. These experiments showed indirectly that growth by atmospheric chemical processes took place primarily on particles in the 0.1 to 1.0 μm size range. The new Harbor Freeway data,

SC524.25FR

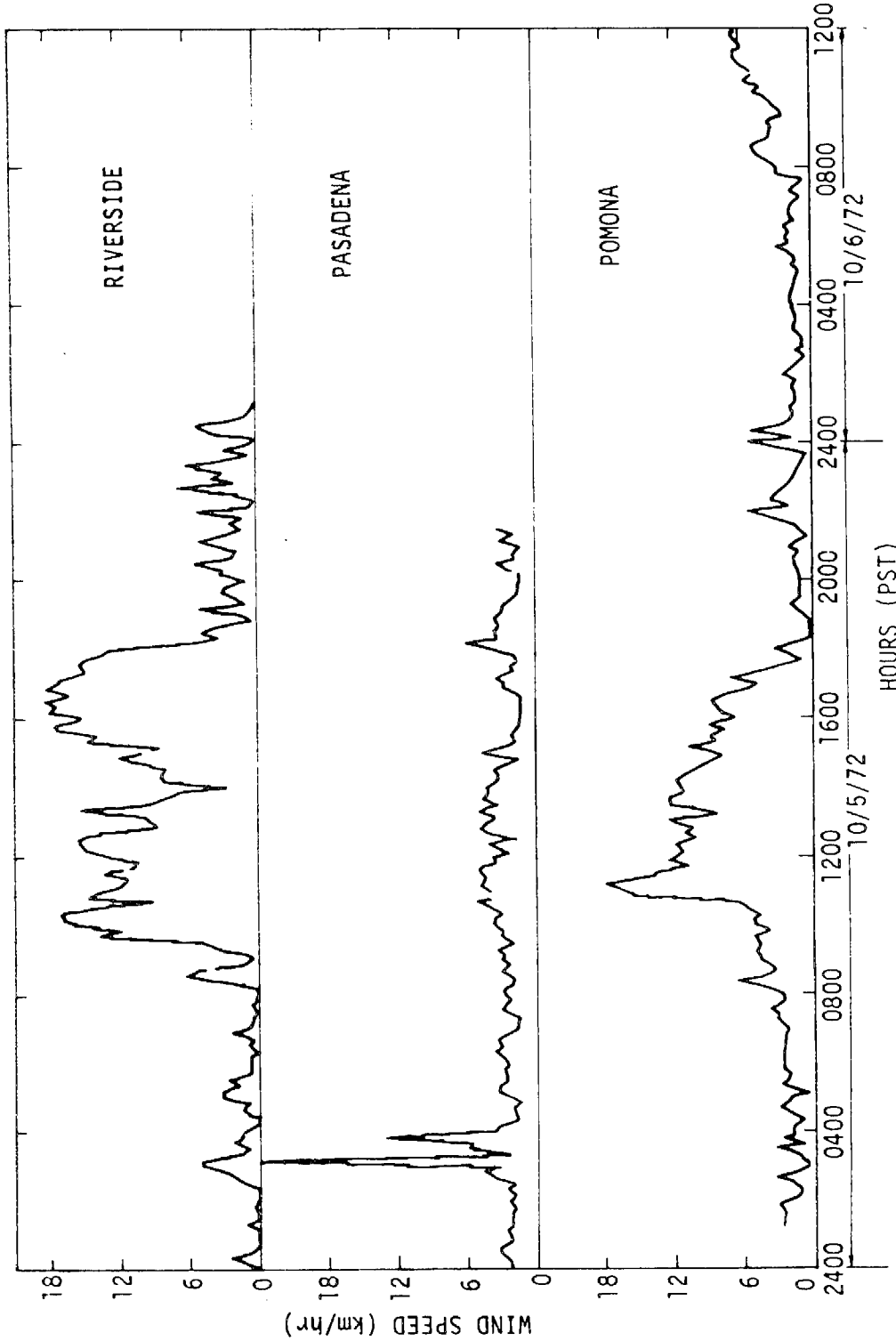
however, show that the extremely high nuclei production by heteromolecular processes linked to oxidation of SO_2 (for example) cannot be ruled out in the Los Angeles Basin, particularly in the western portion. Further work is required to clarify this point.

3. SOUTH COAST BASIN - OCTOBER 5 AND 6, 1972

This is the second episode chosen in the fall of 1972 in which all three of the South Coast Basin stations were running an intensive experiment on the same day. In this case, the mobile laboratory was at Pomona, so the results reflect an aerometric survey from west to east - beginning with Pasadena, then at Pomona, and finally reaching Riverside. Again, this day was characterized, as discussed in Volume III, Section VI, by mild Santa Ana conditions, good visibility, and reasonably dry, desertlike air. It represents, as September 20 did, a case of very low photochemical smog activity. The diurnal curves are shown in Figure 4-8. The winds in the eastern portion of the basin during midday reached 12 to 18 km/hr, while Pasadena remained quite calm. The values of b_{scat} , in general, were less than 10^{-3} m^{-1} . Pomona and Riverside showed a maximum in the morning hours. No systematic diurnal activity in b_{scat} for the three stations was observed on this day.

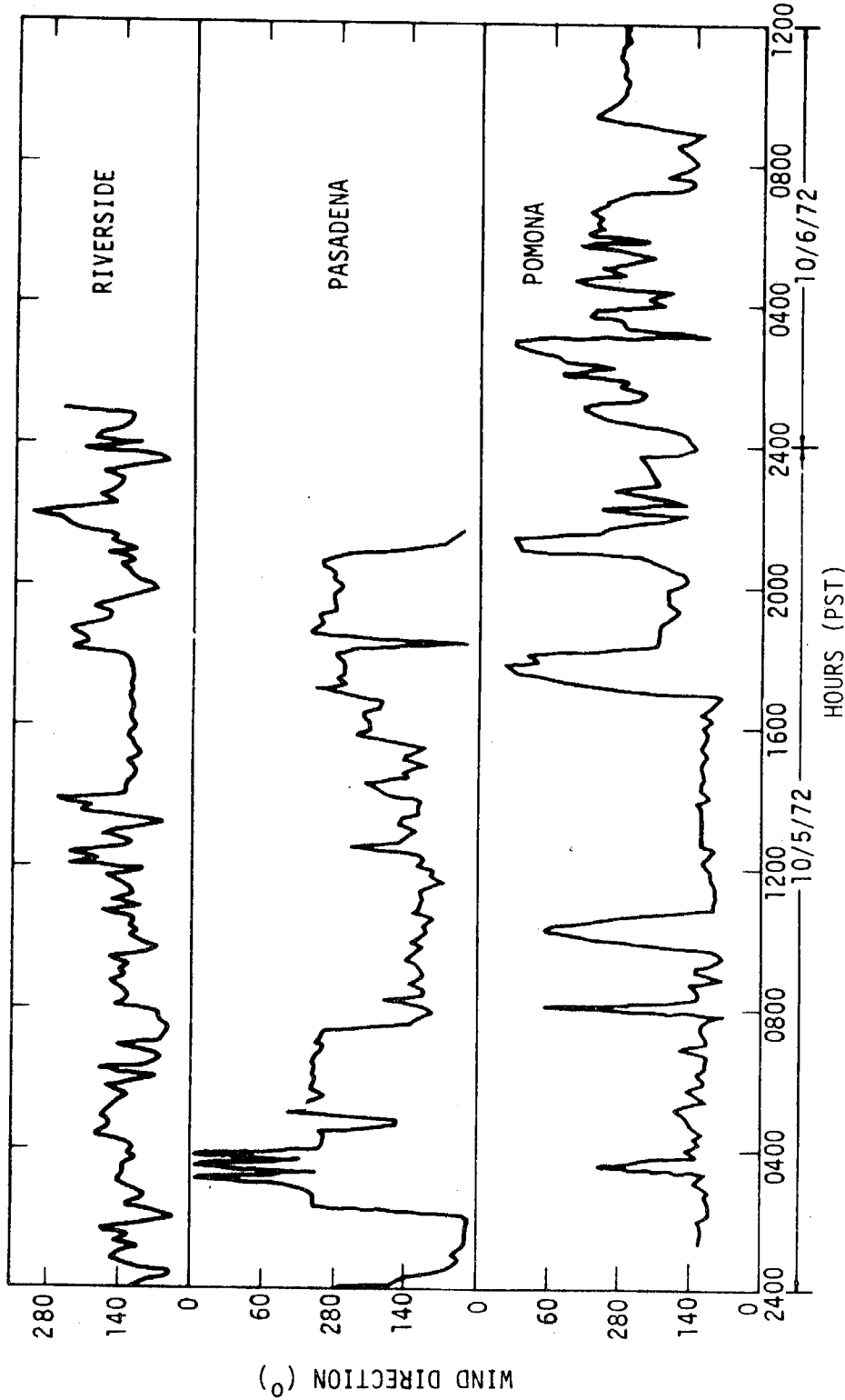
The ozone levels were very low at all three stations, but the classical midday peak was observed. The Pomona and Riverside peaks appeared to be somewhat broader than the peak at Pasadena. The NO_2 concentrations were generally low at all three stations. Of considerable interest, however, is the fact that there appear to be conditions at times, where a morning maximum of NO_2 is followed by a secondary peak of NO_2 later in the day. This is particularly marked in the Pasadena data. It is not understood, at this time, why there is a secondary maximum in NO_2 late in the day. The NO concentrations on this day were generally quite low, with a morning maximum at essentially similar times at Riverside, Pomona, and Pasadena, with a significant increase in NO late at night at Pasadena which did not occur at the other stations. Total hydrocarbon data indicate a peak in total hydrocarbon concentration accompanying the NO peak. Similarly, the CO peaks out in the early morning and in the evening, presumably from the increased heavy traffic, reflecting local traffic patterns, surround the three stations. The condensation

SC524.25FR



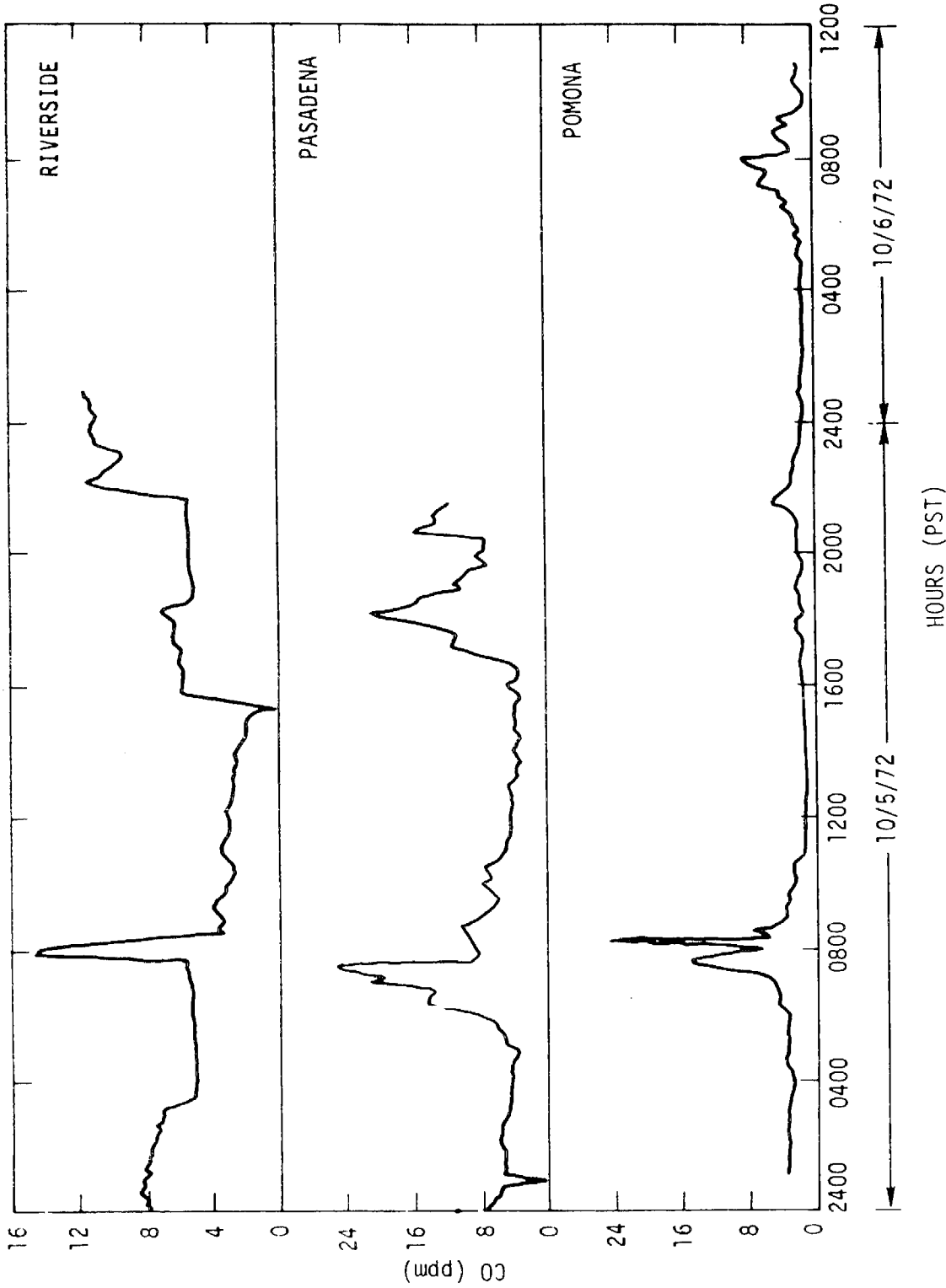
a. Wind Speed
Figure 4-8. Diurnal Patterns for Riverside, Pasadena, and Pomona
on October 5-6, 1972 (Sheet 1 of 9)

SC524.25FR



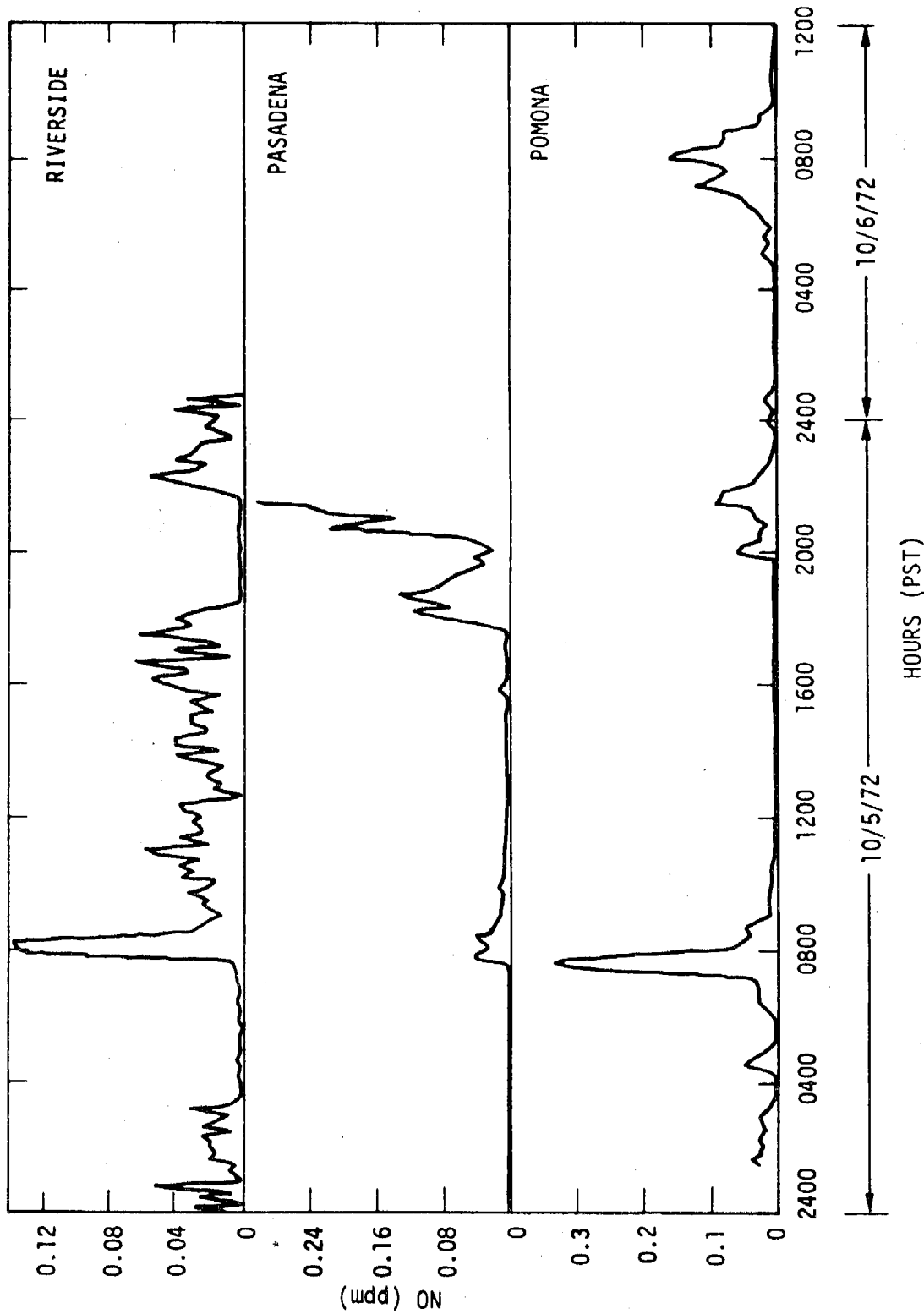
b. Wind Direction
Figure 4-8. Diurnal Patterns for Riverside, Pasadena, and Pomona
on October 5-6, 1972 (Sheet 2 of 9)

SC524.25FR



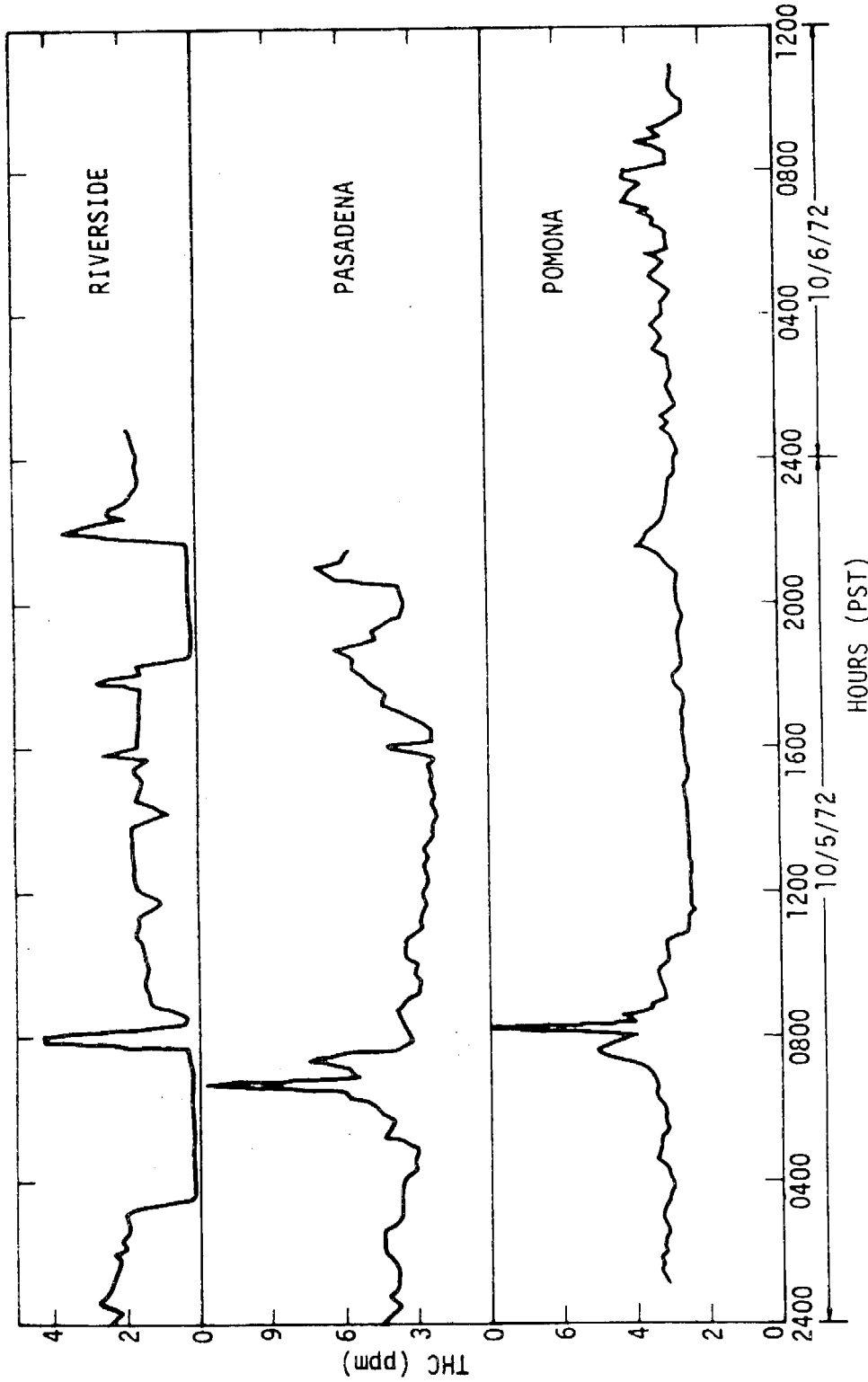
c. Carbon Monoxide
Figure 4-8. Diurnal Patterns for Riverside, Pasadena, and Pomona
on October 5-6, 1972 (Sheet 3 of 9)

SC524.25FR



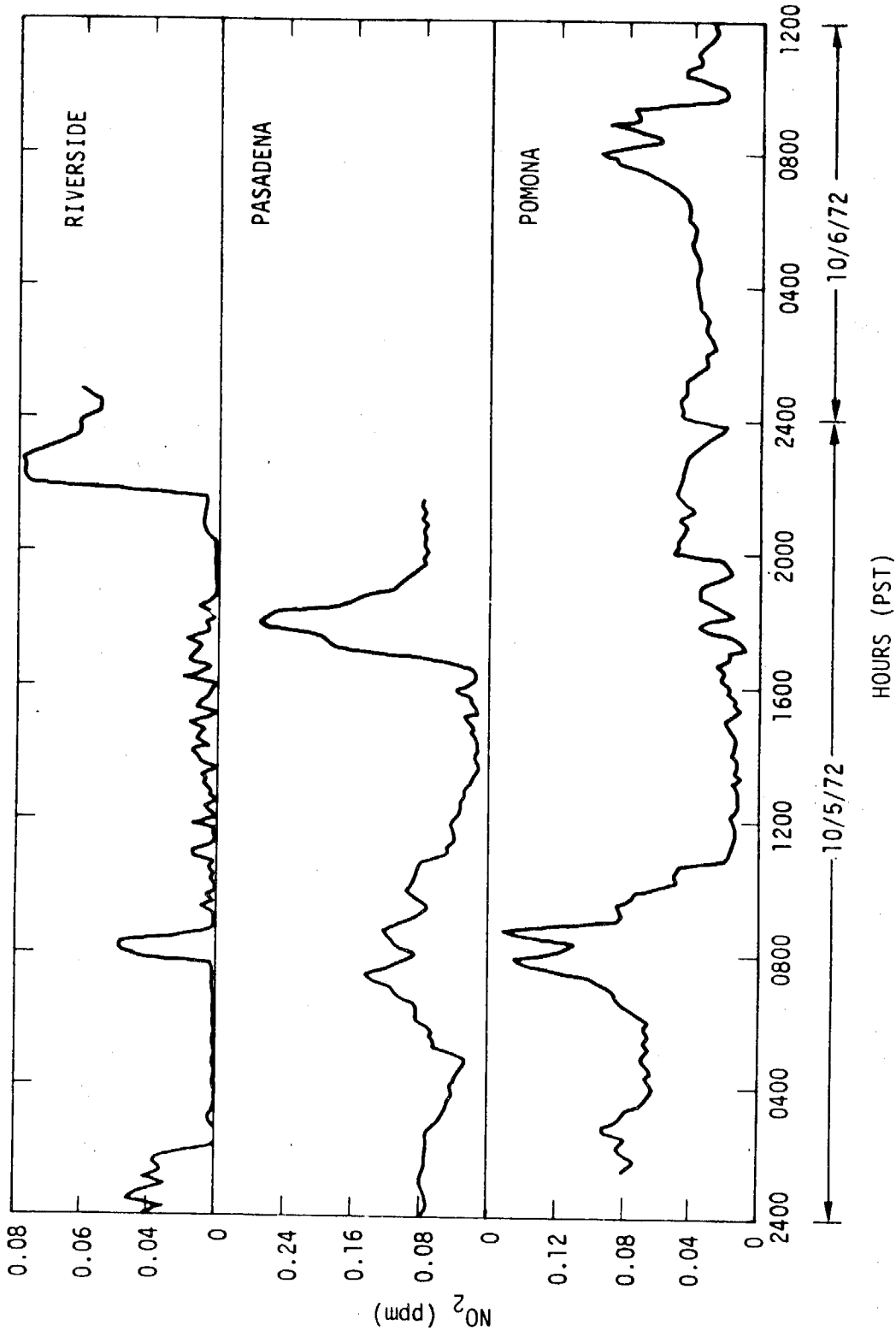
d. Nitric Oxide
Figure 4-8. Diurnal Patterns for Riverside, Pasadena, and Pomona
on October 5-6, 1972 (Sheet 4 of 9)

SC524.25FR



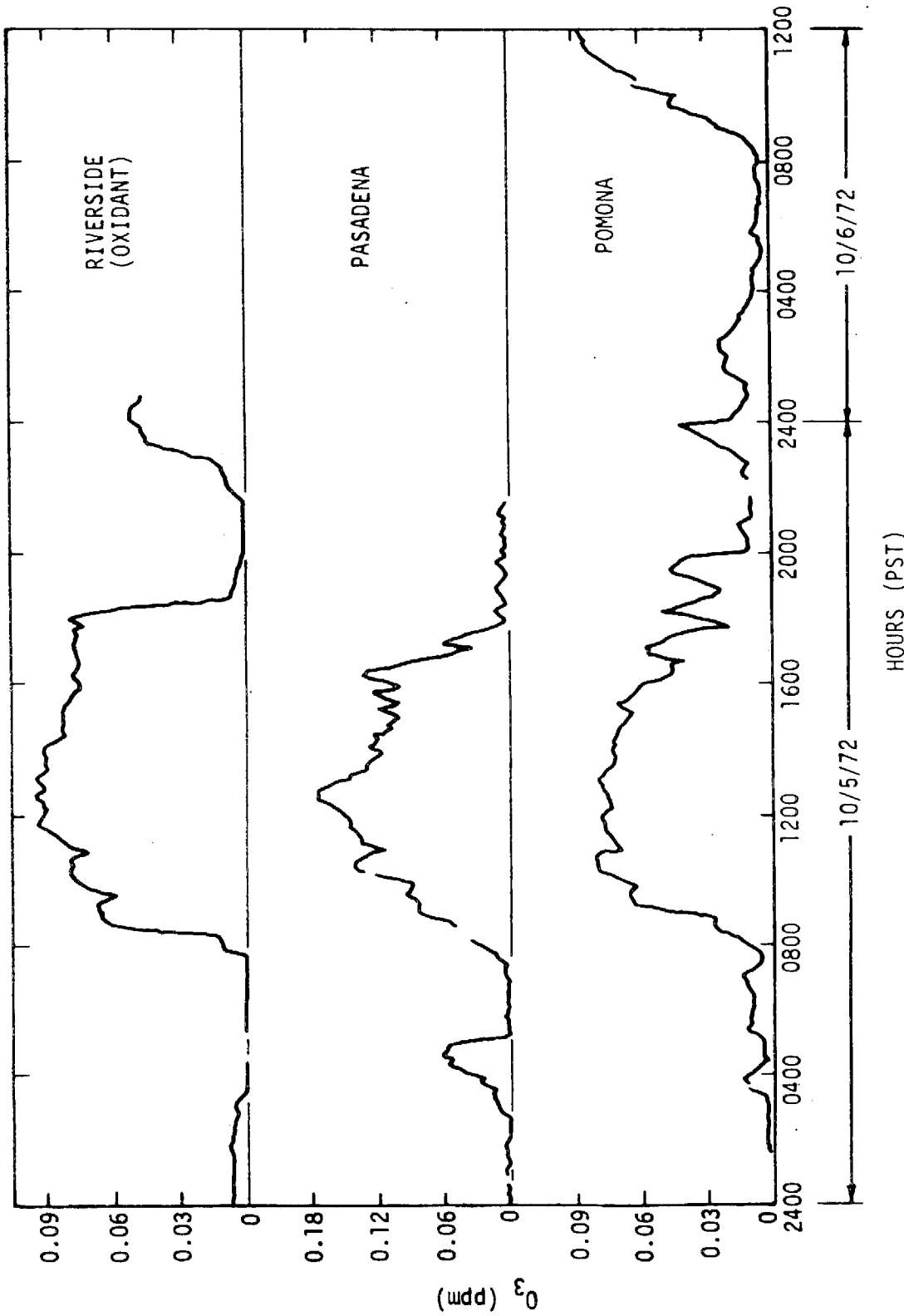
e. Total Hydrocarbons
Figure 4-8. Diurnal Patterns for Riverside, Pasadena, and Pomona
on October 5-6, 1972 (Sheet 5 of 9)

SC524.25FR



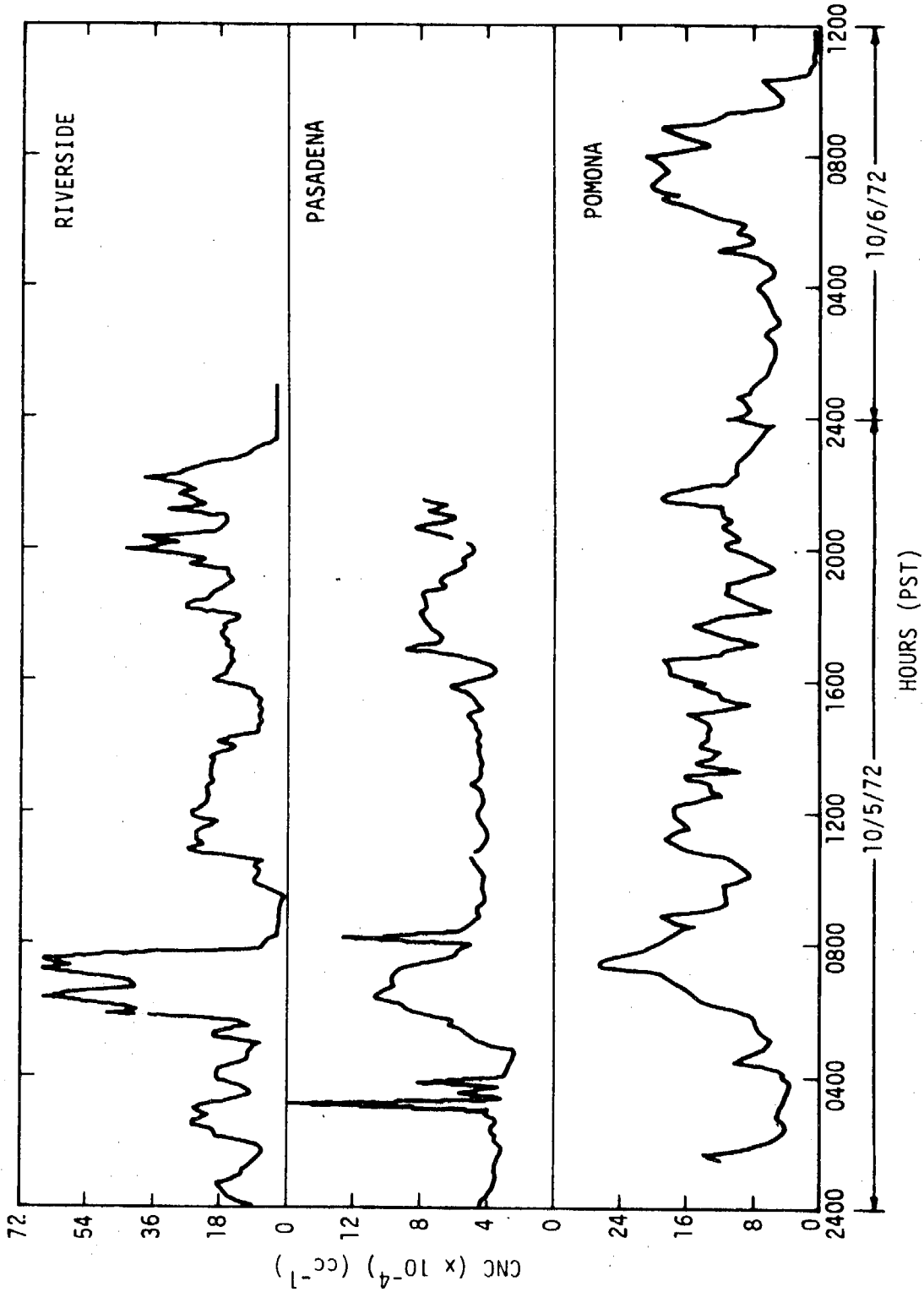
f. Nitrogen Dioxide
Figure 4-8. Diurnal Patterns for Riverside, Pasadena, and Pomona
on October 5-6, 1972 (Sheet 6 of 9)

SC524.25FR



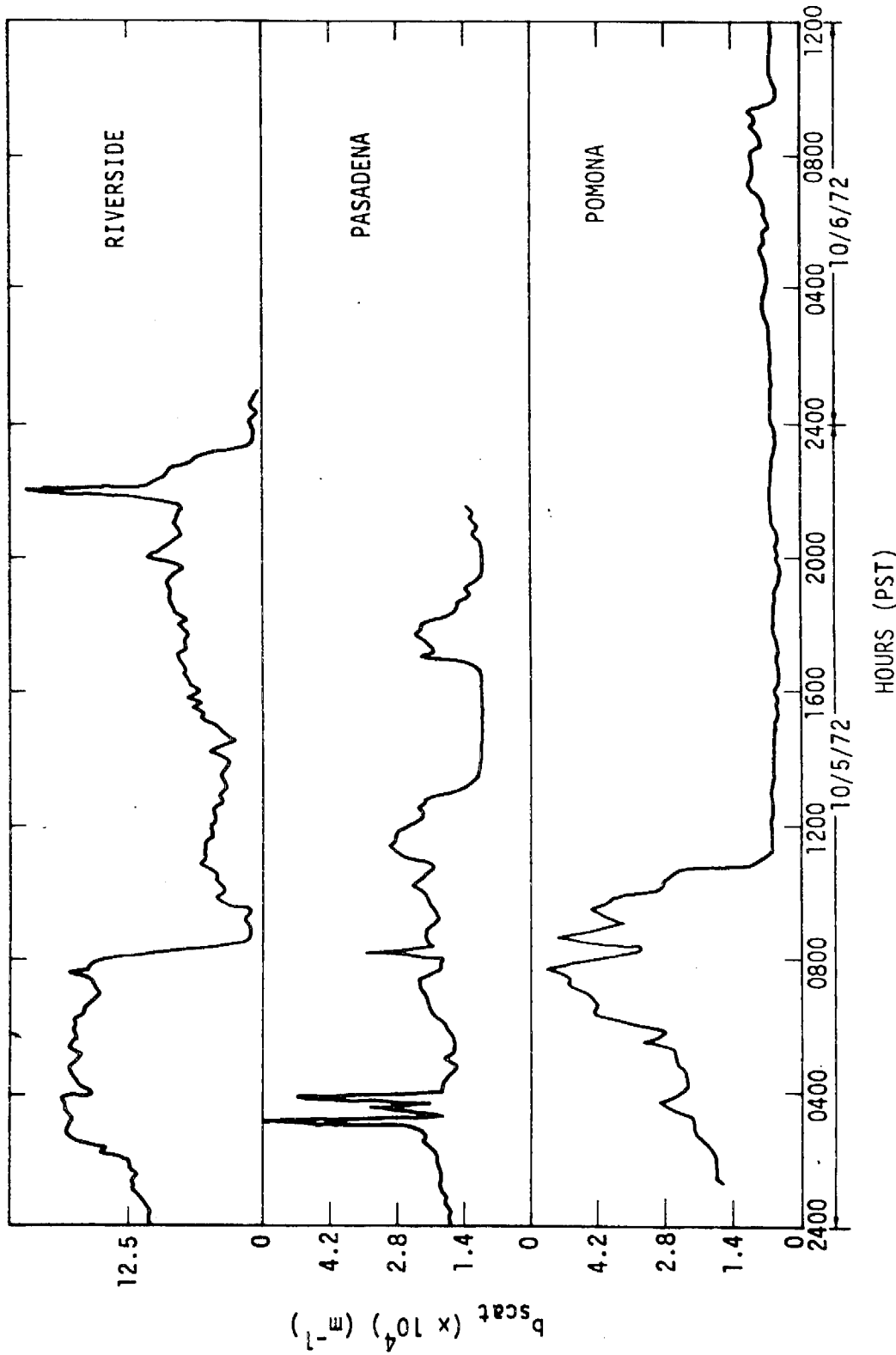
g. Ozone
Figure 4-8. Diurnal Patterns for Riverside, Pasadena, and Pomona
on October 5-6, 1972 (Sheet 7 of 9)

SC524.25FR



h. Condensation Nuclei Concentration
Figure 4-8. Diurnal Patterns for Riverside, Pasadena, and Pomona
on October 5-6, 1972 (Sheet 8 of 9)

SC524.25FR



i. Extinction Coefficient Due to Light Scattering
Figure 4-8. Diurnal Patterns for Riverside, Pasadena, and Pomona
on October 5-6, 1972 (Sheet 9 of 9)

SC524.25FR

nuclei patterns indicate the early morning peaks associated with motor vehicle traffic and increased anthropogenic activity related to combustion. The values, in general, were $\sim 10^5$ particles/cc. The secondary weak maximum was observed, particularly in Riverside and Pasadena, in the evening. Essentially no systematic particle growth in the large particle range was seen on this day, which is expected if there is a strong contribution of photochemical aerosol to the growth of the large particle fraction during the daylight hours.

Figure 4-9 shows the patterns for the heavy elements in Pomona on October 5 and 6. Here the lead and bromine show a strong peak with the morning traffic, and a minimum at midday. Zinc appears to follow lead and bromine reasonably well; however, the iron and calcium appear to be somewhat less well correlated with the lead. In any case, all of the heavy elements show the morning maximum on this day.

4. BACKGROUND MEASUREMENTS

The measurement of background conditions are of considerable interest in the establishment of baseline data for air pollution in the State of California. Three different background locations were selected for this program. The first was in a remote area just east of the Big Sur region, on the Hunter-Liggett Military Reservation. It was chosen to seek diurnal changes related to emissions of hydrocarbon vapors from vegetation in a fairly dry, semi-arid region, characteristic of large areas in Southern California that do not have large, densely clustered stands of conifer trees. The second location, at Goldstone Tracking Station in the Mohave Desert, was chosen for desert background.* The third location was a marine-source-dominated site at Pt. Arguello.

Some of the most interesting data, from the standpoint of air chemistry, were obtained in the remote sites. In general, the levels of trace gases normally considered pollutant gases were surprisingly high at all three locations. Of particular interest was the high oxidant levels experienced at Pt. Arguello and at Hunter-Liggett. All of the pollutants, except for the sulfur gases, were in the concentration ranges that were detectable by the instrumentation of the mobile laboratory. Some of these contaminants were

* See Appendix B

SC524.25FR

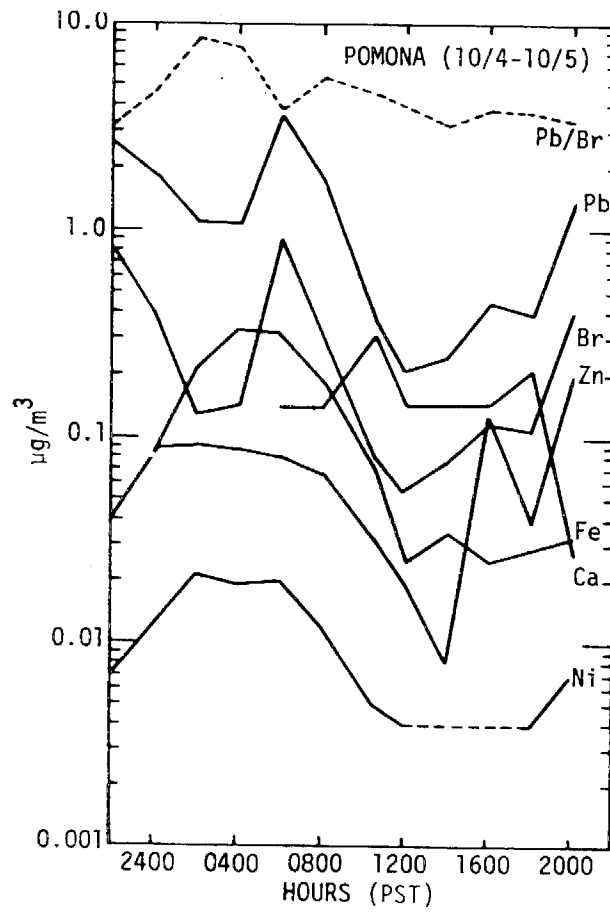


Figure 4-9. Diurnal Patterns of Heavy Elements for Pomona on October 5-6, 1972

SC524.25FR

unquestionably related to anthropogenic sources in aged air masses traveling through these remote regions. On the other hand, there are certainly ample natural sources for many pollutants, which would provide sufficient levels, even in background areas.

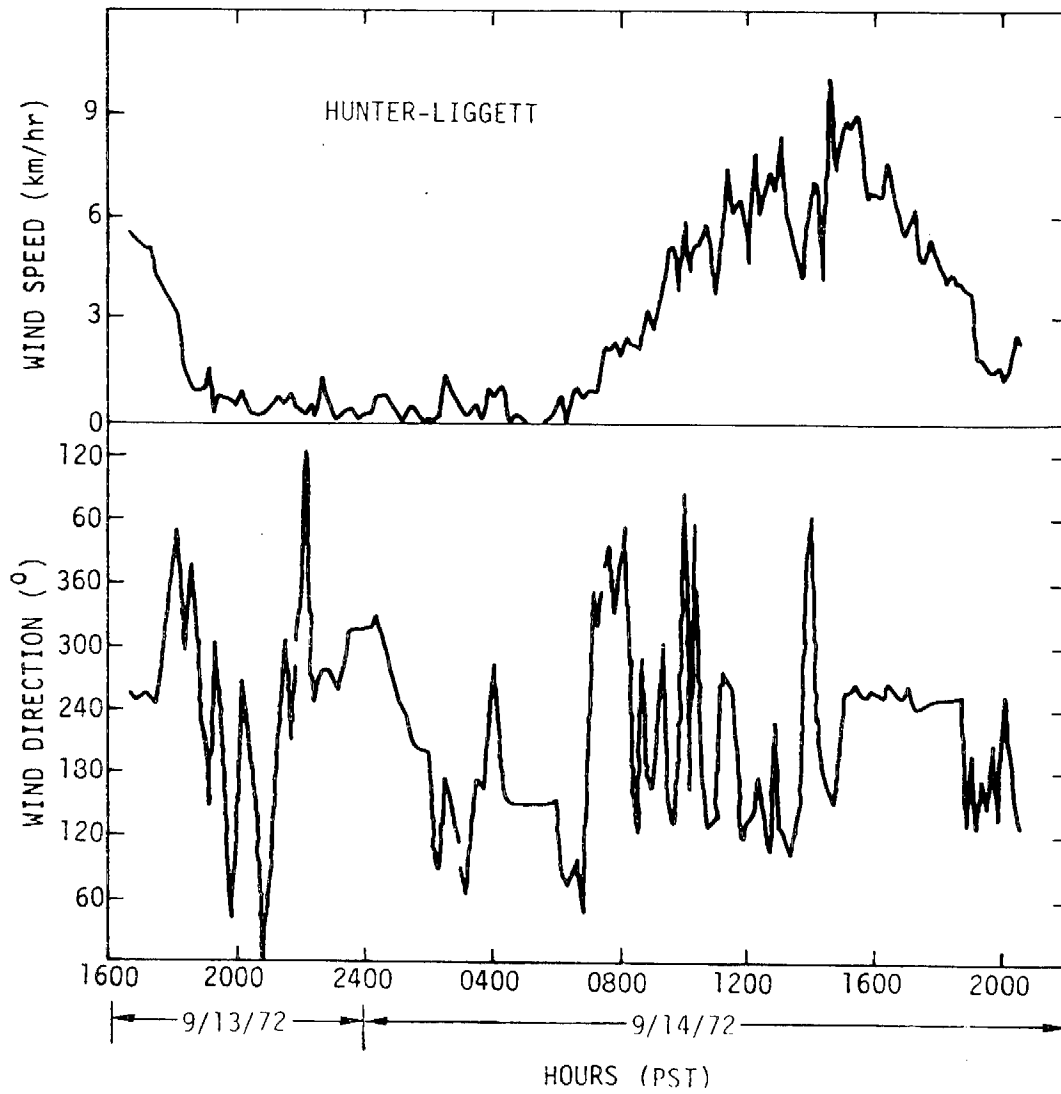
Data taken at Goldstone reflected extremes in conditions that might be expected away from the ocean. On the first day of sampling, the air was quite clean, associated with the leeward side of a weak storm front that had passed through. On this particular occasion, virtually no aerosols were observed in the air, despite the fact that there was a brisk wind blowing. This is rather surprising, in view of the fact that windblown dust is known to be a significant natural contaminant. For example, one expects a systematic increase with wind speed. In the particular case examined, however, there was extensive shower activity one to two days before sampling. The compaction of ground from rainfall may have been responsible for the conditions observed at Goldstone.

On the other extreme, toward the end of the period at Goldstone, the wind shifted from the northwest sector to the southwest sector. The southerly winds brought in an air mass containing aged pollutants. There was a significant increase in pollutant gases, as well as aerosol particles in the sub-micron range that penetrated the Goldstone area. Presumably, this material was a tracer of a contaminated air mass passing westward from the South Coast Basin.

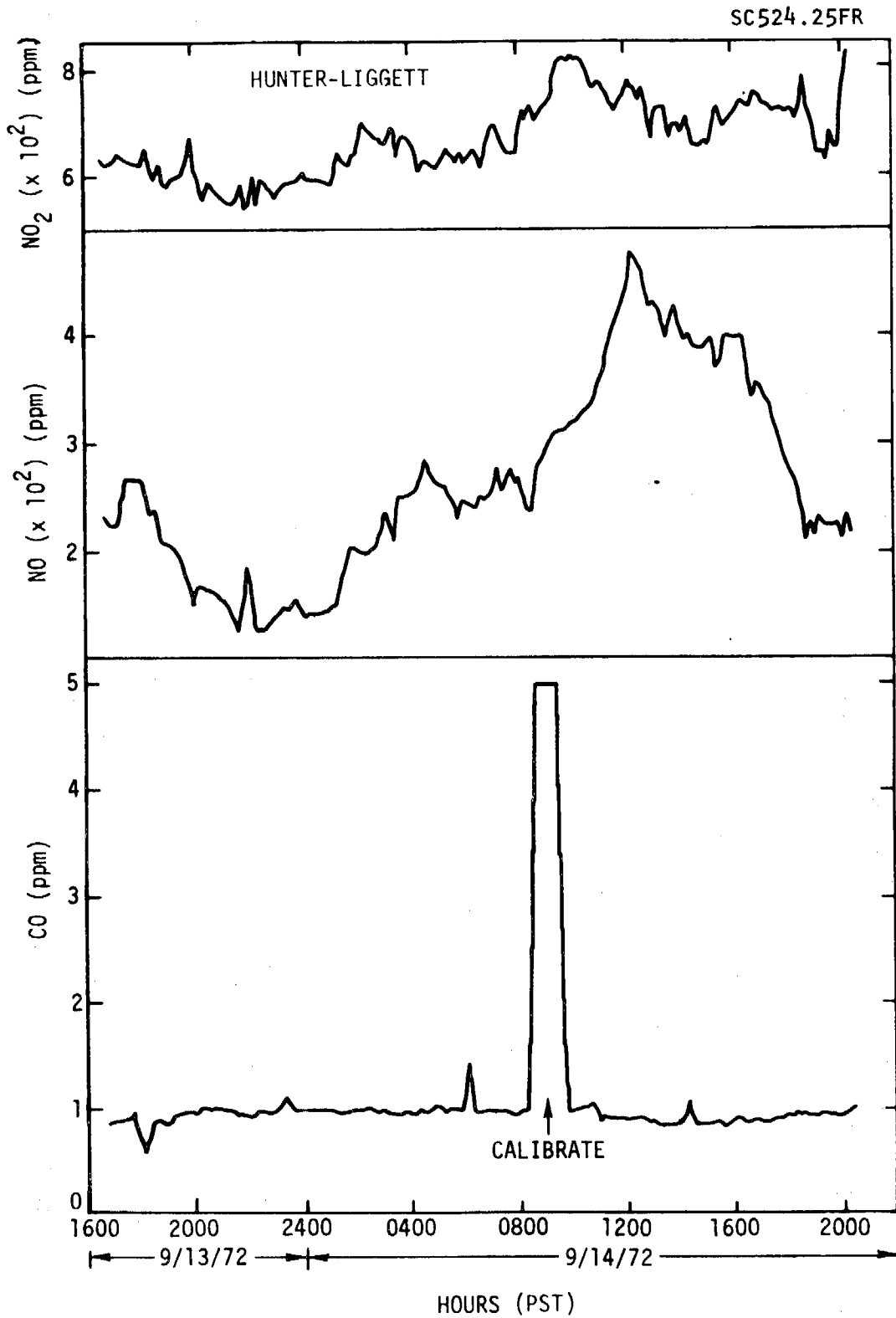
In Pt. Arguello, the air was essentially dominated by the ocean. The site that was selected was within 100 yards of the sea and about 50 ft above the surf zone. The atmosphere was disturbed during the period of sampling by another weak storm front passing through central and Southern California. The period was characterized by a wide range of conditions, from weak winds to rather high winds. During the high wind period, when the ocean was quite agitated, there was a strong influx of sea spray that was easily detected by the instruments on the trailer.

To illustrate the data taken under background conditions, the set of diurnal plots for the Hunter-Liggett Military Reservation are shown in Figure 4-10. Data for SO_2 and H_2S were below the limits of detectability for the Varian (i.e., < 5 ppb). The episode at Hunter-Liggett was taken on a very warm day, with light winds coming from different directions. The

SC524.25FR

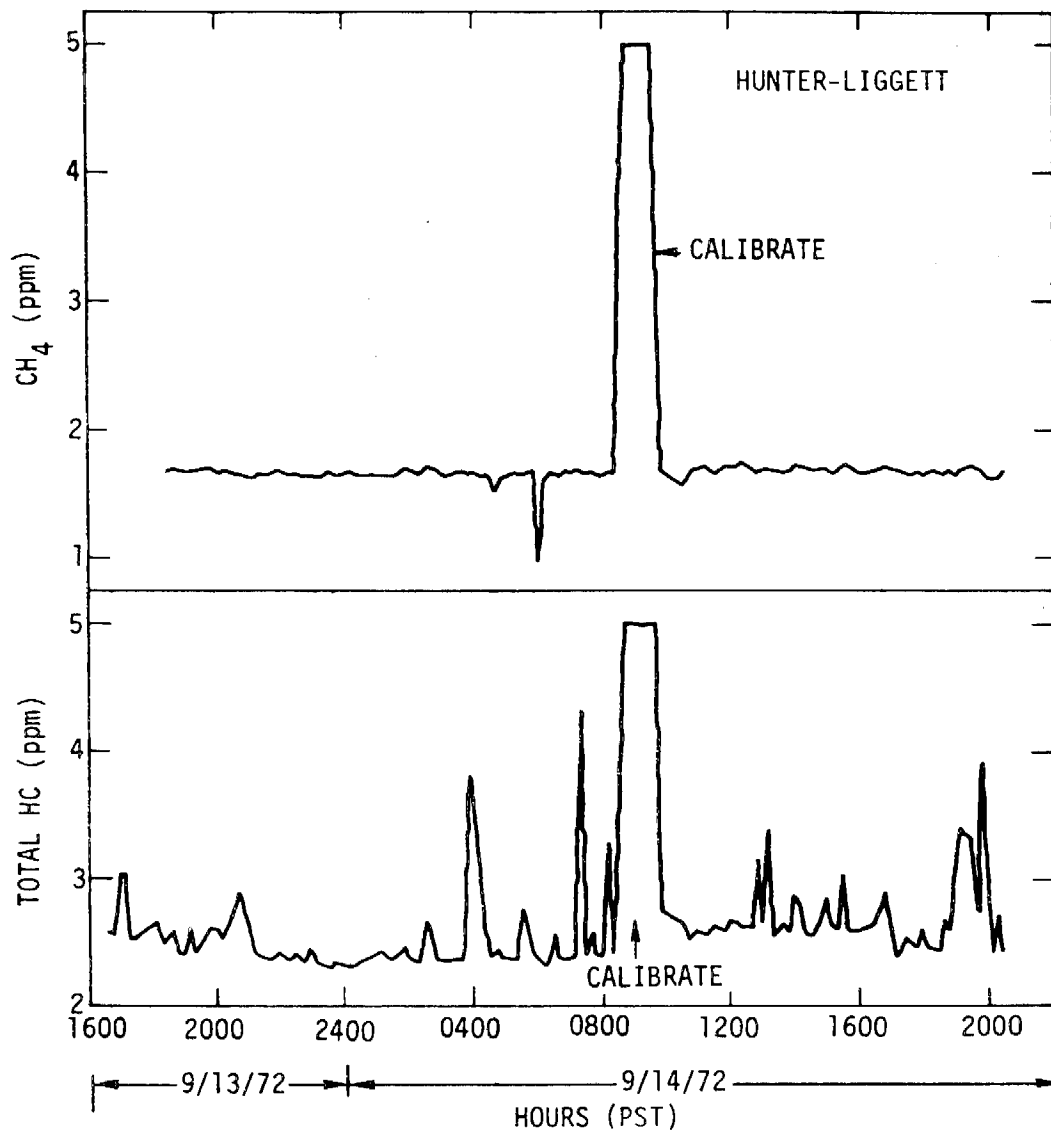


a. Wind Speed and Direction
Figure 4-10. Diurnal Patterns for Hunter-Liggett
on September 13-14, 1972 (Sheet 1 of 4)



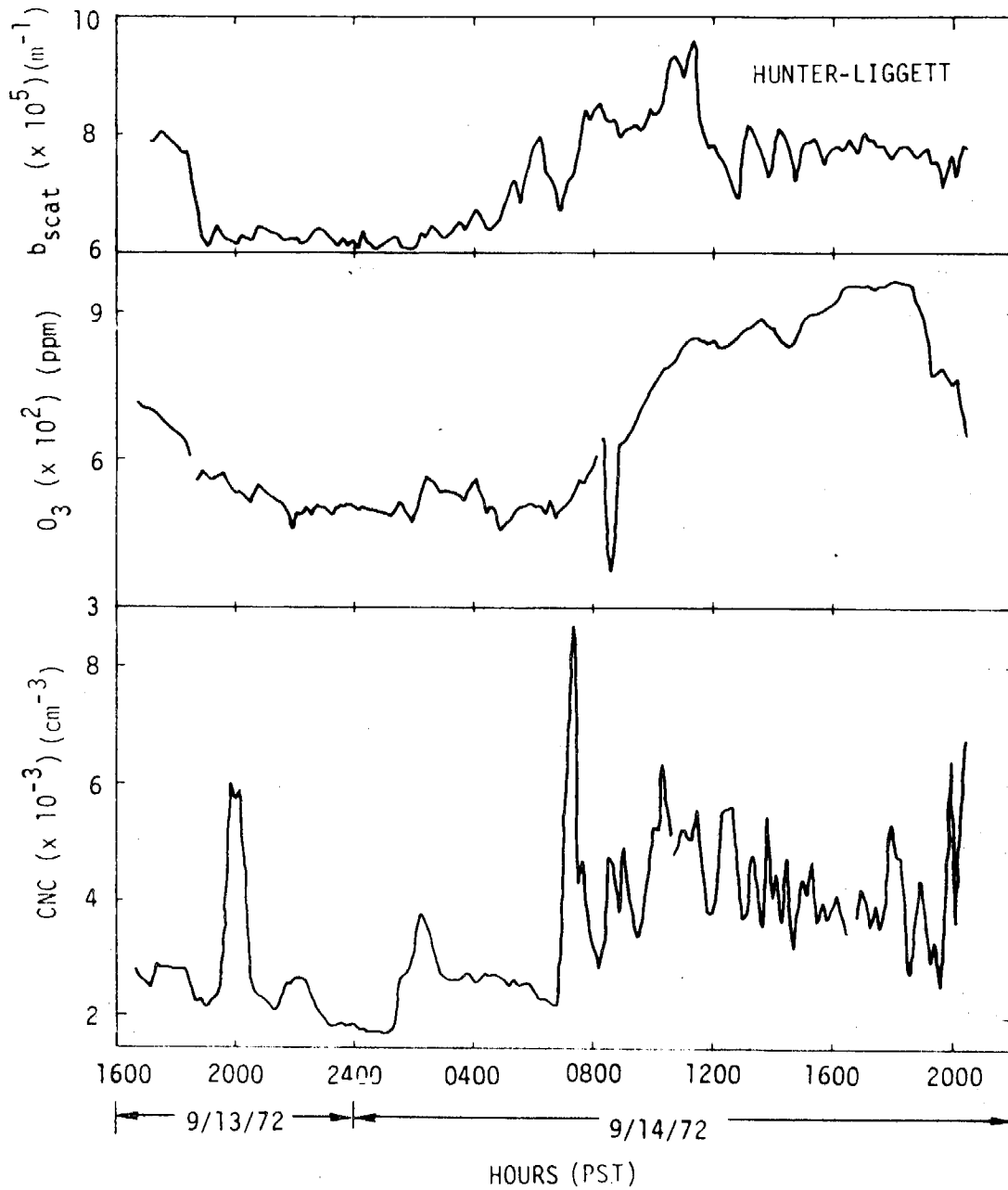
b. Nitrogen Dioxide, Nitric Oxide, and Carbon Monoxide
Figure 4-10. Diurnal Patterns for Hunter-Liggett on
September 13-14, 1972 (Sheet 2 of 4)

SC524.25FR



c. Methane and Total Hydrocarbons
Figure 4-10. Diurnal Patterns for Hunter-Liggett
on September 13-14, 1972 (Sheet 3 of 4)

SC524.25FR



d. Extinction Coefficient, Ozone, and Condensation Nuclei Concentration
Figure 4-10. Diurnal Patterns for Hunter-Liggett
on September 13-14, 1972 (Sheet 4 of 4)

SC524.25FR

variability in wind direction is indicated in Figure 4-10a. The general direction of the wind was from the south or southeast. The wind was calm during the early part of September 14, with an increasing afternoon speed, as indicated in Figure 4-10a. In general, b_{scat} was measured to be extremely low ($< 10^{-4} \text{ m}^{-1}$) during the episode. There was a weak but systematic increase in b_{scat} through the afternoon period, with the increase in wind. It is not clear, from this data whether that increase was associated with blowing dust or whether it may have been related to weak photochemical aerosol formation. The condensation nuclei count showed a similar pattern to that of b_{scat} ; the levels were generally quite low ($< 10^4$ particles/cc), with a weak maximum in the midafternoon. The ozone levels achieved at Hunter-Liggett were of particular interest; since, late in the midday, a value of 0.1 ppm was observed. This, of course, exceeds the air quality limits established for oxidant by federal standards. Accompanying the increased ozone level was a systematic increase in NO , peaking out at approximately the same time the ozone did. However, the NO_2 levels generally remained quite low, with only a weak peak developing in midday, coming somewhat before the NO peak.

The methane hydrocarbons were essentially constant at a level around 2 ppm. Total hydrocarbons were somewhat more variable, potentially reflecting spikes associated with occasional movement of military vehicles at some distance from the trailer. The general background level was $\sim 2\text{-}1/2$ ppm for total hydrocarbon. The CO levels were remarkably low; somewhat < 1 ppm at Hunter Liggett. The interpretation of the Hunter-Liggett data is difficult at this point, particularly because the wind pattern on that day was from a direction that was not climatologically typical. It is possible that the oxidant level measured on that day, with the accompanying NO , could be related to aged air contaminants showing up from the Moss Landing Power Plant region, and drifting back over Hunter-Liggett with the wind reverses. The Hunter-Liggett data are rather unique, in their characterization of low-level diurnal patterns of photochemical activities in a region that is quite remote from major anthropogenic activity.